FOSSIL ENERGY

DOE/MC/23075--3002

DE92 003008

MEASUREMENT AND MODELING OF ADVANCED COAL CONVERSION PROCESSES

17th Quarterly Report #523043-51
October 1, 1990 to December 31, 1990

By
Peter R. Solomon
Michael A. Serio
David G. Hamblen
L. Douglas Smoot
B. Scott Brewster

Work Performed Under Contract No. DE-AC21-86MC23075

For
U.S. Department of Energy
Office of Fossil Energy
Morgantown Energy Technology Center
Morgantown, West Virginia
Dr. Richard Johnson
COTR

By

Contractor

Advanced Fuel Research, Inc.
87 Church Street
East Hartford, CT 06108
(203) 528-9806

Program Director

Peter R. Solomon
President

Subcontractor

Brigham Young University
Provo, Utah 84602
(801) 378-4326

Program Director

L. Douglas Smoot
Dean and Professor

DISCLAIMER

PATENT STATUS

ABSTRACT

The overall objective of this program is the development of predictive capability for the design, scale up, simulation, control and feedstock evaluation in advanced coal conversion devices. This technology is important to reduce the technical and economic risks inherent in utilizing coal, a feedstock whose variable and often unexpected behavior presents a significant challenge. This program will merge significant advances made at Advanced Fuel Research, Inc. (AFR) in measuring and quantitatively describing the mechanisms in coal conversion behavior, with technology being developed at Brigham Young University (BYU) in comprehensive computer codes for mechanistic modeling of entrained-bed gasification. Additional capabilities in predicting pollutant formation will be implemented and the technology will be expanded to fixed-bed reactors.

The foundation to describe coal-specific conversion behavior is AFR's Functional Group (FG) and Devolatilization, Vaporization, and Crosslinking (DVC) models, developed under previous and on-going METC sponsored programs. These models have demonstrated the capability to describe the time dependent evolution of individual gas species, and the amount and characteristics of tar and char. The combined FG-DVC model will be integrated with BYU's comprehensive two-dimensional reactor model, PCGC-2, which is currently the most widely used reactor simulation for combustion or gasification. The program includes: i) validation of the submodels by comparison with laboratory data obtained in this program, ii) extensive validation of the modified comprehensive code by comparison of predicted results with data from bench-scale and process scale investigations of gasification, mild gasification and combustion of coal or coal-derived products in heat engines, and iii) development of well documented user friendly software applicable to a "workstation" environment.

Success in this program will be a major step in improving the predictive capabilities for coal conversion processes including: demonstrated accuracy and reliability and a generalized "first principles" treatment of coals based on readily obtained composition data.

The progress during the seventeenth quarter of the program is summarized below.

For Subtask 2.a., most of the effort was on using the set of rank dependent kinetic parameters obtained from low heating rate experiments to predict high heating rate data from pyrolysis experiments in our Transparent Wall Reactor (TWR) and Heated Tube Reactor (HTR). We also did simulations of high heating rate pyrolysis data from the literature, such as the heated grid experiments of Gibbins, the wire grid experiments of Fong and coworkers of MIT, and the TWR experiments of Fletcher at Sandia.

Some problems were obtained in predicting the changes in the tar yield and tar molecular weight distributions with heating rate for low rank coals using the current version of the model. It was decided to re-examine the assumptions on the model input parameters, such as 1) the crosslinking efficiencies, 2) the tar vaporization law, and 3) the ΔP parameter. Changes in the crosslinking efficiencies were thoroughly evaluated and found to be largely unnecessary.

The effects of the tar vaporization law and the ΔP parameter were found to be very important. The change in the original vaporization law from the expression proposed by Suuberg to a factor of 10 higher was found to be mainly responsible for the inability to predict the high heating rate Zap data. By changing to Suuberg X1, and allowing ΔP to be the sole adjustable parameter, the predictions are much better. The main unresolved question is the appropriate choice for ΔP and how this could be functionalized. It appears that the model predictions of the FIMS data are very sensitive to the choice of this parameter. Possible solutions would be to: 1) parameterize ΔP; 2) improve the description of the external transport of tar to resolve the problem of the higher molecular weight tars coming out earlier than expected.

For Subtask 2.b., progress was made in increasing the signal-to-noise ratio of the optical particle imaging system so that small particles at low temperature can be measured. The modified reactor collection system was operated successfully under devolatilization conditions. Under independent funding, coal devolatilization tests were successfully conducted using the modified reactor collection system. Computer software was written to support the data acquisition and heater control hardware that was previously interfaced to the reactor instrumentation and heaters, and was successfully used during the devolatilization tests.

For Subtask 2.c., discussions were held with BYU on the future direction of the work on modeling the tomography data from the TWR coal flame experiments. Some discrepancies exist in the measured and predicted particle temperatures which could result from problems with the measurements and/or the model. A rate limiting step in comparing the model with the data is the generation of suitable plots. A new approach which involves output of the predictions of the model into a spreadsheet format was agreed upon.

For Subtask 2.d., no work was scheduled during the past quarter.

For Subtask 2.e., the work on the modified AFR fixed-bed reactor (FBR) system continued. It includes two independently heated stages. The reactor system was assembled and tested and is now being used for lignin pyrolysis experiments under independent funding. It appears to work as planned. As expected, the quantitation of gas and tar is much better than in the old system and a wider range of sample sizes and flow rates can be used.

For Subtask 2.f., the decision was made previously to construct an experimental facility that would connect to the HPCP reactor of Subtask 2b. Of the two experimental approaches considered in the previous reports, the decision has been made to develop the "cantilever beam insert." In this approach the sample will be mounted horizontally to one or two of the optical access ports of the HPCP reactor. A summary of the design of this facility was prepared and sent to a few principal investigators active in fields of closely related research for their comments and criticisms. The suggestions received have been included in the details for the design of this facility. Construction of this "cantilever beam insert" will start during this next quarter. Analytical procedures for monitoring rates of oxidation of large particles continue to be evaluated. Further data analysis of large particle oxidation in air in platinum crucibles shows a marked dependence of mass reactivity on the initial mass of the large particles. This is in contrast to a dependance on temperature, which was expected.

For Subtask 2.g., the method used to determine atomic oxygen concentrations in the NO_x submodel was revisited. Further insight into the best quasi-equilibrium expression to use for predicting atomic oxygen concentrations in lean, swirling-flow, natural gas flames was gained. Work continued on the integration and evaluation of a SO_x/sorbent reaction computerized submodel. This submodel has been integrated into PCGC-2 and is currently being evaluated. Experimental data are being sought to determine H_2S capture rates to use in an H_2S sulfation subroutine.

For Subtask 3.a., work continued on code evaluation and user-friendliness. Data from four reactors were identified for code evaluation. Simulations were performed for a natural gas flame in the BYU controlled-profile reactor and for the near-burner field of a full-scale industrial boiler. Two-dimensional combustor data were requested from Imperial College. A set of minimum specifications for a foundational, entrained-bed code that will satisfy the terms of the contract was identified. These specifications were documented in a letter to AFR and METC. Two menu-driven post-processors were developed for converting PCGC-2 plotting files for gas and particle properties into a format that can be used by spreadsheet programs.

For Subtask 3.b., work continued on developing and evaluating the one-dimensional fixed-bed model. The model response to variations in operating conditions was validated by simulating several such test cases. Predicted temperature profiles were compared to measurements for the atmospheric, air-blown Wellman-Galusha gasifier fired with Elkhorn bituminous, Jetson bituminous, Leucite Hills subituminous, and Utah Blind Canyon bituminous coals. These test cases included temperature profiles at different operating conditions. Discussions with AFR, about the single particle FG-DVC submodel for integration into the fixed-bed code, continued. Development of the user's manual for the fixed-bed code was initiated. The first draft of the manual was prepared.

For Subtask 3.c., PCGC-2 was modified to allow sorbent injection in the primary stream.

For Subtask 4.a., potential application cases for demonstrating the entrained-bed code were identified. A post-doctoral research associate was recruited to work on this subtask.

For Subtask 4.b., work continued on collecting fixed-bed design and test data from the open literature as well as by direct contact of the individuals and the organizations active in the field. No new data sets have been obtained. No new test cases were identified or simulated.

"MEASUREMENT AND MODELING OF COAL CONVERSION PROCESSES"

Contract No. DE-AC21-86MC23075

Table of Contents

SECTION I. INTRODUCTION

I.A. PROGRAM BACKGROUND AND DESCRIPTION

During the past 5 years, significant advances have been made at Brigham Young University (BYU) in comprehensive two-dimensional computer codes for mechanistic modeling of entrained-bed gasification and pulverized coal combustion. During the same time period, significant advances have been made at Advanced Fuel Research, Inc. (AFR) in the mechanisms and kinetics of coal pyrolysis and secondary reactions of pyrolysis products. This program presents a unique opportunity to merge the technology developed by each organization to provide detailed predictive capability for advanced coal conversion processes. This predictive capability will incorporate advanced coal characterization techniques in conjunction with comprehensive computer models to provide accurate process simulations.

The program will streamline submodels existing or under development for coal pyrolysis chemistry, volatile secondary reactions, tar formation, soot formation, char reactivity, and SO_x-NO_x pollutant formation. Submodels for coal viscosity, agglomeration, tar/char secondary reactions, sulfur capture, and ash physics and chemistry will be developed or adapted. The submodels will first be incorporated into the BYU entrained-bed gasification code and subsequently, into a fixed-bed gasification code (to be selected and adapted). These codes will be validated by comparison with small scale laboratory and PDU-scale experiments. The validated code could then be employed to simulate and to develop advanced coal conversion reactors of interest to METC.

I.B. OBJECTIVES

The objectives of this study are to establish the mechanisms and rates of basic steps in coal conversion processes, to integrate and incorporate this information into comprehensive computer models for coal conversion processes, to evaluate these models and to apply them to gasification, mild gasification and combustion in heat engines.

I.C. APPROACH

This program is a closely integrated, cooperative effort between AFR and BYU. The program consists of four tasks: 1) Preparation of Research Plans, 2) Submodel Development and Evaluation, 3) Comprehensive Model Development and Evaluation, and 4) Applications and Implementation.

I.D. CRITICAL TECHNICAL ISSUES

To achieve the goals of the program, the computer models must provide accurate and reliable descriptions of coal conversion processes. This will require the reduction of very complicated and interrelated physical and chemical phenomena to mathematical descriptions and, subsequently, to operational computer codes. To accomplish this objective, a number of technical issues must be addressed as noted below. The status of each of these tasks is also indicated.

A	Separation of Rates for Chemical Reaction, Heat Transfer, and Mass Transfer
A	Particle Temperature Measurements Using FT-IR E/T Spectroscopy
A	Functional Group Description of Coal, Char, and Tar
A	Tar Formation Mechanisms
I	Char Formation Mechanisms
A	Viscosity/Swelling
A	Intraparticle Transport
I	Pyrolysis of Volatiles and Soot Formation
I	Secondary Reaction of Tar
I	Particle Ignition
A	Char Reactivity
I	Ash Chemistry and Physics
A	Particle Optical Properties
I	Code Efficiency and Compatibility for Submodels
I	Coupling of Submodels with Comprehensive Codes
I	Comprehensive Code Efficiency
I	Turbulence

I SO_x and NO_x

I Generalized Fuels Model

I Fixed-Bed Model

(o) to be addressed; (I) initiated; (A) almost completed; (C) completed.

These technical issues are addressed in the three Tasks as described in Sections II-IV.

I.E. SEVENTEENTH QUARTER PROGRESS

Subtask 2.a. Coal to Char Chemistry Submodel Development and Evaluation

During the past quarter, most of the effort was on using the set of rank dependent kinetic parameters obtained from low heating rate experiments to predict high heating rate data from pyrolysis experiments in our Transparent Wall Reactor (TWR) and Heated Tube Reactor (HTR). We also did simulations of high heating rate pyrolysis data from the literature such as the heated grid experiments of Gibbins, the wire grid experiments of Fong and coworkers of MIT, and the TWR experiments of Fletcher at Sandia.

Some problems were obtained in predicting the changes in the tar yield and tar molecular weight distributions with heating rate for low rank coals using the current version of the model. In addition, we could not predict the extractables yields for the high heating rate data of Fong and coworkers on the Pittsburgh Seam coal with the current kinetic parameters. It was decided to re-examine the assumptions on the model input parameters, such as 1) the bridge breaking rate, 2) the crosslinking efficiencies, 3) the tar vaporization law, and 4) the ΔP parameter. It was found that a modest change in the activation energy for the bridge breaking rate (from 25 to 27 kcal/mole) allowed for good predictions of the Fong data. Changes in the crosslinking efficiencies were thoroughly evaluated and found to be largely unnecessary. A decision was made to use $10^{14} sec^{-1}$ for the bridge breaking pre-exponential and values of the crosslinking efficiencies = 1.

The effects of the tar vaporization law and the ΔP parameter were found to be very important. The change in the original vaporization law from the expression proposed by Suuberg to a factor of 10 higher was found to be mainly

responsible for the inability to predict the high heating rate Zap data. By changing to Suuberg X1, and allowing ΔP to be the sole adjustable parameter, the predictions are much better. A decision was initially made to use the law proposed by Fletcher, since it had been subjected to a rather thorough validation with model compounds. However, in the intermediate molecular weight range where the model is sensitive to the vaporization law, the two models are comparable. Therefore, either Fletcher or Suuberg X1 can be employed. The main unresolved question is the appropriate choice for ΔP and how this could be functionalized. It appears that the model predictions of the FIMS data are very sensitive to the choice of this parameter. At low heating rates, a choice of ΔP = 0 gives the best prediction of the tar yield. A choice of ΔP = 0.2 gives the best prediction of the tar MWD. Possible solutions would be to: 1) parameterize ΔP; 2) improve the description of the external transport of tar to resolve the problem of the higher molecular weight tars coming out earlier than expected.

Subtask 2.b. Fundamental High-Pressure Reaction Rate Data

During the last quarter, progress was made in increasing the signal-to-noise ratio of the optical particle imaging system so that small particles at low temperature can be measured. The modified reactor collection system was operated successfully under devolatilization conditions. The time required for size classification of pulverized coal was further reduced, the quality of the classification was improved, and sufficient quantities of narrow size ranges of three of the five test coals were produced for upcoming char preparation and oxidation tests. Under independent funding, coal devolatilization tests were successfully conducted using the modified reactor collection system. Computer software was written to support the data acquisition and heater control hardware that was previously interfaced to the reactor instrumentation and heaters, and was successfully used during the devolatilization tests.

Subtask 2.c. Secondary Reaction of Pyrolysis Products and Char Burnout

Discussions were held with BYU on the future direction of the work on modeling the tomography data from the TWR coal flame experiments. Some discrepancies exist in the measured and predicted particle temperatures which could result from problems with the measurements and/or the model. A rate limiting step in comparing the model with the data is the generation of suitable plots. A new approach which involves output of the predictions of the model into a spreadsheet format was agreed upon.

Subtask 2.d. Ash Physics and Chemistry Submodel

No work scheduled during the past quarter.

Subtask 2.e. Large Particle Submodels

The work on the modified AFR fixed-bed reactor (FBR) system continued. It includes two independently heated stages. The reactor system was assembled and tested and is now being used for lignin pyrolysis experiments under independent funding. It appears to work as planned. A redesign of the upper reactor chamber was required in order to eliminate a tar deposition problem. As expected, the quantitation of gas and tar is much better than in the old system and a wider range of sample sizes and flow rates can be used. Some problems were encountered with the software used to quantify the IR data, but these appear to have been resolved.

Subtask 2.f. Large Char Particle Oxidation at High Pressure

For this subtask, the decision was made previously to construct an experimental facility that would connect to the HPCP reactor of Subtask 2b. Of the two experimental approaches considered in the previous reports, the decision has been made to develop the "cantilever beam insert." In this approach the sample will be mounted horizontally to one or two of the optical access ports of the HPCP reactor. A summary of the design of this facility was prepared and sent to a few principal investigators active in fields of closely related research for their comments and criticisms. The suggestions received

have been included in the details for the design of this facility. Construction of this "cantilever beam insert" will start during this next quarter. Analytical procedures for monitoring rates of oxidation of large particles continue to be evaluated. Further data analysis of large particle oxidation in air in platinum crucibles shows a marked dependence of mass reactivity on the initial mass of the large particles. This is in contrast to a dependance on temperature, which was expected.

Subtask 2.g. SO_x-NO_x Submodel Development

During the past quarter, the method used to determine atomic oxygen concentrations in the NO_x submodel was revisited. Further insight into the best quasi-equilibrium expression to use for predicting atomic oxygen concentrations in lean, swirling-flow, natural gas flames was gained. Work continued on the integration and evaluation of a SO_x/sorbent reaction computerized submodel. This submodel has been integrated into PCGC-2 and is currently being evaluated. Experimental data are being sought to determine H_2S capture rates to use in an H_2S sulfation subroutine.

Subtask 3.a. Integration of Advanced Submodels into Entrained-Flow Code, with Evaluation and Documentation

Work continued on code evaluation and user-friendliness. Data from four reactors were identified for code evaluation. Simulations were performed for a natural gas flame in the BYU controlled-profile reactor and for the near-burner field of a full-scale industrial boiler. Two-dimensional combustor data were requested from Imperial College. The graphical user interface for editing input files was extended to particle combustion. Diagnostic messages were added to the code to help users detect errors in code input. A set of minimum specifications for a foundational, entrained-bed code that will satisfy the terms of the contract was identified. These specifications were documented in a letter to AFR and METC. Additional features that would enhance code performance were also identified. Two menu-driven post-processors were developed for converting PCGC-2 plotting files for gas and particle properties into a format that can be used by spreadsheet programs.

Subtask 3.b. Comprehensive Fixed-Bed Modeling Review, Development, Evaluation, and Implementation

During the last quarter, work continued on developing and evaluating the one-dimensional fixed-bed model. The model response to variations in operating conditions was validated by simulating several such test cases. Predicted temperature profiles were compared to measurements for the atmospheric, air-blown Wellman-Galusha gasifier fired with Elkhorn bituminous, Jetson bituminous, Leucite Hills subituminous, and Utah Blind Canyon bituminous coals. These test cases included temperature profiles at different operating conditions. Discussions with AFR, about the single particle FG-DVC submodel for integration into the fixed-bed code, continued. Development of the user's manual for the fixed bed code was initiated. The first draft of the manual was prepared. A progress report on fixed-bed model development was presented at the Peer Review Meeting in Pittsburgh and the Project Review Meeting in Morgantown. An article on fixed-bed model development was prepared and published in ACERC's Burning Issues.

Subtask 3.c. Generalized Fuels Feedstock Submodel

PCGC-2 was modified to allow sorbent injection in the primary stream.

Subtask 4.a. Application of Generalized Pulverized Coal Comprehensive Code

Potential application cases for demonstrating the entrained-bed code were identified. A post-doctoral research associate was recruited to work on this subtask.

Subtask 4.b. Application of Fixed-Bed Code

Work continued on collecting fixed-bed design and test data from the open literature as well as by direct contact of the individuals and the organizations active in the field. No new data sets have been obtained. No new test cases were identified or simulated.

SECTION II. TASK 2. SUBMODEL DEVELOPMENT AND EVALUATION

Objectives

The objectives of this task are to develop or adapt advanced physics and chemistry submodels for the reactions of coal in an entrained-bed and a fixed-bed reactor and to validate the submodels by comparison with laboratory scale experiments.

Task Outline

The development of advanced submodels for the entrained-bed and fixed-bed reactor models will be organized into the following categories: a) Coal Chemistry (including coal pyrolysis chemistry, char formation, particle mass transfer, particle thermal properties, and particle physical behavior); b) Char Reaction Chemistry at high pressure; c) Secondary Reactions of Pyrolysis Products (including gas-phase cracking, soot formation, ignition, char burnout, sulfur capture, and tar/gas reactions); d) Ash Physics and Chemistry (including mineral characterization, evolution of volatile, molten and dry particle components, and ash fusion behavior); e) Large Coal Particle Effects (including secondary reactions within the particle and in multiple particle layers; f) Large Char Particle Effects (including oxidation); g) SO_x-NO_x Submodel Development (including the evolution and oxidation of sulfur and nitrogen species); and h) SO_x and NO_x Model Evaluation.

II.A. SUBTASK 2.a. - COAL TO CHAR CHEMISTRY SUBMODEL DEVELOPMENT AND EVALUATION

Senior Investigators - David G. Hamblen and Michael A. Serio
Advanced Fuel Research, Inc.
87 Church Street, East Hartford, CT 06108
(203) 528-9806

Objective

The objective of this subtask is to develop and evaluate, by comparison with laboratory experiments, an integrated and compatible submodel to describe the organic chemistry and physical changes occurring during the transformation from coal to char in coal conversion processes.

Accomplishments

During the past quarter, most of the effort was on using the set of rank dependent kinetic parameters obtained from low heating rate experiments to predict high heating rate data from pyrolysis experiments in our Transparent Wall Reactor (TWR) and Heated Tube Reactor (HTR). We also did simulations of high heating rate pyrolysis data from the literature such as the heated grid experiments of Gibbins, the wire grid experiments of Fong and coworkers of MIT, and the TWR experiments of Fletcher at Sandia.

Some problems were obtained in predicting the changes in the tar yield and tar molecular weight distributions with heating rate for low rank coals using the current version of the model. In addition, we could not predict the extractables yields for the high heating rate data of Fong and coworkers on the Pittsburgh Seam coal with the current kinetic parameters. It was decided to re-examine the assumptions on the model input parameters, such as 1) the bridge breaking rate, 2) the crosslinking efficiencies, 3) the tar vaporization law, and 4) the ΔP parameter. It was found that a modest change in the activation energy for the bridge breaking rate (from 25 to 27 kcal/mole) allowed for good predictions of the Fong data. Changes in the crosslinking efficiencies were thoroughly evaluated and found to be largely unnecessary. A decision was made

to use $10^{14}sec^{-1}$ for the bridge breaking pre-exponential and values of the crosslinking efficiencies = 1. The final set of rank dependent parameters is summarized in Table II.A-1.

The effects of the tar vaporization law and the ΔP parameter were found to be very important. The change in the original vaporization law from the expression proposed by Suuberg to a factor of 10 higher was found to be mainly responsible for the inability to predict the high heating rate Zap data. By changing to Suuberg X1, and allowing ΔP to be the sole adjustable parameter, the predictions are much better. A decision was initially made to use the law proposed by Fletcher, since it had been subjected to a rather thorough validation with model compounds. However, in the intermediate molecular weight range where the model is sensitive to the vaporization law, the two models are comparable. Therefore, either Fletcher or Suuberg X1 can be employed. The main unresolved question is the appropriate choice for ΔP and how this could be functionalized. It appears that the model predictions of the FIMS data are very sensitive to the choice of this parameter. At low heating rates, a choice of ΔP = 0 gives the best prediction of the tar yield. A choice of ΔP = 0.2 gives the best prediction of the tar MWD. Possible solutions would be to: 1) parameterize ΔP; 2) improve the description of the external transport of tar to resolve the problem of the higher molecular weight tars coming out earlier than expected.

Work continued on testing the fluidity model in conjunction with the changes in the FG-DVC model discussed above. For certain coals, such as Illinois No. 6 and Pocahontas, it is difficult to provide very good fits to both the fluidity and pyrolysis data. We also do not predict the fluid behavior of low rank coals which soften when heated to very high heating rates. However, we have achieved excellent agreement with the majority of data obtained so far.

Work also continued on the swelling model. The changes in the FG-DVC model discussed above result in better predictions of the Free Swelling Index (FSI) for the majority of coals. There are still problems in fitting the FSI for the Pocahontas coal, which has a high FSI and a low Geissler fluidity.

TABLE II-A-1 - RANK DEPENDENT KINETIC PARAMETERS FOR ARGONNE PREMIUM COALS

KINETIC PARAMETERS		ZAP	WYO	ILL	UTAH	LS	PIT	UPF	POC
Bridge Breaking	A	1.0×10^{14}	1.0×10^{14}	1.0×10^{14}	1.0×10^{14}	1.0×10^{14}	1.0×10^{14}	1.0×10^{14}	1.0×10^{14}
	E/R	26,000	26,000	26,000	27,000	27,250	27,500	28,250	29,500
	σ/R	1,000	1,000	1,000	1,250	1,000	1,250	1,250	750
CH_4 Loose	A	3.0×10^{13}	3.0×10^{13}	3.0×10^{13}	3.0×10^{13}	3.0×10^{13}	3.0×10^{13}	3.0×10^{13}	3.0×10^{13}
	E/R	28,000	28,000	28,000	28,000	28,000	28,000	28,750	29,500
	σ/R	2,500	2,250	1,800	1,500	1,200	1,300	800	750
	wt.%	1.04	1.26	1.63	1.64	1.49	1.80	1.92	1.59
CH_4 Tight	A	6.0×10^{13}	6.0×10^{13}	6.0×10^{13}	6.0×10^{13}	6.0×10^{13}	6.0×10^{13}	6.0×10^{13}	6.0×10^{13}
	E/R	32,000	32,000	32,000	32,000	32,000	32,000	32,000	33,000
	σ/R	2,200	2,000	2,200	2,200	2,200	2,200	2,000	1,700
	wt.%	0.56	0.84	2.17	2.56	3.02	3.20	3.73	2.71
CO_2 X-Loose	A	5.0×10^{12}	5.0×10^{12}	5.0×10^{12}	5.0×10^{12}	5.0×10^{12}	5.0×10^{12}	5.0×10^{12}	5.0×10^{12}
	E/R	18,000	18,000	20,500	21,000	21,250	21,500	22,000	23,000
	σ/R	1,500	1,500	3,000	4,000	3,500	3,600	2,000	2,500
	wt.%	0.74	0.54	0.12	0.10	0.08	0.10	0.05	0.06
CO_2 Loose	A	5.0×10^{12}	5.0×10^{12}	5.0×10^{12}	5.0×10^{12}	5.0×10^{12}	5.0×10^{12}	5.0×10^{12}	5.0×10^{12}
	E/R	23,500	24,000	24,750	25,000	26,000	26,500	27,000	28,000
	σ/R	2,000	2,500	1,750	1,250	3,000	3,000	3,000	2,500
	wt.%	3.35	3.29	0.35	0.29	0.19	0.25	0.14	0.08
CO_2 Tight	A	7.5×10^{12}	7.5×10^{12}	7.5×10^{12}	7.5×10^{12}	7.5×10^{12}	7.5×10^{12}	7.5×10^{12}	7.5×10^{12}
	E/R	31,000	32,000	32,000	32,000	32,000	32,000	32,000	33,500
	σ/R	3,000	2,800	2,750	5,000	3,200	2,500	2,500	2,700
	wt.%	2.11	1.57	0.53	1.22	0.73	0.65	0.31	0.46
H_2O Loose	A	5.0×10^{12}	5.0×10^{12}	5.0×10^{12}	5.0×10^{12}	5.0×10^{12}	5.0×10^{12}	5.0×10^{12}	5.0×10^{12}
	E/R	16,000	16,000	25,000	25,000	25,500	26,000	27,500	28,000
	σ/R	1,500	1,500	1,000	1,250	1,250	1,250	1,250	1,250
	wt.%	0.64	0.47	1.46	3.11	2.63	2.30	1.60	0.51
H_2O Tight	A	2.0×10^{14}	2.0×10^{14}	2.0×10^{14}	2.0×10^{14}	2.0×10^{14}	2.0×10^{14}	2.0×10^{14}	2.0×10^{14}
	E/R	28,500	28,500	32,000	32,000	32,000	32,000	34,000	35,000
	σ/R	4,750	3,500	5,000	2,500	2,500	2,500	3,600	3,000
	wt.%	12.13	8.89	9.79	5.08	4.88	4.28	3.73	0.96
CO Loose	A	5.0×10^{12}	5.0×10^{12}	5.0×10^{12}	5.0×10^{12}	5.0×10^{12}	5.0×10^{12}	5.0×10^{12}	5.0×10^{12}
	E/R	24,500	24,750	25,000	25,000	25,500	26,000	28,000	29,000
	σ/R	3,000	2,500	1,000	1,250	1,100	1,250	750	1,250
	wt.%	1.80	1.70	0.30	0.40	0.20	0.25	0.20	0.15
CO Tight	A	5.0×10^{12}	5.0×10^{12}	5.0×10^{12}	5.0×10^{12}	5.0×10^{12}	5.0×10^{12}	5.0×10^{12}	5.0×10^{12}
	E/R	30,000	30,250	30,500	30,500	30,500	30,750	31,500	32,000
	σ/R	3,000	3,000	2,000	2,000	1,600	1,900	1,400	1,500
	wt.%	2.82	3.54	1.69	2.32	1.36	1.51	0.74	0.15
CO X-Tight	A	2.0×10^{14}	2.0×10^{14}	2.0×10^{14}	2.0×10^{14}	2.0×10^{14}	2.0×10^{14}	2.0×10^{14}	2.0×10^{14}
	E/R	39,000	39,750	40,000	40,000	40,000	40,000	40,000	40,000
	σ/R	2,500	2,500	3,000	2,500	3,000	2,800	2,250	3,200
	wt.%	5.25	5.00	3.20	2.80	3.00	2.30	1.37	1.90

Some work was done on incorporating the redistribution of functional groups into the FG-DVC model. The current assumption is that the breaking of two ethylene bridges creates two methyl groups. However, this leads to an overprediction of the amount of methyls, especially in the case of low rank coals.

The current state of the FG-DVC model was summarized in a paper titled "Can Coal Science be Predictive?" which is included as Appendix A. The paper was originally prepared by Peter Solomon for his keynote address at the 1990 Australian Coal Science Conference (delivered in 12/90). It was revised for his Storch Award lecture (tc be delivered in 4/91) and that version is included in Appendix A.

Plans

Complete work on the fluidity model. Resume work on the swelling model and the optical properties model. Initiate work on studying the evolution of sulfur and nitrogen species. Complete work on definition of submodel for char reactivity.

II.B. SUBTASK 2.B. - FUNDAMENTAL HIGH-PRESSURE REACTION RATE DATA

Senior Investigators - Geoffrey J. Germane and Angus U. Blackham
Brigham Young University
Provo, Utah 84602
(801) 378-2355 and 6536

Student Research Assistants - Charles R. Monson, Gary Pehrson,
David Wheeler, and James Rigby

Objective

The overall objective of this subtask is to measure and correlate reaction rate coefficients for pulverized-coal char particles as a function of char burnout in oxygen at high temperature and pressure.

Accomplishments

Three components of the subtask have been identified to accomplish the objectives outlined above: 1) develop the laminar-flow, high-pressure, controlled-profile (HPCP) reactor, 2) prepare char at high temperature and pressure, and 3) determine the kinetics of char-oxygen reactions at high pressure. The HPCP reactor, capable of functioning at 400 psi (27 atmospheres), has been constructed to perform the fundamental reaction rate measurements required for the study. Data from another char oxidation study (atmospheric pressure) conducted at Brigham Young University will also be used.

Work continued during the last quarter on development of the optical particle imaging system and the reactor collection system. In additionΦ, progress was made in preparing coal samples with the proper size classification for the upcoming char preparation and reaction rate tests.

High Pressure Reactor Development and Characterization

Work during the reporting period focused mainly on automating the facility for the reactivity tests, and assembly of the optical instrument. Computer software was written to support the data acquisition and heater control hardware that was previously interfaced to the reactor instrumentation and heaters. This software was successfully used during the reporting period for devolatilization tests. The program allows the microcomputer to record and provide readout of reactor temperatures, pressure, and gas flow rates. Algorithms operate in real time to convert sensor signals into engineering units and display them on the monitor. These data along with information concerning heater controllers, reactor configuration, coal/char type and size, particle feedrate, and oxidizer concentration is written to a file every minute during a test to provide a detailed record.

The program also provides control of the reactor heaters. After the user inputs a desired zone temperature, the heater controller setting is determined by the microcomputer using temperature measurements from the heat zone and a proportional/integral control scheme. The microcomputer then sends the proper control signal to the controller through a 4 - 20 mA current loop. The four heat zones are controlled concurrently. In addition to maintaining the desired reactor temperature, the control algorithm checks for suspect thermocouple measurements, ensures that the heaters stay below their maximum allowable temperature and controls the rate of temperature change to prevent breakage of ceramics in the reactor because of thermal shock. The control system reduces temperature deviation during a test and improves repeatability of reactor conditions for duplicate tests. The ease of reactor operation is also increased.

It has become apparent during testing that the preheater capacity was too low to provide high secondary gas temperatures with the 5.1 cm ID reaction tube at conditions of high pressure and short residence time. Modifications are being made to the preheater to improve its capacity. The preheater heating element will be surrounded by a 12.7 cm ID alumina tube. The secondary gas will flow through a bed of alumina pieces that will fill the void between the alumina tube and the preheater insulation. The large

increase in available heat transfer area in the bed will significantly improve the capacity of the preheater. The situation will also be improved through the use of a smaller reaction tube. The required gas flow rate and preheater capacity will be reduced by 86% when using a 1.9 cm ID reaction tube. High temperature ceramic fixtures are being designed to properly locate the small reaction tube within the large tube.

Under separate funding, the gas mixing station is being assembled. The station will consist of the hardware necessary to meter and mix two gas flows. Nitrogen and air will be mixed during char oxidation experiments to provide the desired oxygen concentration for the primary and secondary gas flows. All components of the system have been received and assembly is in progress.

Optical Instrumentation - The optical instrument is patterned after a system developed at Sandia National Laboratories for *in situ* measurement of single particle temperature, velocity and diameter (Tichenor *et al.*, 1984). This system obtains temperature measurements by two-color pyrometry and particle velocity and diameter measurements through the use of an image-plane, coded-aperture technique. A description of the instrument and its operation was given in the 15th Quarterly Report. Implementation of the optical instrument to accurately determine particle temperature history during char oxidation experiments will improve the accuracy of the reaction rate parameter determination.

A great deal of work has been carried out in cooperation with a separate, independently-funded research group at the Brigham Young University Combustion Laboratory that is developing a particle imaging and temperature measuring instrument nearly identical to the one under development for this project. During the reporting period, most of this joint effort has centered on the photomultiplier tube (PMT) signal conditioning. In its original configuration the dynamic response of the PMT signal was too slow to allow particle size measurements. A number of amplifiers and configurations have been tried in an effort to improve the signal. Circuits that provide current-to-voltage conversion and preamplification of the PMT output have been developed that provide sufficient dynamic response and signal level. Work is ongoing to increase the signal-to-noise ratio through filtering, thereby

improving particle size measurements and extending the detection limit to smaller, lower temperature particles, which will be important for both char oxidation and coal devolatilization studies.

The final obstacle to be overcome with the optical system is proper operation of the laser trigger. A large fraction of the laser radiation scattered from a particle is lost as the light passes through the lenses, coded aperture, and especially the beamsplitter of the system. Sufficient light is not available at the laser detector to discriminate between a particle and noise. It appears that the laser beam will need to be focused from its 800 mm waist diameter to 100 mm diameter at the optical control volume in order to increase the intensity of scattered light. A prism may also be used to redirect the scattered light to the laser detector, bypassing the beamsplitter. Simple signal conditioning of the laser detector output will also be required.

Tar/Char/Gas Collection System - The modifications to the collection and separation system, involving a quenched and sintered stainless steel tube which extends from the entrance of the collection probe to the virtual impactor nozzle, were completed under independent funding. Coal devolatilization tests in the HPCP were successfully conducted by researchers from two separate independent projects, in which the collection system performed properly.

Char Preparation at High Temperature and High Pressure

During the reporting period, efforts continued to decrease the particle size range of the fractions of the selected coals and to produce sufficient coal in the desired size ranges for the char oxidation tests. Presently, Utah Blind Canyon bituminous coal, North Dakota lignite and Pittsburgh No. 8 bituminous coal have been sized and stored in sufficient quantities for the test program.

A sample of Utah bituminous coal was studied with a scanning electron microscope to assess the size distribution of the coal particles. The coal had been sieved to a range of 64-75 μm but there was some uncertainty whether

any fine particles (<10 μm) had adhered to the larger coal particles of the desired range. The scanning electron micrographs (SEM) in Figures II.B-1 and 2 show a range of particle size from about 60-80 μm. There are so few smaller particles that their possible effect on devolatilization and subsequent oxidation is considered to be insignificant. Also, there don't appear to be any fine particles attached to larger coal particles.

Kinetics of Char-Oxygen Reactions at High Pressure

While the literature review continues, no results in this area were obtained during the reporting period since the optical particle temperature and imaging system is not yet operable.

Plans

Modifications to the preheater will be made to increase heat transfer to the primary air and the gas mixing station will be completed and placed into service. Final alignment of the optical instrument will be completed and signal conditioning for the PMT outputs will be improved to provide stronger, noise free signals. Modifications will be made to the laser trigger to provide proper operation. The instrument will also be completely enclosed in a light-tight cover that will attach to the HPCP reactor. Since any stray light introduced into the optical system drastically increases noise, this will improve the instrument accuracy and allow operation of the system with the room lights on.

Work will continue to carefully size coal particles prior to char preparation and oxidation. An experimental plan for char oxidation will be finalized using a predictive reaction code to suggest test conditions. It is hoped that the optical system will be completed so that char preparation and oxidation for some of the test coals can be initiated under carefully controlled conditions in the HPCP reactor.

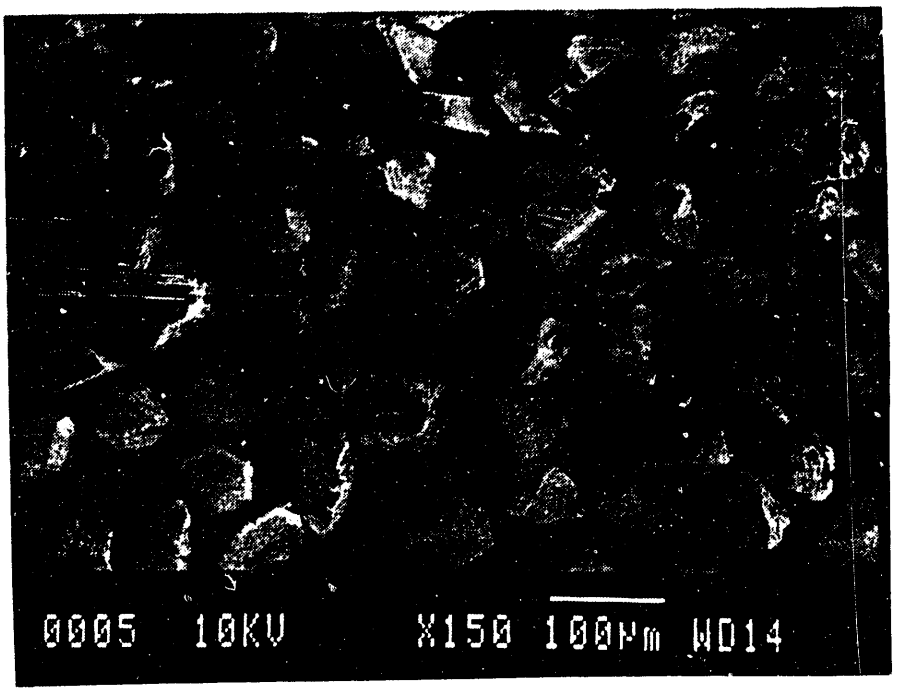

Figure II.B-1. Scanning electron micrograph of Utah Blind Canyon bituminous coal sieved to 64 - 75 μm.

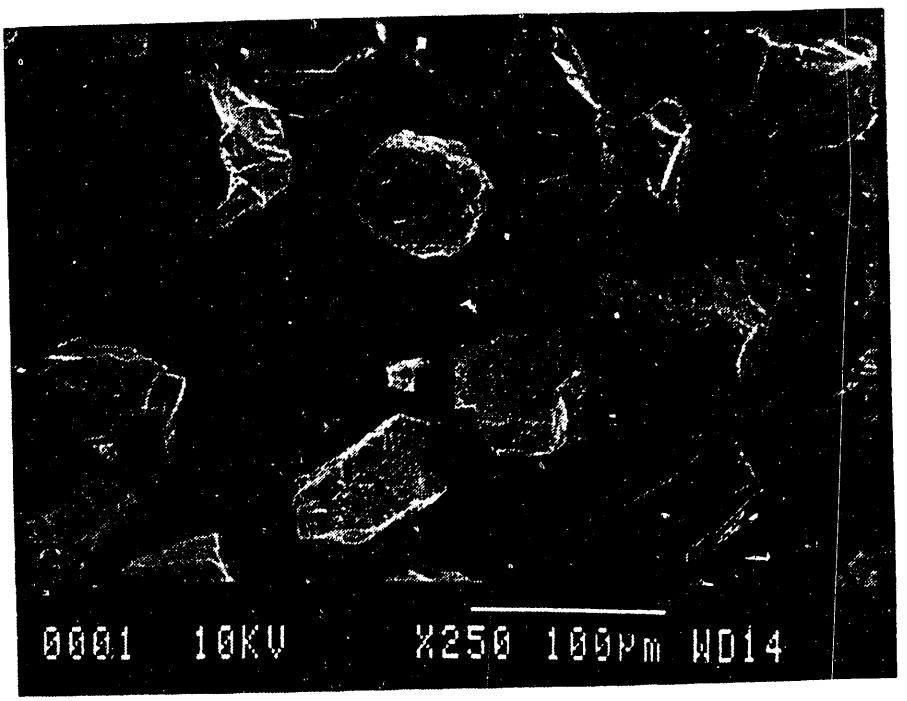

Figure II.B-2. Scanning electron micrograph of sieved 64 - 75 μm Utah Blind Canyon bituminous coal showing the extent of very small interspersed particles.

II.C. SUBTASK 2.c. - SECONDARY REACTION OF PYROLYSIS PRODUCTS AND CHAR BURNOUT

SUBMODEL DEVELOPMENT AND EVALUATION

Senior Investigator - James R. Markham and Michael A. Serio
Advanced Fuel Research, Inc.
87 Church Street, East Hartford, CT 06108
(203) 528-9806

Objective

The objective of this subtask is to develop and evaluate by comparison with laboratory experiments, an integrated and compatible submodel to describe the secondary reactions of volatile pyrolysis products and char burnout during coal conversion processes. Experiments on tar cracking, soot formation, tar/gas reactions, char burnout, and ignition will continue during Phase II to allow validation of submodels.

Accomplishments

Discussions were held with BYU on the future direction of the work on modeling the tomography data from the TWR coal flame experiments. Some discrepancies exist in the measured and predicted particle temperatures which could result from problems with the measurements and/or the model. A rate limiting step in comparing the model with the data is the generation of suitable plots. A new approach which involves output of the predictions of the model into a spreadsheet format was agreed upon.

Plans

Continue work with BYU on modeling the TWR coal flame experiments. Define submodels for ignition and soot formation.

II.D. SUBTASK 2.d. - ASH PHYSICS AND CHEMISTRY SUBMODEL

Senior Investigator - James Markham
Advanced Fuel Research, Inc.
87 Church Street, East Hartford, CT 06108
(203) 528-9806

Objective

The objective of this task is to develop and validate, by comparison with laboratory experiments, an integrated and compatible submodel to describe the ash physics and chemistry during coal conversion processes. AFR will provide the submodel to BYU together with assistance for its implementation into the BYU PCGC-2 comprehensive code.

To accomplish the overall objective, the following specific objectives are: 1) to develop an understanding of the mineral matter phase transformations during ashing and slagging in coal conversion; 2) To investigate the catalytic effect of mineral matter on coal conversion processes. Data acquisition will be focused on: 1) design and implementation of an ash sample collection system; 2) developing methods for mineral characterization in ash particles; 3) developing methods for studying the catalytic effects of minerals on coal gasification.

Accomplishments

No work scheduled during the past quarter.

Plans

Complete definition of submodel for ash chemistry and physics.

II.E. SUBTASK 2.e. - LARGE PARTICLE/THICK BED SUBMODELS

Senior Investigator - Michael A. Serio
Advanced Fuel Research, Inc.
87 Church Street
East Hartford, CT 06108
(203) 528-9806

Objective

The objectives of this task are to develop or adapt advanced physics and chemistry submodels for the reactions of "large" coal particles (i.e., particles with significant heat and/or mass transport limitations) as well as thick beds (multiple particle layers) and to validate the submodels by comparison with laboratory scale experiments. The result will be coal chemistry and physics submodels which can be integrated into the fixed-bed (or moving-bed) gasifier code to be developed by BYU in Subtask 3.b. Consequently, this task will be closely coordinated with Subtask 3.b.

Accomplishments

The work on the modified AFR fixed-bed reactor (FBR) system continued. It includes two independently heated stages. The reactor system was assembled and tested and is now being used for lignin pyrolysis experiments under independent funding. It appears to work as planned. A redesign of the upper reactor chamber was required in order to eliminate a tar deposition problem. As expected, the quantitation of gas and tar is much better than in the old system and a wider range of sample sizes and flow rates can be used. Some problems were encountered with the software used to quantify the IR data, but these appear to have been resolved.

Plans

Complete testing of new fixed-bed reactor system. Complete initial set of experiments on secondary reaction effects in thick beds. Continue development of single particle model with BYU. Begin work on tar repolymerization model.

II.F. SUBTASK 2.F. - LARGE PARTICLE OXIDATION AT HIGH PRESSURES

Senior Investigators: Angus U. Blackham and Geoffrey J. Germane
Brigham Young University
Provo, Utah 84602
(801) 378-2355 and 6536

Student Research Assistants: Ken Bateman, Gary Pehrson and Wade Riser

Objectives

The overall objective for this subtask is to provide data for the reaction rates of large char particles of interest to fixed-bed coal gasification systems operating at pressure. The specific objectives for this quarter included:

1. Review appropriate literature.
2. Select the experimental approach.
3. Design the apparatus to use in conjunction with the HPCP reactor of Subtask 2b.
4. Request support information concerning the proposed "cantilever beam insert."
5. Continue evaluation of analytical procedures for monitoring the kinetics of oxidation of large particles.
6. Conduct additional preliminary oxidation experiments.

Accomplishments

Two components of this subtask to accomplish the overall objective have been suggested in the plans outlined earlier: 1) high-pressure, large-particle reactor design, fabrication and preliminary data; 2) experimental reaction rate data for chars from five coals. The general features of the experimental unit will be a "large particle insert" to be connected to the HPCP facility of Subtask 2b. The "large particle insert" will consist of: (a) the reactor tube, (b) the balance unit, and (c) the connecting channel. Of the two experimental approaches considered in previous reports, the decision has been made to develop the "cantilever beam insert." In this

approach, the sample will be mounted horizontally from a force transducer connected to one or two of the optical access ports of the HPCP reactor.

In this quarter, a summary of the design of the "cantilever beam insert" was prepared and sent to a few principal investigators active in fields of closely related research for their comments and criticisms. Some responses have been received and evaluated. These suggestions have expanded the basis on which the design details of the cantilever beam insert are now progressing.

A few additional experimental exercises with the load cell have given additional information on the properties of the load cell. Because of a change in personnel on this subtask the evaluation of the CO/CO_2 chromatographic column has not yet been completed. The report of this evaluation will be included in the next quarterly report. The air oxidation of sets of large coal particles in platinum crucibles is continuing. The variables in these preliminary studies are coal type, size and temperature. These results will be compared with the results of the preliminary oxidation of the Utah bituminous coal reported previously in the 4th Annual Report (Solomon, 1990).

High-Pressure, Large-Particle Reactor Design

Experimental Approach - Reactor Design - After the decision was made to develop the "cantilever beam insert," a summary of the features of this proposed experimental facility was prepared and given to a few principal investigators active in fields of research closely related to our project of large coal particle oxidation with a request for their suggestions concerning the design features. This five page "Request for Informal Design Review" is included in the appendix of this quarterly report. The responses received have been reviewed and evaluated. Some design features have been added or modified as a result of these responses. The general design, however, has remained unchanged, and the detailed drawings for the "cantilever beam insert" are being prepared. Construction of the facility will start in this next quarter.

Experimental Approach - Force Transducer - During this quarter, a few additional tests were made with the load cell (force transducer) to determine its properties. Measurements of maximum load, stability, and sensitivity were made as a function of lever-arm length. Lever-arms of 10, 15 and 20 cm were studied. The maximum loads measured were 25, 22 and 19 g, respectively. The drift of the transducer was a maximum at 10 mg/hr showing good stability at maximum loads. The sensitivity is still ~3 mg per division at each length. Improving this sensitivity to 1 mg per division in still considered possible as further testing and adjusting of the amplifier-indicator is accomplished.

Experimental Reaction Rate Data

Preliminary Large Particle Oxidation Measurements - For the principal purpose of providing experience in experimental procedures associated with large coal particles, a series of sets of large particles of a Utah bituminous coal have been devolatilized and oxidized in platinum crucibles. A lump of coal was crushed to provide some particles with dimensions about 0.5-1.0 cm on a side. The first set (six particles) was heated with Mekker burners. The results were given in the 14th Quarterly Report (Solomon et al., 1990). A second set (six particles) was heated in a muffle furnace and reported in the 15th Quarterly Report (Solomon, 1990). Four sets of samples (four particles in each set) were heated at different temperatures in the muffle furnace. The results were reported in the 4th Annual Report (Solomon et al., 1990).

An additional study of the data of these last four sets has been made, resulting in a correlation not noted in the earlier reports. Graphs of each of the four sets of data have been prepared with the log of the normalized mass remaining for each particle plotted against the time of oxidation. The slope of each curve therefore is an indication of mass reactivity. The average mass reactivities for the sixteen particles reported in Table II.F - 2 of the 4th Annual Report are included in Figures II.F-1, 2, 3, and 4 along with the initial mass of each large particle. Our expectation was that average mass reactivity would correlate with temperature of oxidation. There was a slight indication of this because the highest observed mass reactivity was at the highest oxidation temperature (0.112 min^{-1} at 1420-1470 K). However the spread of reactivities of the four particles in this temperature

Experimental Approach - Force Transducer - During this quarter, a few additional tests were made with the load cell (force transducer) to determine its properties. Measurements of maximum load, stability, and sensitivity were made as a function of lever-arm length. Lever-arms of 10, 15 and 20 cm were studied. The maximum loads measured were 25, 22 and 19 g. respectively. The drift of the transducer was a maximum at 10 mg/hr showing good stability at maximum loads. The sensitivity is still ~3 mg per division at each length. Improving this sensitivity to 1 mg per division in still considered possible as further testing and adjusting of the amplifier-indicator is accomplished.

Experimental Reaction Rate Data

Preliminary Large Particle Oxidation Measurements - For the principal purpose of providing experience in experimental procedures associated with large coal particles, a series of sets of large particles of a Utah bituminous coal have been devolatilized and oxidized in platinum crucibles. A lump of coal was crushed to provide some particles with dimensions about 0.5-1.0 cm on a side. The first set (six particles) was heated with Mekker burners. The results were given in the 14th Quarterly Report (Solomon et al., 1990). A second set (six particles) was heated in a muffle furnace and reported in the 15th Quarterly Report (Solomon, 1990). Four sets of samples (four particles in each set) were heated at different temperatures in the muffle furnace. The results were reported in the 4th Annual Report (Solomon et al., 1990).

An additional study of the data of these last four sets has been made, resulting in a correlation not noted in the earlier reports. Graphs of each of the four sets of data have been prepared with the log of the normalized mass remaining for each particle plotted against the time of oxidation. The slope of each curve therefore is an indication of mass reactivity. The average mass reactivities for the sixteen particles reported in Table II.F - 2 of the 4th Annual Report are included in Figures II.F-1, 2, 3, and 4 along with the initial mass of each large particle. Our expectation was that average mass reactivity would correlate with temperature of oxidation. There was a slight indication of this because the highest observed mass reactivity was at the highest oxidation temperature (0.112 min-1 at 1420-1470 K). However the spread of reactivities

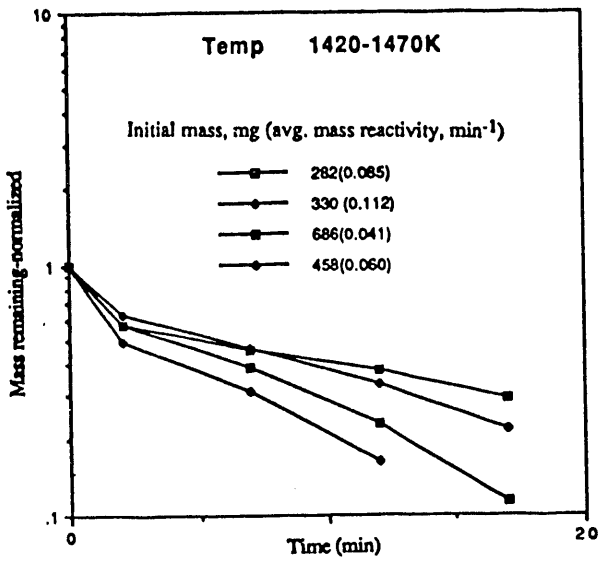

Figure II.F-1. Mass of large coal particles remaining (normalized) as a function of reaction time at 1420 - 1470 K.

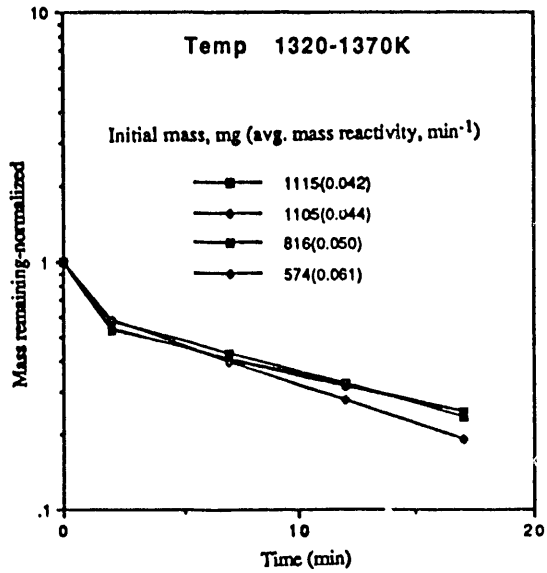

Figure II. F-3. Mass remaining (normalized as a function of reaction time at 1320 - 1370 K.

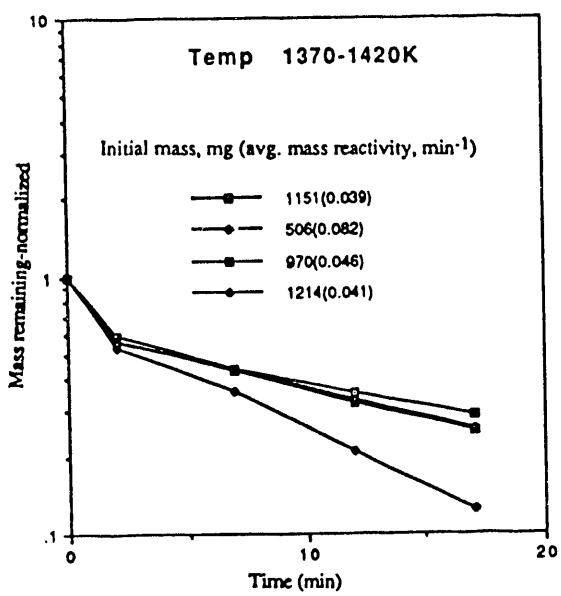

Figure II.F-2. Mass remaining (normalized) as a function of reaction time at 1370 - 1420 K.

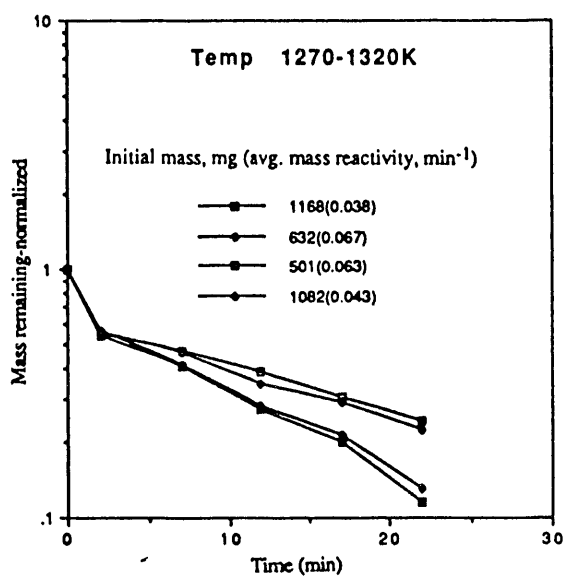

Figure II. F-4. Mass remaining (normalized) as a function of reaction time at 1270 - 1320 K.

range was quite broad (0.041 to 0.112 min^{-1}) and appeared to be a function of the initial particle mass. When the average mass reactivity for all sixteen particles was plotted against initial particle mass, the correlation presented in Figure II.F-5 was obtained. All four temperature ranges are represented in the cluster of points for initial masses greater than 1 gram. Therefore, in the overall temperature range for these oxidations, mass reactivity does not appear to change significantly with temperature but decreases with increasing particle mass. This observation suggests that the factor of most influence under these conditions is the movement of gas through the developing ash residue for this range of temperatures (1270-1470K).

This preliminary conclusion, along with those suggested in the previous reports, indicates that further experiments of this preliminary nature with platinum curcibles at atmospheric pressure will help in determining the issues that need to be considered as plans are being made for measurements at high pressure in the facility to be constructed for this subtask. Accordingly, experiments are currently in progress in which the variables are coal type, size and temperature.

Plans

During the next quarter, construction of the "cantilever beam insert" will start. The study of the load cell will continue as it is incorporated into the balance unit. Evaluation of the CO/CO_2 gas chromatographic column will be completed. Additional preliminary experiments will be completed and compared with those discussed here and in previous reports.

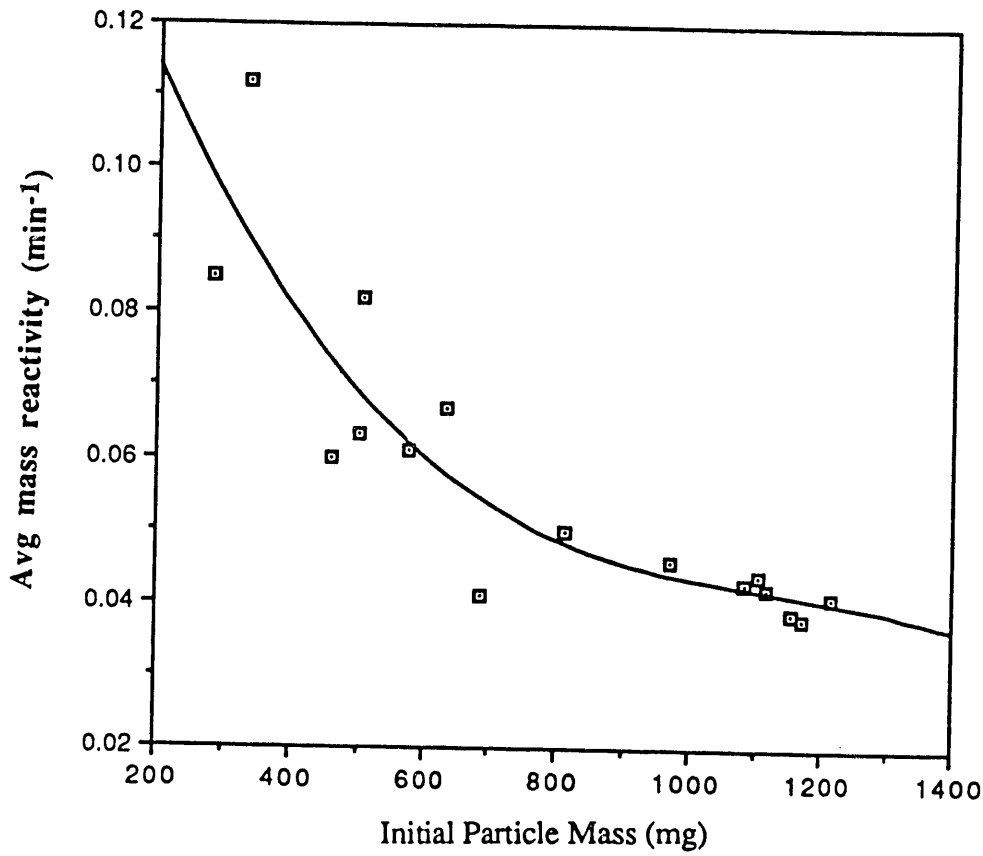

Figure II. F-5. Effect of initial particle mass on average mass reactivity for various temperatures from 1270 - 1470 K.

II.G. SUBTASK 2.G. - SO_x/NO_x SUBMODEL DEVELOPMENT

Senior Investigators: L. Douglas Smoot and B. Scott Brewster
Brigham Young University
Provo, Utah 84602
(801) 378-4326 and (801) 378-6240

Research Assistant: Richard D. Boardman

Objectives

The objectives of this subtask are 1) to extend an existing pollutant submodel in PCGC-2 for predicting NO_x formation and destruction to include thermal NO, 2) to extend the submodel to include SO_x reactions and SO_x-sorbent reactions (effects of SO_3 nonequilibrium in the gas phase will be considered), and 3) to consider the effects of fuel-rich conditions and high-pressure on sulfur and nitrogen chemistry in pulverized-fuel systems.

Accomplishments

The task of extending the NO_x submodel to include thermal NO has been completed. The fuel-NO mechanism was also generalized to test alternative global rate expressions, including NH_3 as an intermediate species. An evaluation of the NO_x submodel was completed and reported in the 4th Annual Report (Solomon et al., 1990). During the past quarter, the method used to determine atomic oxygen concentrations was revisited. Further insight into the best quasi-equilibrium expression to use for predicting atomic oxygen concentrations in lean, swirling-flow, natural gas flames was gained.

Work has continued on the development and evaluation of a SO_x/sorbent reaction computerized submodel. The framework for this submodel was presented and briefly discussed in the 4th Annual Report (Solomon et al., 1990). This code has been integrated into PCGC-2 and is currently being evaluated. Several simplifications are made in this "first-generation" model which may

not be valid for all reactor conditions. The complexity of the model can be increased after demonstration of a suitable sulfur capture model.

In the current quarterly report, the theory of the SO_x submodel is further discussed. A preliminary prediction that was completed is discussed. Work is continuing to verify that the model predicts correct results, prior to a more extensive evaluation of the model.

NO_x Submodel Development

Investigation of the expression used to estimate atomic oxygen concentrations was further explored using the NO formation rate expression derived from the Zel'dovich thermal-NO mechanism (Westenberg, 1971):

$$\frac{d[NO]}{dt} = 2k_{A6}[O][N_2] \quad \text{gmole cm}^{-3}\,\text{s}^{-1} \qquad \text{(II.G-1)}$$

This expression is obtained by assuming the reverse Zel'dovich mechanism steps are negligible and that OH concentrations are small.

Two quasi-equilibrium expressions are often used to estimate O concentrations. Oxygen equilibrium (Eq. II.G-2) has been recommended for fuel-lean zones in the combustor while carbon equilibrium (Eq. II.G-3) has been suggested for fuel-rich regions where primary fuel oxidation occurs.

$$[O] = \left\{K'_{eq}[O_2]\right\}^{1/2} \qquad \text{(II.G-2)}$$

$$[O] = K'_{eq}\frac{[O_2][CO]}{[CO_2]} \qquad \text{(II.G-3)}$$

The sensitivity of the NO model to these expressions was examined to determine if either or both expressions should be used to predict atomic oxygen concentrations. Figure II.G-1 compares the predicted NO concentrations with the experimental values measured in the ACERC controlled-profile reactor (with independent funding) over a narrow range of overall fuel-to-oxidizer equivalence ratios with an experimental secondary-air swirl number of 1.5. Separate NO model predictions were made using either oxygen equilibrium or carbon equilibrium at every computational node in the reactor to predict

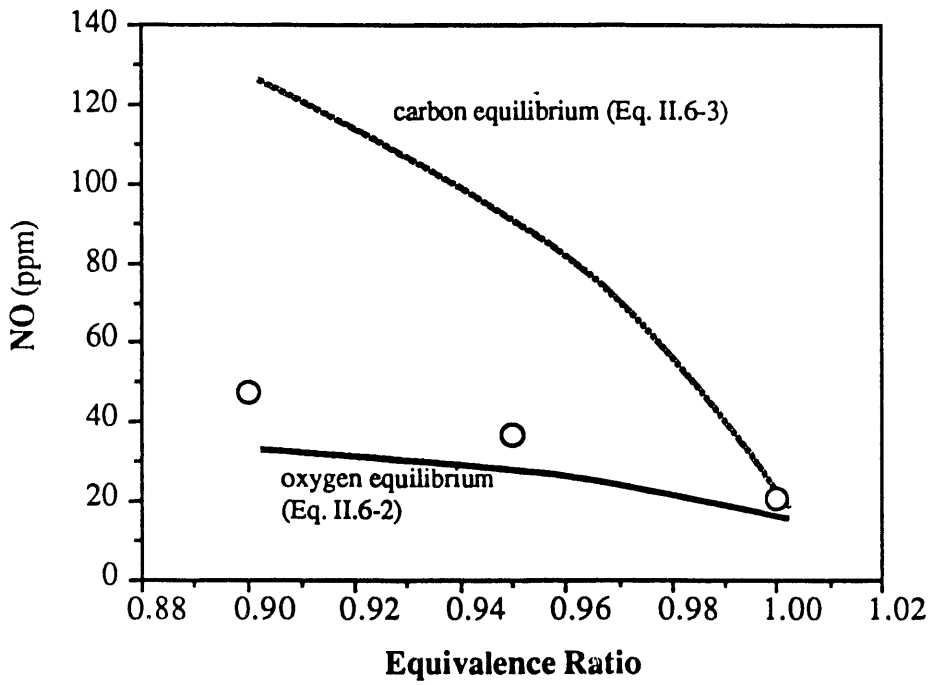

Figure II. G-1. Comparison of prediction methods used to estimate atomic oxygen concentrations with measured data (circles) for natural gas combustion in the ACERC controlled-profile reactor: Secondary swirl no. - 1.5; heating rate = 147 kW.

atomic oxygen concentrations. The upper theoretical curve shows that thermal NO concentrations are overpredicted at lower equivalence ratios (fuel-lean conditions) when carbon equilibrium is assumed. When oxygen equilibrium is assumed, predicted NO concentrations are lower than the measured data. Predictions were not made for higher equivalence ratios for which the importance of carbon equilibrium may lead to better prediction of atomic oxygen concentrations. The results in this study are thus limited, but hopefully provide guidance for using the NO model for practical burner conditions, which are normally fuel-lean to achieve complete combustion.

SO_x-Sorbent Particle Reaction Submodel

Submodel Description - Implementation of a SO_x/sorbent-reactions submodel into PCGC-2 is broken down into three components: 1) describing the simultaneous conversion of coal sulfur to gaseous species, 2) tracking the injected sorbents while accounting for simultaneous calcination, sintering, and sulfation, and 3) predicting simultaneous capture of sulfur species (usually H_2S and SO_2) by the sorbent particles. The approach taken to develop a SO_x/sorbent-reactions predictive model is to simplify the description of these three components as much as possible in order to first demonstrate the feasibility of predicting sorbent capture with a submodel of PCGC-2. Then, after an evaluation of the "first-generation" model is completed, assumptions can be relaxed as warranted by the verification procedure and other experimental evidence.

In the 4th Annual Report (Solomon et al., 1990), a brief discussion of the SO_x/sorbent-reactions submodel foundation was given. Figure II.G-2 illustrates the solution algorithm for the SO_x/sorbent-reactions submodel which is called after converging PCGC-2. As individual particle trajectories are integrated, the capture of SO_2 and H_2S is calculated at each time step by the shrinking-core grain model of Silcox (1985). Figure II.G-3 shows the individual steps contained in the sulfation submodel using the set of equations listed in Table II-G-1.

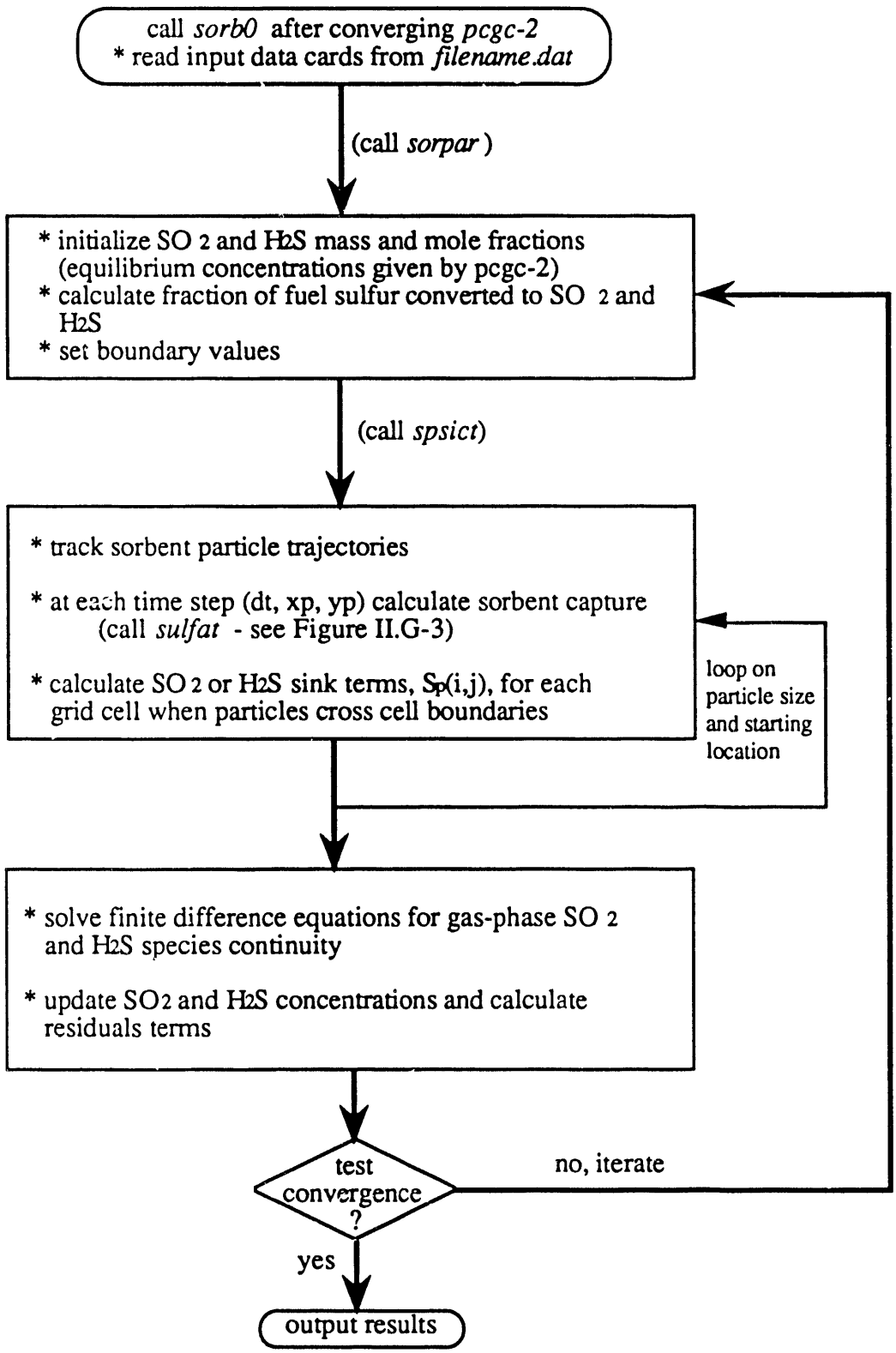

Figure II.G-2. SOx/sorbent reaction submodel solution algorithm.

sulfat (calculation of sorbent sulfation)
Called from spsict at time step along particle trajectory path

initialization
* select number of subshells to descibe sorbent particles
* calculate the radius of grains based on BET surface area of sorbent particles
* at each particle starting location, set initial conversion of grains to 1E-10 to avoid division by zero at first time step
  Also, set radius of unreacted CaO to (1.0-1E-10)*(initial grain radius) for each subshell and assign the concentration profiles of SO_2 and H_2S through the particles
* select order of sulfation reaction

at each time step (xp,yp, dt)
* calculate gas temperature, [SO_2], and [H_2S] by 2-D interpolation
* set the concentration of SO_2 and H_2S at the sorbent particles surface (node n) equal to [SO_2], and [H_2S]
* calculate the interfacial area available for reaction at each subshell
* calculate the particle void fraction as a function of sorbent particle radius
* calculate the extended grain radius (due to increase in the molar volume of $CaSO_4$ product) at each subshell
* calculate bulk and Knudsen diffusivity at each subshell
* calculate the effective diffusivity at each subshell
* calculate product layer diffusivity at each subshell
* calculate the reaction rate constant (assumed to be constant throughout the sorbent particle since particles are isothermal)

calculate new concentration profiles through the sorbent particle using material balance differential equation

first-order reaction
* assemble coefficients for matix solution
* use Thomas algorithm to solve tri-diagonal system of equation

half-order reaction
* assemble coefficients for matrix solution
* use Newton-Raphson technique to calculate concentration at each sorbent particle subshell

determine sorbent particle conversion due to reaction occurring during dt (differential time step)
* calculate change in grain radius due to reaction
* calculate conversion for each subshell
* obtain overall conversion for sorbent particle by summing up subshell
  conversion (integration procedure used)

return to *spsict*

Figure II.G-3. Sulfation model procedure outline. (See Table II.G-1 for equations).

Figure II.G-4 ***Predicted Sorbent SO_2 Capture***
Wyo. subbit. coal, 1:10 sorbent/coal feed

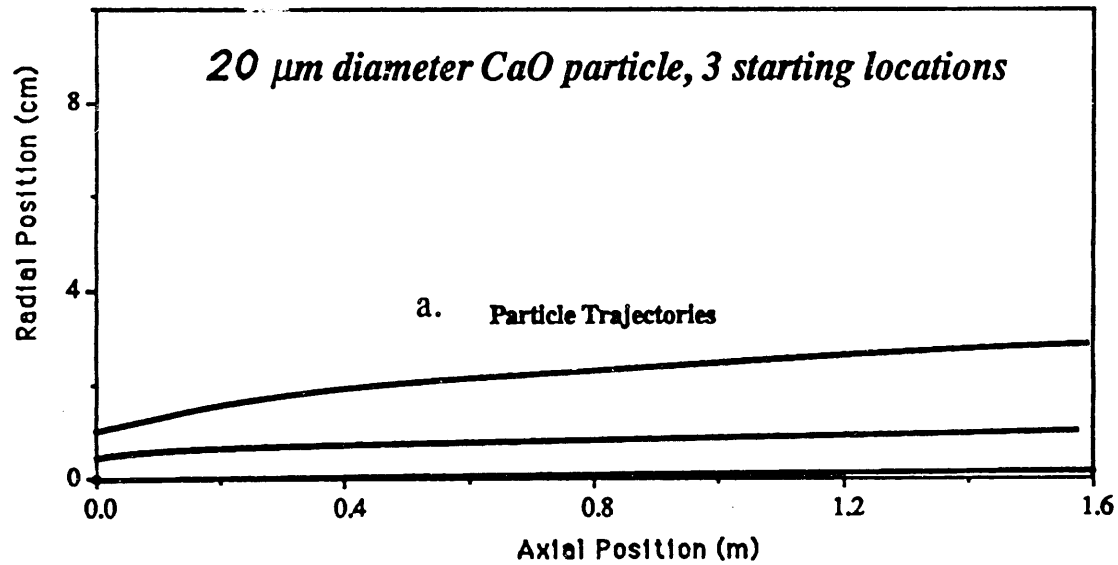

b. SO_2 *Concentration: without sorbent injection ——; with sorbent injection ——*

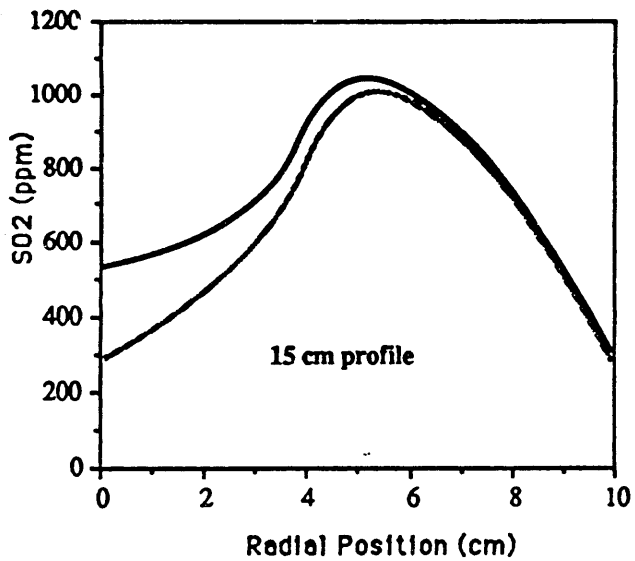

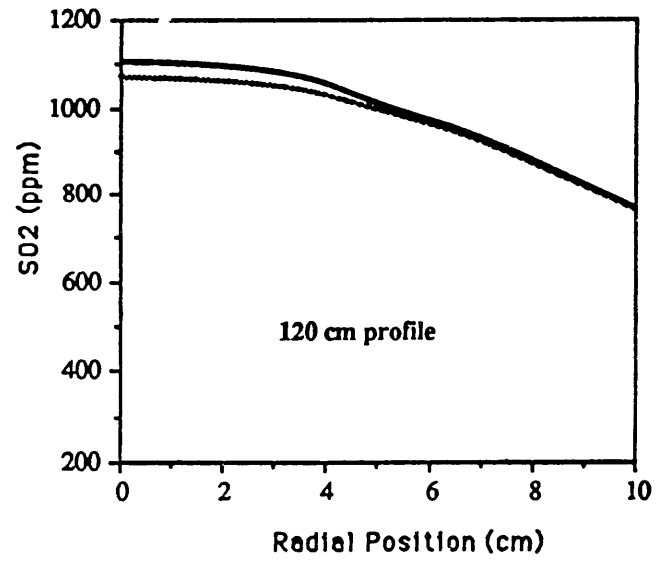

Table II.G-1. Sorbent-Reaction Submodel Equation Set

Equation	Definition	Eq. No.s
$\frac{d^2[SO_2]}{dR^2}+\left(\frac{2}{R}+\frac{1}{D_{eff}}\frac{dD_{eff}}{dR}\right)\frac{d[SO_2]}{dR}-\frac{N}{D_{eff}}=0.$	Material balance on SO_2 in a spherical shell Used to calculate $[SO_2]$ at each sorbent particle subshell.	4.7
$@R=0.;\ \frac{d[SO_2]}{dR}=0.$ $@R=R_p;\ [SO_2]_{R_p}=[SO_2]_{xp,yp,dt}$	Boundary conditions	4.9
$N=k_{½}A[SO_2]^{½}_{r_{cor(i)}}$	Half-order volumetric consumption rate	4.10
$N=k_1A[SO_2]^{1}_{r_{cor(i)}}$	First-order volumetric consumption rate	4.11
$A=3z(1-e_c)\frac{r^3}{r^3_{cor(i)}}$	Interfacial area available for reaction at ith subshell	4.15
$z=\left\{\frac{\rho_{CaO}}{\rho_{MgO}}\left(\frac{1}{W}-1\right)+1\right\}^{-1}$	Fraction of grains which are CaO	4.16
$W=\left\{1+\left(\frac{1-Y}{Y}\right)\left(\frac{M_{MgO}M_{CaCO_3}}{M_{MgCO_3}M_{CaO}}\right)\right\}^{-1}$	Weight fraction of CaO in the calcine on an "impurity-free" basis	4.17
$\frac{dr_{cor(i)}}{dt}=\left(\frac{-M_{CaO}}{\rho_{CaO}}\right)K_n[SO_2]^n_{r_{cor(i)}}$	Material balance on CaO at product-CaO interface for nth order reaction	4.13 4.14
$[SO_2]_{r_{cor(i)}}=\frac{D_{sp}[SO_2]_{R_{(i)}}}{D_{sp}+K_1r_{cor(i)}\left(1-\frac{r_{cor(i)}}{r_{ext(i)}}\right)}$	Interfacial concentration for ith subshell for first-order reaction rate	4.23
$[SO_2]_{r_{cor(i)}}=\frac{2[SO_2]_{R_{(i)}}-\alpha-\left(-4[SO_2]_{R_{(i)}}\alpha+\alpha^2\right)^{\frac{1}{2}}}{2}$ $where,\ \alpha=-\left(\frac{K_{½}r_{cor(i)}}{D_{sp}}\right)^2\left(1-\frac{r_{cor(i)}}{r_{ext(i)}}\right)^2$	Interfacial concentration for ith subshell for half-order reaction rate	4.24
$r_{ext(i)}=\left\{\left(\frac{r_g^3-r_{cor(i)}}{1-e_s}\right)\left(\frac{\rho_{CaO}M_{CaSO_4}}{\rho_{CaSO_4}M_{CaO}}\right)+r^3_{cor(i)}\right\}^{\frac{1}{3}}$	Extended grain radius	4.26

Table II.G-1 Continued

Equation	Definition	Eq. No. §
$r_g = \frac{3}{\rho_{CaO}(BET\ surface\ area)}$	Initial grain radius	4.84
$e_x = 1-(1-e_c)\left\{1+\left(\frac{\left(\frac{a}{1-e_s}-1\right)X}{1+\frac{\rho_{CaO}(1-W)}{\rho_{MgO}W}}\right)\right\}$	Particle void fraction	4.28
$X_{R(i)} = 1-\left(\frac{r_{cor(i)}}{r_g}\right)^3$	Extent of grain conversion at ith subshell	4.27
$X(t) = \frac{3}{R_p^3}\int_0^{R_p} R_{(i)}^2 X_{R(i)} dR$	Overall conversion of sorbent particle	4.44
$K_1 = 291\exp\left(\frac{-7510}{T}\right) \quad cm\,sec^{-1}$	First-order reaction rate constant	4.79a
$K_{1/2} = 0.0307\exp\left(\frac{-6970}{T}\right) \quad gmol^{\frac{1}{2}}\,cm^{-\frac{1}{2}}\,sec^{-1}$	Half-order reaction rate constant	4.79b
$D_{eff} = \left(\frac{1}{\frac{1}{D_M}+\frac{1}{D_K}}\right)e_x^2$	Effective diffusivity	4.80
$D_M = \exp(1.66\ln(T)-11.3) \quad cm^2\,sec^{-1}$	Bulk diffusivity for SO_2-air binary-pair	-
$D_K = 19,400\frac{e_c}{\rho_{CaO}(BET\ surface\ area)}\sqrt{\frac{T}{M_{SO_2}}} \quad cm^{-2}\,sec^{-1}$	Knudsen diffusion coefficient	4.82
$D_S = 0.0124\exp\left(\frac{-12,200}{T}\right) \quad cm^2\,sec^{-1}$	Product layer diffusion coefficient	4.83

§ Equations reference number in Silcox (1985). Rate constants and diffusion coefficients derived by Silcox from experimental data as cited by Silcox (1985)

As individual particles pass through computational cells in the reactor domain, the extent of sorbent conversion by the reactions:

$$CaO + SO_2 + 1/2O_2 \dashrightarrow CaSO_4 \qquad \text{(II.G-4)}$$

$$CaO + H_2S \dashrightarrow CaS + H_2O \qquad \text{(II.G-5)}$$

is predicted. Thus, the submodel predicts the loss (or sink) of gaseous sulfur species occurring in each computational cell. Species continuity is then solved for H_2S and/or SO_2 to determine the steady-state concentrations throughout the reactor. The complete source term for each cell also includes the release of sulfur species from the coal, given by the sulfur-species equilibrium ratio predicted by PCGC-2. As sulfur is captured by the sorbents, the gaseous sulfur species are assumed to re-equilibrate to the equilibrium ratio that is predicted without sulfur capture. These assumptions make it possible to decouple the SO_x/sorbent-reactions submodel from the main code.

The algorithm is iterative since the sulfation submodel is dependent on the concentrations of SO_2 and H_2S in the gas. Convergence is determined by summing up residual terms for species continuity and comparing these values with a small tolerance. This is a rigorous approach and ensures convergence of the differential equations for all regions of the reactor.

Key Submodel Assumptions - In the current SO_x/sorbent-reactions submodel the following assumptions are made with respect to the individual three components:

(.) Prediction of Gaseous SO_x Species Formation:

- Both inorganic and organic sulfur are released from coal at a rate proportional to total coal mass loss.
- Gaseous sulfur is instantaneously converted to an equilibrium composition of SO_2, SO_3, H_2S, COS, CS2, etc. as soon as the sulfur is released from the coal and mixed locally with the bulk gas.
- As sulfur is captured by injected sorbents, the pool of sulfur species is proportionally reduced.
- Species continuity is solved to determine the steady-state concentration of sulfur species accounting for simultaneous sulfur release by coal and capture by sorbents.

(2) Sorbent Particle Calcination and Dispersion:

- Variable particle sizes are allowed.
- Particles are injected with the coal feed inlets (generalized inlet injections will be implemented later).
- Particles are rapidly calcined by the high temperatures encountered near the coal injection regions.
- Calcination gas (CO_2 if $CaCO_3$ sorbents or H_2O if $Ca(OH)_2$ sorbents) is added to the inlet carrier gas.
- Particles are in thermal equilibrium with the adjacent gas temperature.
- Particles are isothermal.
- Particles follow gas streamlines, accounting for turbulent dispersion effects.
- Energy and momentum coupling between sorbents and the gas are neglected (i.e., radiation absorption and attenuation are ignored).

(3) Sulfation of Sorbents (SO_2 Capture):

- Sorbent particles are comprised of tiny spherical grains of CaO, determined from BET surface area.
- Intra-particle CaO grains at each descrete radius from the particle center (i.e. subshell levels) react with sulfur species at an equal rate. The number of subshells used to describe particles is variable but should be at least 10 (Silcox, 1985).
- Individual grains shrink as CaO is consumed and swell as $CaSO_4$ is formed.
- Bulk diffusion to the sorbent particle surface is not limiting.
- Intra-particle diffusion is important. The effective diffusivity includes Knudsen and bulk-gas diffusion.
- Variable void-space due to grain swelling is calculated at each time step.
- Diffusion through $CaSO_4$ product layer is an important but not always a limiting resistance.
- Reaction of CaO with SO_2 is irreversible.
- The reaction order with respect to SO_2 can be half- or first-order.
- The reaction order with respect to oxygen for SO_2 capture is zero (i.e. oxygen is always in excess of SO_2).

One significant assumption that is made in the current sorbent-reaction submodel is that particles are instantaneously calcined as they enter with the coal particles in the primary inlet stream. Silcox (1985) showed that this is a reasonable assumption for sorbents injected into high-temperature regions. His calculations showed that particle heat-up and calcination occur over a short period of time relative to the time required for sulfination by SO_2. Silcox also notes that thermodynamic considerations rule out simultaneous calcination and sulfation if the sorbent is injected into the burner zone. If the sorbent is injected downstream of the burner zone in cooler flame regions, then simultaneous calcination and sulfation can occur. A model to predict joint calcination and sulfation was developed by Milne (1990) at the University of Utah. Whether or not this theory can be used to include simultaneous calcination in the current sorbent-reaction submodel framework has not been determined. The major limitation is the added complexity of the mathematical formulation and difficulty in obtaining numerical solutions.

Currently, a H_2S sulfation subroutine needs to be developed. This will require an examination of the controlling resistances in the particle and correlation of intrinsic reaction rates. There is a general lack of information in the open literature to elucidate the H_2S capture rates and important physical processes. Experimental data are currently being sought to complete this objective.

Model Prediction - A list of the Fortran subroutines for the SO_x/sorbent submodel is given in Table II.G-2. A des·ription of input data is given in Table II.G-3. A hypothetical case has been predicted to demonstrate the model for combustion of subbituminous coal for which sulfur pollutant data are available (Asay, 1982). In the experiments, no sorbents were actually injected into the reactor. Figure II.G-4a shows the predicted particle trajectories for sorbents injected with the coal feed for the subbituminous combustion case and Figure II.G-4b show the changes in SO_2 concentration predicted after sorbent capture at two aft locations.

Table II.G-2. List of SO_x/Sorbent-Reaction Submodel FORTRAN Subroutines

Subroutine	Description
calcsj	Calculates sorbent particle number density
calso2	Solves finite difference equation for SO_2 species continuity
calh2s	Solves finite difference equation for H_2S species continuity
sorb0	Reads in input data from *filename*.dat and initializes sorbent particle number density
sorpar	Main submodel driver, calculates source terms for SO_2 and H_2S (sulfur entering with the coal or gas inlet streams), determines if convergence is obtained, prints out final results
spsict	Performs particle trajectory integration and calculates the capture of SO_2 and H2S in each computational cell, also calculates sink terms for SO_2 and H_2S species continuity
sulfat	calculates the change in conversion of calcined $CaCO_3$ particles to $CaSO_4$ according to the shrinking-core model of Silcox (1985)
RATESX.INC	include statements unique to SO_x/sorbent-reactions submodel
SOXRTE.INC	

Table III.G-3. SO_x/Sorbent-Reactions Submodel Data Input Description

Input in PCGC-2 *filename*.dat

```
***************************** PCSORB ******************************
*************** SOX/H2S-SORBENT REACTIONS SUBMODEL  *************
   ****************************      ****************************
   3,1                                !NSLS,NPSS
   0.0200, 1340.                      !SPLOAD,SPDEN
   0.0000,0.0000,0.0000,              !YPS(ISL),ISL = 1,5
   20.00E-06,                         !PDS(IPS),IPS = 1,3
   1.0000,                            !PMFS(IPS),IPS = 1,5
   F  F                               !LSPBUG,LYPS
   0.9500,0.0200,                     !YPSH,YPSL
   0.3500,                            !PRKS(IPS),IPS = 1,5
```

Definition of Input data

Variable	Description
NSLS	number of starting location for sorbent particles
NPSS	number of particle sizes for sorbent particles
SPLOAD	sorbent particle loading (ratio of sorbent particle mass to the mass of gas in the primary inlet) (kg s-1)
SPDEN	sorbent particle density (*i.e.*, density of CaO) (kg m-3)
YPS(ISL)	particle starting location for isl particle trajectory
PDS(IPS)	particle diameter for ips particle size
PMFS(IPS)	particle mass fraction (fraction of sorbent mass) for ips particle size
LSPBUG	logical to specify intermediate debugging printout
LYPS	
YPSH	
YPSL	
PRK(IPS)	turbulent Prandtl-Schmidt number for sorbent particles
nsubsh	number of sorbent particle subshell (specified in PARAMETER.INC)
nsnode	number of sorbent particle nodes (specified in PARAMETER.INC)
iorder	order of sorbent particle reaction with respect to SO2 (assigned in *sulfat.F*) iorder = 1; first order reaction iorder = 2; half order reaction

Work is in progress to verify that these first results are correct. Subsequently, the SO_x/sorbent reaction submodel will be evaluated for other cases. The data collected under Subtask 2.H (Huber, 1989) will be used to evaluate fuel-rich capture after a subroutine to predict H2S capture is added to the submodel.

Plans

During the upcoming quarter, the evaluation of the SO2-capture submodel will continue. Completion of the H2S capture subroutine will be pursued. Researchers at The University of Utah (Silcox, 1990) may have experimental data available to develop H2S/sorbent-reaction rate expressions and diffusion expressions.

SECTION III. TASK 3. COMPREHENSIVE MODEL DEVELOPMENT AND EVALUATION

Objectives

The objective of this task is to integrate advanced chemistry and physics submodels into a comprehensive two-dimensional model of entrained-flow reactors (PCGC-2) and to evaluate the model by comparing with data from well-documented experiments. Approaches for the comprehensive modeling of fixed-bed reactors will also be reviewed and evaluated and an initial framework for a comprehensive fixed-bed code will be employed after submission of a detailed test plan (Subtask 3.b).

Task Outline

This task is being performed in three subtasks. The first covers the full 60 months of the program and is devoted to the development of the entrained-bed code. The second subtask is for fixed-bed reactors and is divided into two parts. The first part (12 months) was devoted to reviewing the state-of-the-art in fixed-bed reactors. This led to the development of the research plan for fixed-bed reactors, which was approved. The code development is being done in the remaining 45 months of the program. The third subtask is to generalize the entrained-bed code to fuels other than dry pulverized coal and will be performed during the last 24 months of the program.

III.A. SUBTASK 3.A. - INTEGRATION OF ADVANCED SUBMODELS INTO ENTRAINED-FLOW CODE, WITH EVALUATION AND DOCUMENTATION

Senior Investigators - B. Scott Brewster and L. Douglas Smoot
Brigham Young University
Provo, UT 84602
(801) 378-6240 and 4326

Research Assistant - Susana K. Berrondo

Objectives

The objectives of this subtask are 1) to integrate the FG-DVC submodel into PCGC-2, 2) incorporate additional submodels and improvements developed under Task 2, 3) evaluate the improved code, 4) improve user-friendliness and robustness, and 5) document the code.

Accomplishments

Work continued on code evaluation and user-friendliness. Minimum specifications for a foundational, entrained-bed code that will satisfy the terms of the contract were identified. Other desirable features that could be considered were also identified. A post-processor was developed to convert PCGC-2 plotting files to spreadsheet-compatible format.

Code Evaluation

Data from four reactors have been identified for code evaluation: the AFR transparent wall reactor (TWR), the BYU/ACERC controlled-profile reactor (CPR), the 2-D furnace at Imperial College, and the near-burner test data from the 80 MWe Goudey Station at Johnson City, New York, operated by New York State Electricity and Gas (NYSEG). Simulations of the TWR flames were described in the 4th Annual Report (Brewster et al., 1990). No further work was conducted on the TWR simulations during the past quarter. Simulations were performed during the past quarter for a natural gas flame in the CPR and for the near-burner field of the NYSEG Goudey plant. The Goudey simulations were performed under independent funding. Also, 2-D data with coal combustion were requested from Imperial College for code evaluation.

Controlled-Profile Reactor (CPR) - A diagram of the CPR reactor is shown in Figure III.A-1. The reactor is referred to as "controlled-profile" because of its computer-controlled wall temperature profile. Using the reactor's access windows, gas temperature, composition, and three velocity components were measured with independent funding in a swirling natural gas flame (Eatough, 1990). Gas temperature, measured with a suction pyrometer, is compared with code predictions in Figure III.A-2. The effect of soot on radiation was investigated theoretically by injecting carbon particles of 1 μm diameter with the primary gas. A loading of 0.1 lb solids/lb gas was assumed. The effect of radiation model type (Varma six-flux or discrete ordinates) was also investigated (Smoot et al., 1988).

The effect of radiation model type was insignificant, except at large axial distances. Both models underpredicted the gas temperature at the outlet, with the underprediction by the flux model being more significant. The underprediction seems unreasonable, since the temperature boundary conditions were higher (1300 K) than the predicted outlet temperature (1150 K for the flux model and 1275 K for the discrete ordinates method). Only the "no soot" simulations underpredicted the temperature. The predicted outlet temperature with soot was 1375 K. The problem is being investigated but has not been resolved.

Particle trajectories for the soot case are shown in Fig. III.A-3. The 1-μm particles were injected at 10 starting locations in the primary duct. The presence of soot particles causes smoother radial temperature profiles. The gas is hotter than otherwise predicted near the centerline and near the wall. The shape of the predicted profile agrees much better with the shape of the measured data at axial locations of 0.26, 0.31, 0.36, 0.46, 0.66, and 0.76 m. The effect of the soot particles, which were considered inert, is thought to occur primarily through radiation. Particles in cold areas of the reactor receive radiation and act as heat sources to the gas. Particles in hot areas radiate heat away and act as heat sinks. These effects can be seen in the comparisons in Fig. III.A-2. In general, however, the temperature is predicted too high, and this investigation is continuing.

Near-Burner Goudey Data - The near-burner region of the Goudey NYSEG plant is being simulated with PCGC-2 under independent funding to see whether 2-D code predictions can be applied to this zone. The plant is located in Johnson City, New York. A schematic of the furnace is shown in Fig. III.A-4a. Near-burner measurements were taken at Level 2, following the probe paths

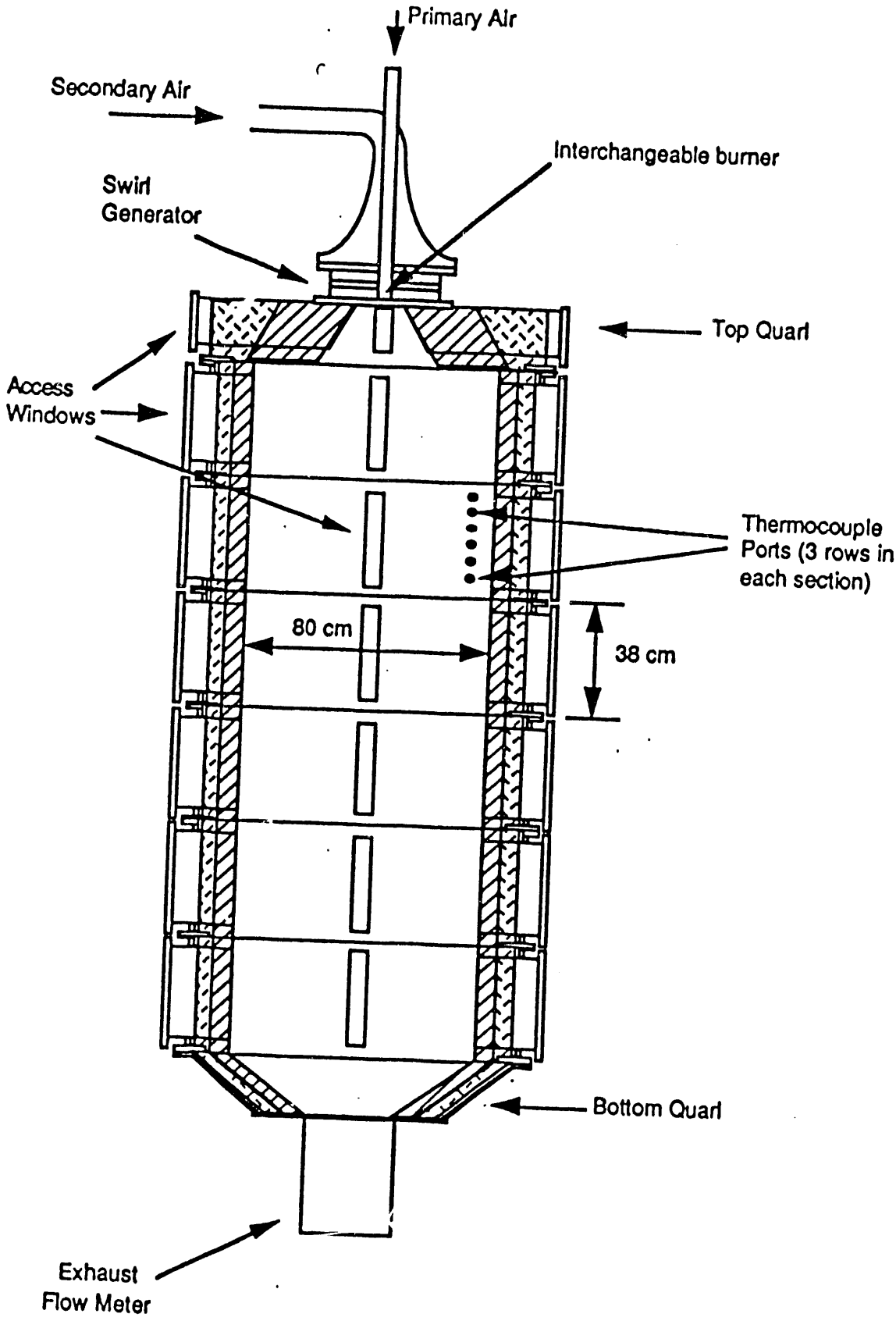

Figure III. A-1. Cross-section diagram of BYU-ACERC controlled profile reactor.

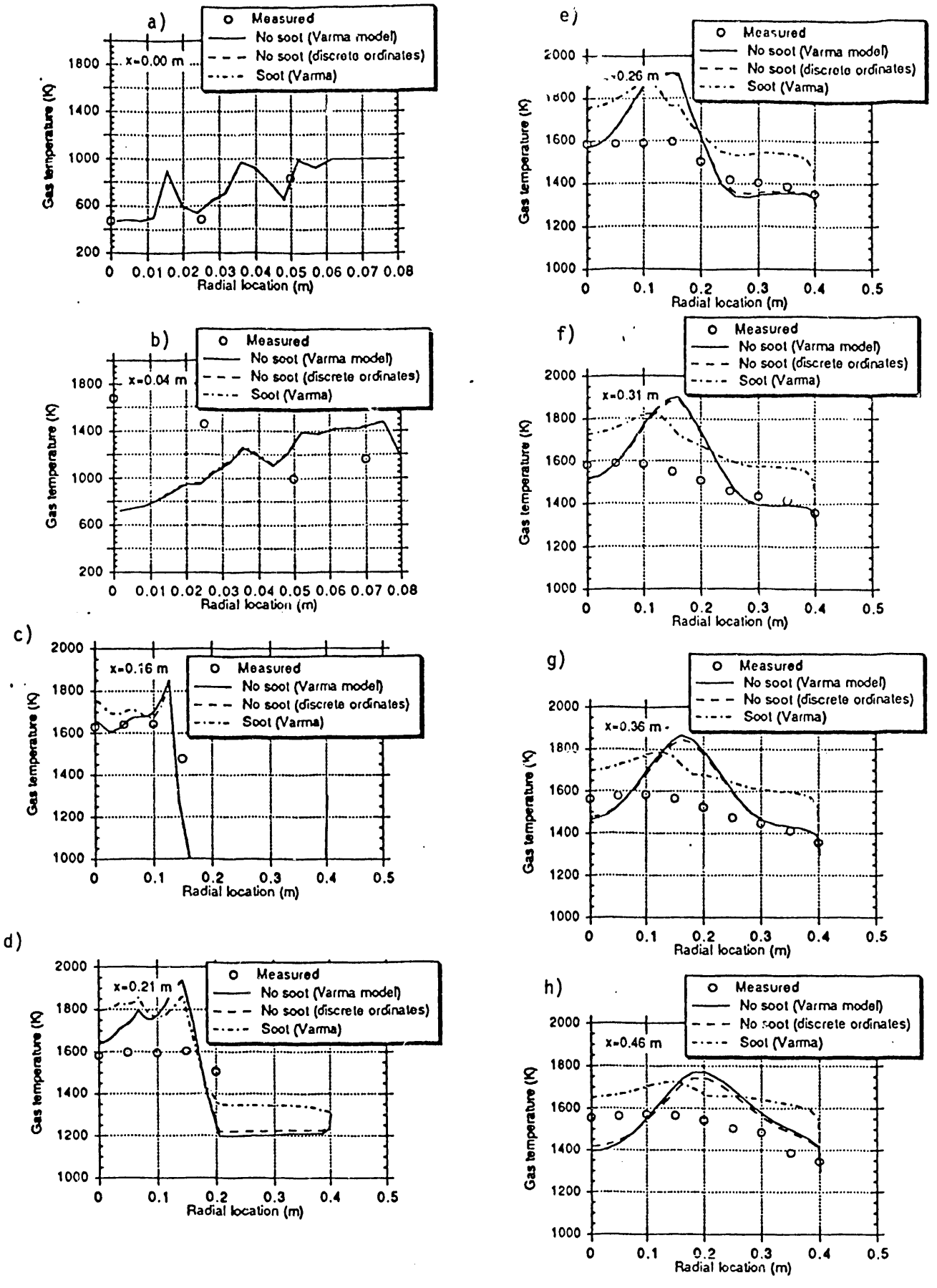

Figure III. A-2. Predicted gas temperature compared with experimental data (Eatough, 1990) for a natural gas flame in the CPR (continued on following page).

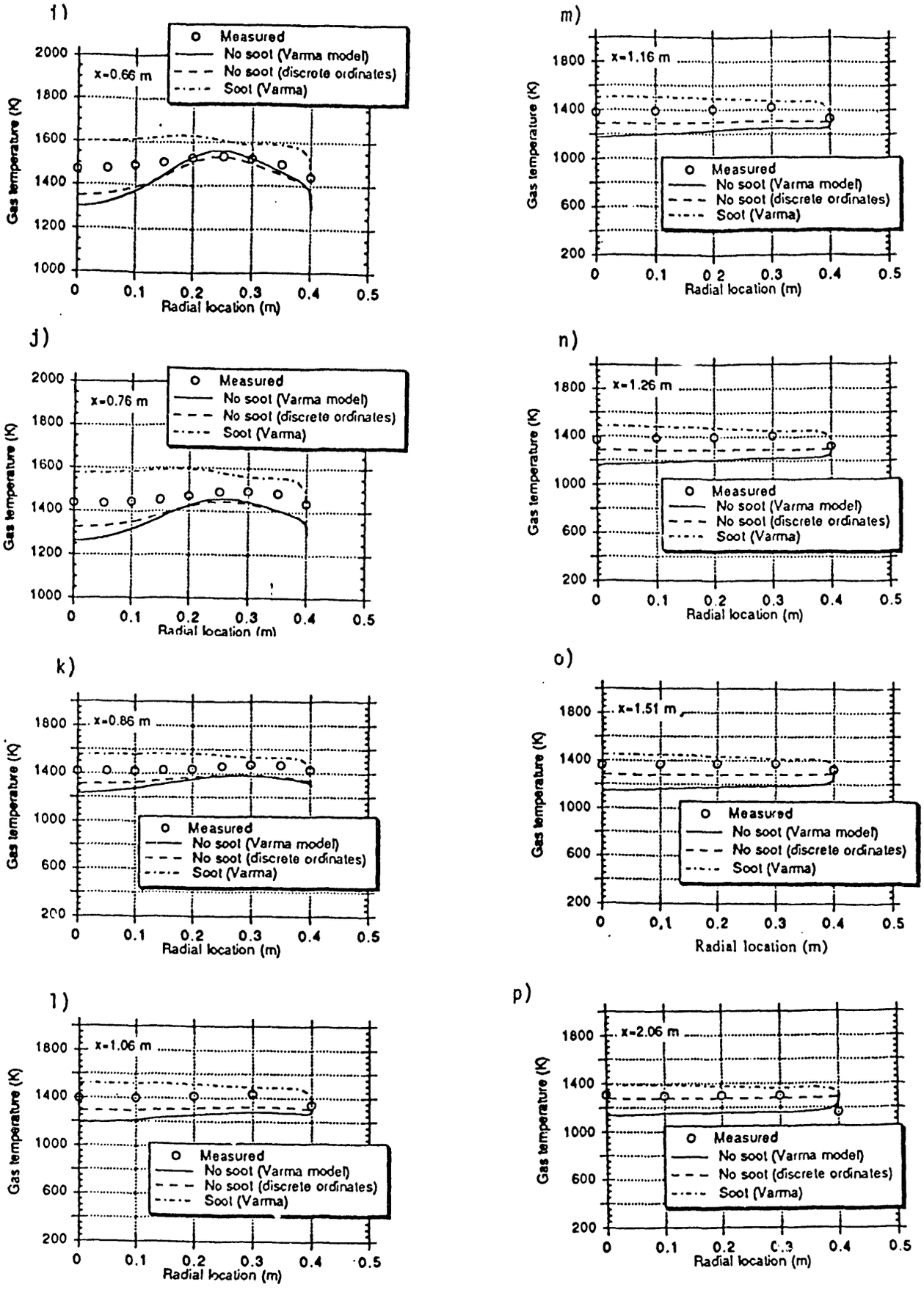

(Continued)
Figure III. A-2. Predicted gas temperature compared with experimental data (Eatough, 1990) for a natural gas flame in the CPR .

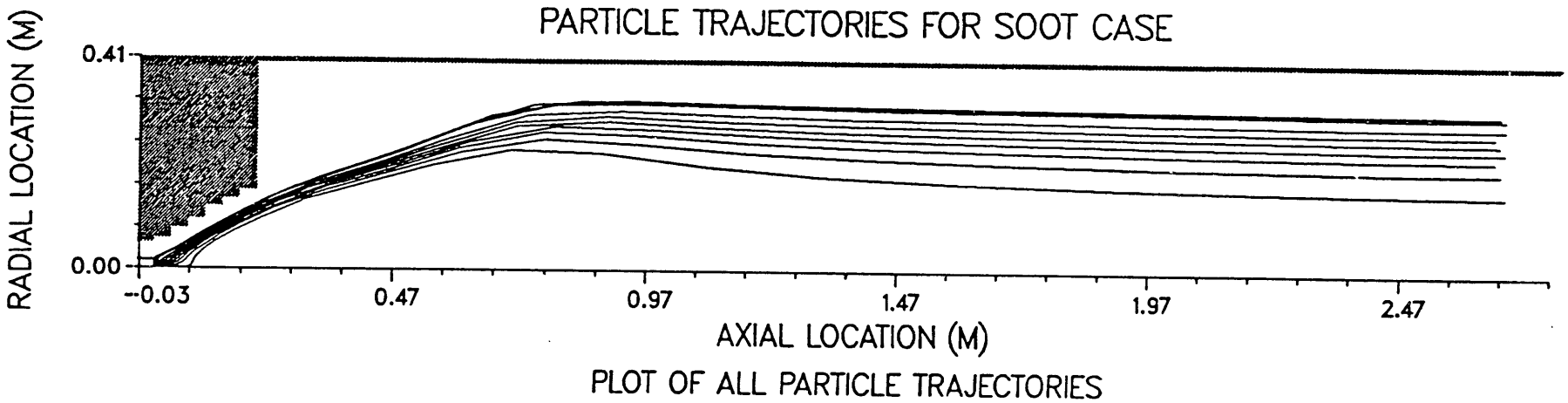

Figure III. A-3 Predicted soot particle trajectories for simulation of natural gas flame in the CPR.

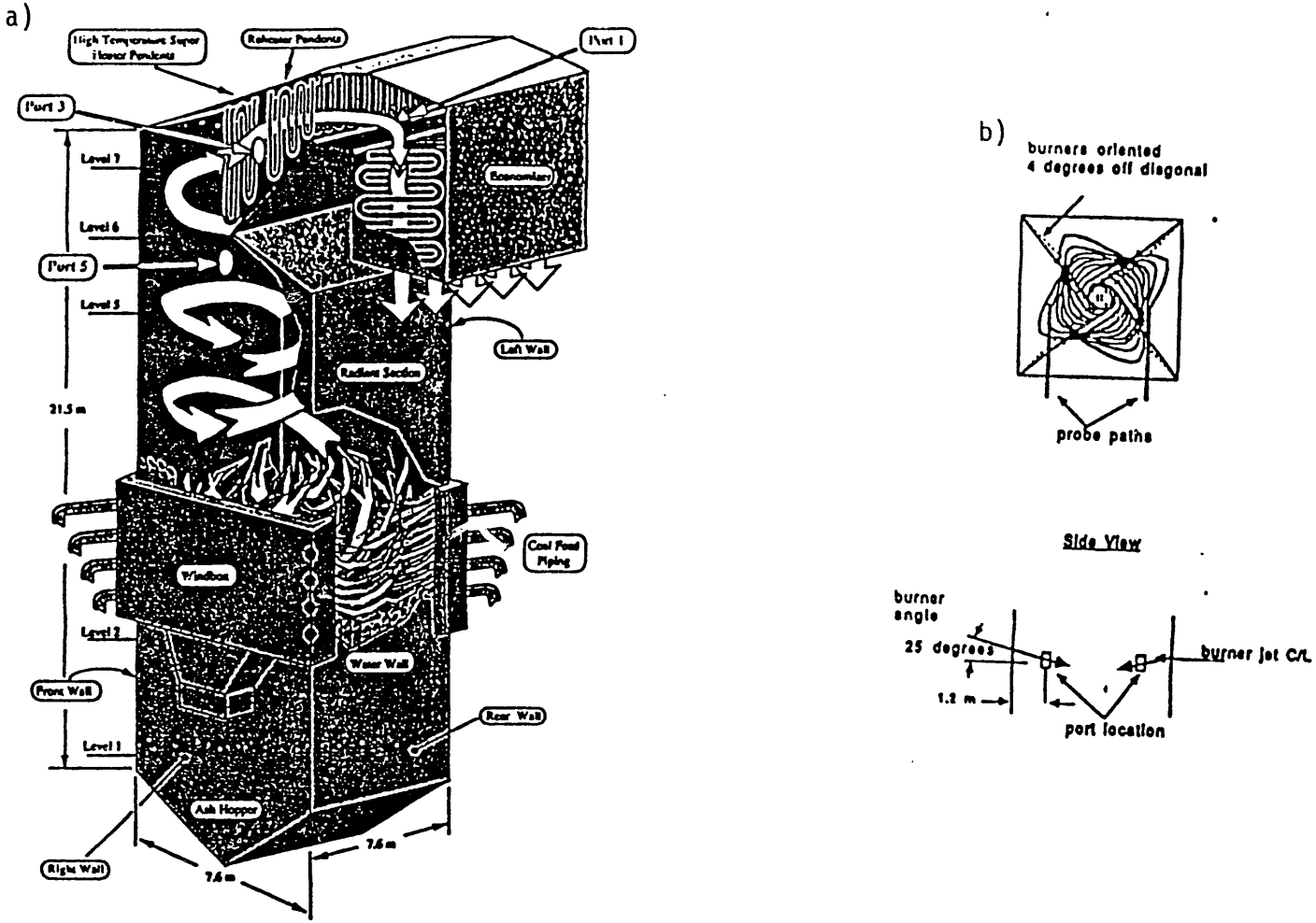

Figure 6D-3. Schematic of Goudey Station Configuration

Figure III. A-4. Schematic of the Goudey NYSEG combustor (taken from Cannon et al., 1990).

shown in Fig. III.A-4b. The data were compared with predictions of the 2-D, axisymmetric code, assuming the axis of symmetry coincides with the centerline of the burner jet. As shown in the figure, the furnace is corner-fired, and the centerline is offset from the 45-degree diagonal by 4 degrees and tilted downward. The equations for coordinate transformation from the Goudey reactor coordinates to the axisymmetric coordinate system with axis corresponding to the burner centerline and origin corresponding the burner inlet are given in the appendix.

A plot of the predicted particle trajectories and assumed geometry for the simulation is shown in Fig. III.A-5. The angle between the reactor wall and burner centerline was assumed to be 45 degrees (i.e. the 4-degree offset was neglected). After a distance equal to half the width of the reactor, the wall was assumed to converge back toward the reactor centerline, in order to prevent recirculation at the exit plane and achieve convergence over a relatively short axial length. Otherwise, the reactor length would have needed to be increased by a factor of 3 or more in order to provide enough distance so as to not have any recirculation at the reactor exit plane. The code cannot converge if there is recirculation at the reactor exit plane. Since it is only the near-burner region of the calculation that is of interest, the modified geometry to achieve convergence for a shorter total axial distance of simulation has no adverse effect. In fact, it allows for more detailed simulation of the near-burner region with the same number of total grid points.

A contour plot of predicted temperature is shown in Fig. III.A-6. The probe path with measurement locations is also shown. Temperature was measured at most, but not all, of the indicated locations. Due to the uncertainty in the burner tilt angle, two values were tried. A plot of predicted and measured temperature along the probe path is shown in Fig. III.A-7. The initial trough in predicted temperature near the wall does not agree with the measurements. The results shown in the figure are very preliminary, and the investigation is continuing. It is not clear at this time whether the 2-D code can be successfully applied to the near-burner field in this 3-D reactor.

Imperial College Data - Costa et al. (1990) recently presented new coal combustion data for gas phase species concentration, temperature, and char burnout for two swirl numbers, obtained in an axisymmetric reactor. The data contain near-field measurements that have brought to light a deficiency in the Imperial College 2-D model (Lockwood et al., 1980, 1984; Lockwood and Salooja,

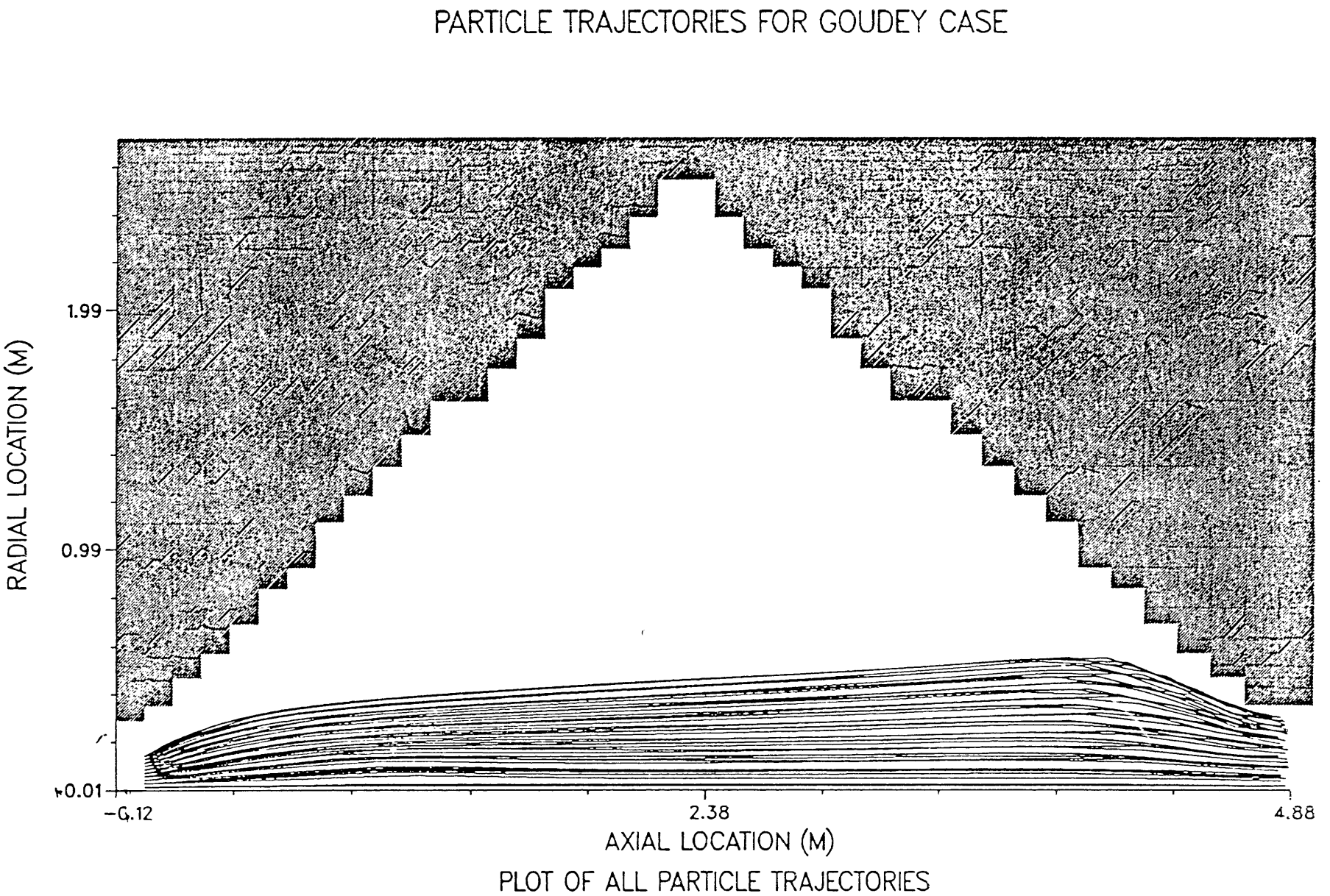

Figure III.A-5. Predicted particle trajectories for Goudey simulation.

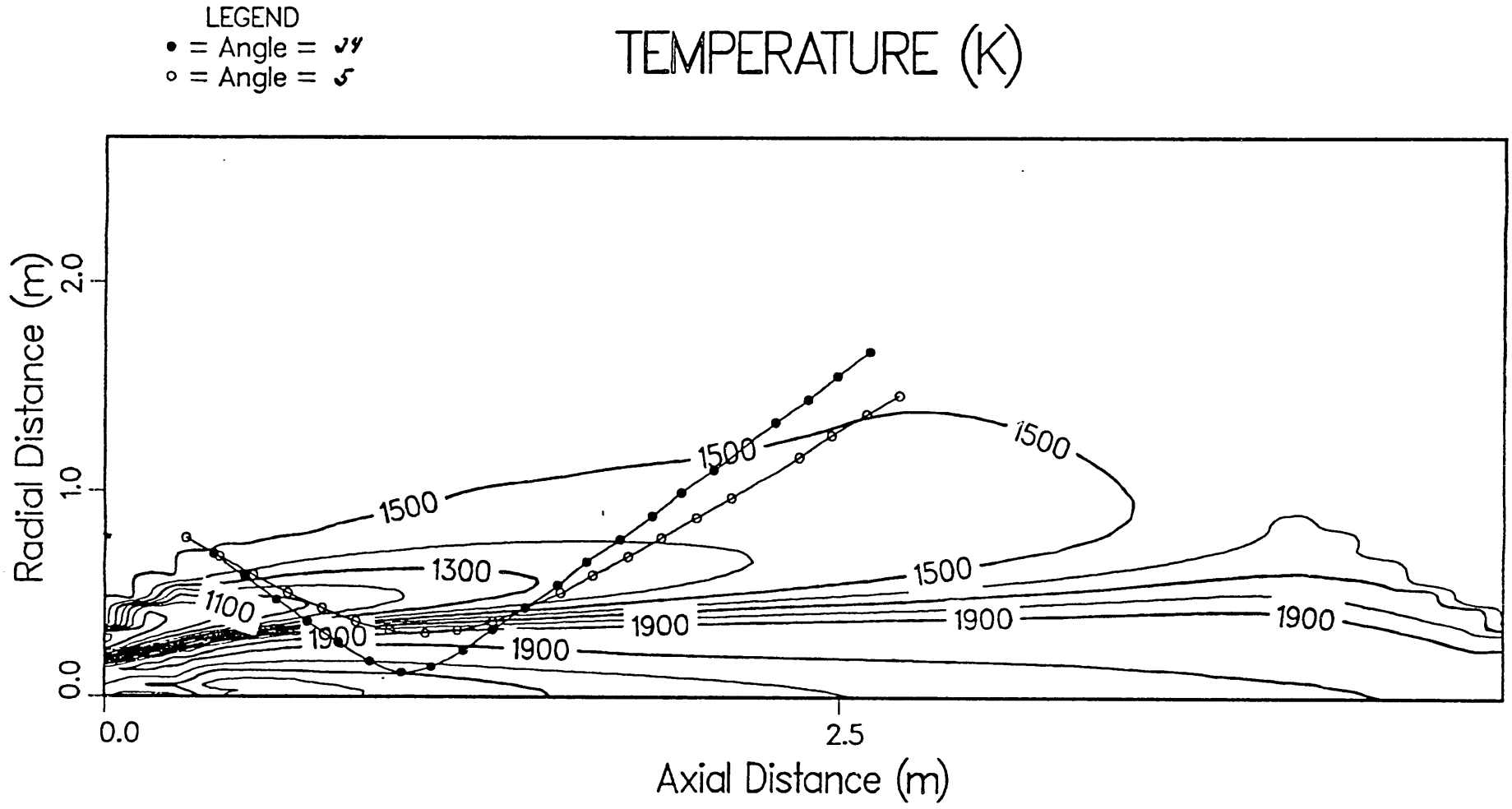

Figure III.A-6. Predicted particle temperature and probe path for two burner tilt angles for Goudey simulation.

PORT 13

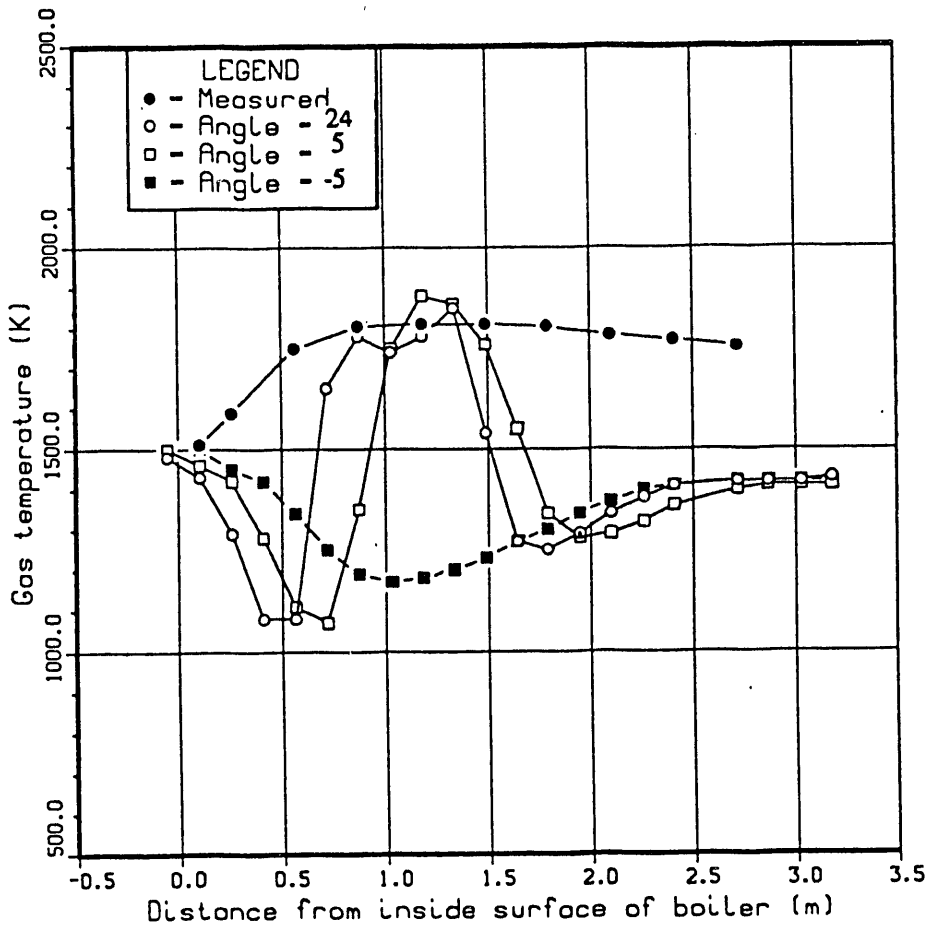

Figure III. A-7. Predicted and measured gas temperature along probe path in Goudey reactor.

1983; Lockwood and Mahmud, 1988), in that the ignition distance is significantly underpredicted. The quality of the data appears to be quite good, e.g. the radial oxygen concentration profiles are quite symmetric around the centerline. Since one of the potential benefits of detailed coal chemistry submodeling is more accurate prediction of particle ignition, these data are significant interest to this study. A copy of the data on computer-readable media has been requested from the Imperial College investigators.

User-Friendliness

Improving code user-friendliness is an on-going activity. During the past quarter, the graphical user interface (GUI) for editing input files was extended to particle combustion cases, and diagnostic messages were added to assist the user in detecting errors in code input. The GUI currently runs under the OPEN LOOK™ windowing system developed by Sun Microsystems. Although it has only been tested on Sun workstations, it should work on any machine with OPEN LOOK. The particle data window is shown in Figure III.A-8. The top part of the window contains logical variables which toggle between their true and false states by clicking the mouse on the arrow. A brief text string by the side of the arrow explains the meaning of the current setting. Below the logical variables are numeric fields for specifying the number of trajectories, particle sizes, etc. These values are changed by using the mouse to position the cursor in the appropriate numeric field and entering the data from the keyboard. Directly below the numeric field for specifying the maximum number of particle iterations for convergence is a stack button for selecting the option for interpolating gas properties. Again, the user can cycle through the available options by clicking the mouse on the box with the arrow. Below the stack button for the gas properties interpolation index is an array of numeric fields for specifying the particle diameters. A stack button for cycling through available unit options is also provided. At the bottom of the window, numeric fields are provided for specifying particle properties. Stack buttons allow the user to select from several unit options.

Diagnostic messages are continually added to the code when problems with code input are encountered. During the past quarter, a problem was encountered in the Goudey plant simulation when the gas stream flowrates were mistakenly input in kg/hr rather than kg/s. This error resulted in the simulation not converging because of extremely high gas velocities at the inlet, far in excess of the speed of sound. Diagnostic messages were therefore added to warn the user when the inlet velocities, calculated from

input flowrate values, exceed a reasonable value. A value greater than 200 m/s is considered unreasonable. Diagnostics were also added to aid the user in selecting the upper temperature limit for the physical properties table. The lower limit is fairly easy to select; it is commonly set equal to the lowest inlet stream temperature entering the reactor. The upper temperature limit is difficult to specify because some regions of the reactor may exchange significant heat through radiation with other regions of the reactor. Therefore, the code was modified to print a message whenever the upper temperature limit specified by the user is inadequate and needs to be modified. The message also suggests what the new value should be.

Foundational Code Specifications

Minimum specifications for a foundational, entrained-bed code that will satisfy the terms of the contract were identified. These specifications are as follows:

1. The percolation version of FG-DVC with rank-dependent kinetics will be included, if available. Additional submodels from AFR will also be included based on availability.

2. The code will operate with a single solids progress variable. Coal offgas composition and enthalpy will be assumed constant.

3. Code output will be provided in a format suitable for hardcopy printout. In addition, electronic data files suitable for use with independent computer graphics programs (e.g. spreadsheets and/or more advanced, commercial software) for plotting will be provided, and experiences with such graphics programs will be documented. Any software (i.e. driver programs) developed under this program in connection with the use of such graphics programs will also be provided.

4. Sorbent injection will be allowable with the coal or through an additional, sidewall inlet.

This list of specifications was presented at the Contract Review Meeting held at METC on October 25th, 1990, and documented in a letter to AFR and METC on November 28th. In order to insure adequate time for code integration, it was requested that the final submodel versions be made available by December 31st,

PARTICLES

LYPS : Uniform mass flux

LPARTP : No particles in Primary

LPARTS : Particles in Secondary

LSPM : No particles Mass Source Term

LSPU : No particles Axial Velocity Term

LSPV : No particles Radial Velocity Term

LSPH : No particles Energy Source Term

LRBND : F

Number of particle trayectory starting locations : 10

Number of particle sizes/types : 5

Solids loading in primary : 5.07955

Particle Density : 1340.00000

Normalized upper bound for particle starting location : 0.950

Normalized lower bound for particle starting location : 0.020

Maximum number of particle phase iterations : 15

Max. no. part. iter. for convergence : 1

Index for gas property interpolation : Gas properties interpolated in both directions

Particles Initial Diameter units: m

1 : 4.5e-05	2: 5.25e-05	3: 6e-05	4: 6.75e-05
5: 7.5e-05	6: 0	7: 0	8 : 0
	9: 0	10: 0	

Particle Properties : Different

Particle Number : 1

Velocity	: 0.950000	units: m/s
Radial Position	: 0.000000	units: m
Temperature	: 1.000000	units: C
Mass Fraction	: 0.200000	units: m
Turbulent Pr/Sc	: 0.350000	

Figure III.A-8. Particle data window for the OPENLOOK GUI.

1990, in the case of FG-DVC, and by March 31st, 1991, in the case of all other submodels.

In addition to identifying a set of minimum specifications for compliance with the contract, additional features that would further enhance code performance were identified. These additional features will be considered once the delivery of a code with the minimum specifications is insured, based on availability of resources and technology. The additional features include additional submodels (these will be difficult to incorporate if unavailable until after March 31st, 1991), an additional solids progress variable for tracking coal offgas (this would greatly increase the code computational burden and introduce technical uncertainties in the turbulent statistics), and aft injection of coal.

Spreadsheet Plotting

As indicated above, it was proposed at the Contract Review Meeting held at METC during the last quarter on October 25th, that an option be provided for plotting PCGC-2 output using spreadsheet programs. Accordingly, post-processors were developed during the past quarter for converting the PCGC-2 plotting files for gas and particle properties to spreadsheet format. These "spreadsheet" post-processors are menu-driven and similar in look and feel to the driver programs that already exist for DISSPLA plotting.

Plans

During the next quarter, work will continue on code evaluation and user-friendliness. The Goudey reactor simulations will be concluded. A coal flame in the CPR reactor will be simulated. Based on availability of data, simulation of the Imperial College reactor will be initiated. If available, integration of the final FG-DVC submodel code version with rank-dependent kinetics will be initiated.

III. B. SUBTASK 3.B. - COMPREHENSIVE FIXED-BED MODELING REVIEW, DEVELOPMENT, EVALUATION, AND IMPLEMENTATION

Senior Investigators - Predrag T. Radulovic and L. Douglas Smoot
Brigham Young University
Provo, Utah 84602
(801) 378-3097 and (801) 378-4326

Research Assistant - Michael L. Hobbs

Objectives

The objectives of this subtask are: 1) to develop an advanced fixed-bed model incorporating the advanced submodels being developed under Task 2, particularly the large-particle submodel (Subtask 2.e), and 2) to evaluate the advanced model.

Accomplishments

Work continued on developing and evaluating the one-dimensional, fixed-bed model. The model response to variations in operating conditions was validated by simulating several such test cases. Predicted temperature profiles were compared to measurements for the atmospheric, air-blown Wellman-Galusha gasifier fired with Elkhorn bituminous, Jetson bituminous, Leucite Hills subbituminous, and Utah Blind Canyon bituminous coals. These test cases included temperature profiles at different operating conditions. Discussions with AFR, about the large-particle FG-DVC submodel for integration into the fixed-bed code, continued. Development of the user's manual for the fixed-bed code was initiated. The first draft of the manual was prepared. A progress report on fixed-bed model development was presented at the Peer Review Meeting in Pittsburgh and the Project Review Meeting in Morgantown. An article on fixed-bed model development was prepared and published in ACERC's Burning Issues.

Comparison of Temperature Profiles at Different Conditions

Several of the Wellman-Galusha experimental test cases included temperature profiles at different operating conditions. Predicted temperature profiles were compared with measurements for the Elkhorn bituminous, Jetson bituminous, Leucite Hills subbituminous, and Utah Blind Canyon bituminous coal cases as shown in Figure III.B-1.

Elkhorn Bituminous Coal Case - A shift in the measured temperature profile due to changing reactant feed rates during gasification of Elkhorn bituminous coal was shown in Figure III.B-1A. The predictive trends were in agreement with the direction of the measured temperature shifts in each case. From the sensitivity analysis, an increase in coal flow rate caused the location of the maximum temperature to move closer to the bottom of the reactor. In general, an increase in either the steam flow rate or air flow rate caused the location of the maximum temperature to move closer to the top of the reactor. In this case the coal and the air flow rates were increased, the steam flow rate was decreased, and the location of the maximum temperature moved toward the reactor bottom. Although the increased air flow rate should have caused the location of the maximum temperature to move toward the reactor top, changes in coal and steam flow rates were more significant for the Elkhorn case.

Jetson Bituminous Coal Case - The effect of varying operational parameters on the location of the maximum temperature was shown in Figure III. B-1B for gasification of Jetson bituminous coal. The direction of the temperature shift was predicted adequately by the one-dimensional model. An increase in the coal, air and steam mass flow rates caused the location of the maximum temperature to move toward the top of the reactor. For the Jetson case, the increase in steam and air mass flow rates was more significant than the increase in the coal mass flow rate.

Leucite Hills Subbituminous Coal Case - Although gasification of low-rank coals seems to be more difficult to simulate, predictions from the one-dimensional model were in agreement with the experimental data for the Leucite Hills subbituminous coal as shown in Figure III.B-1C. The increase in coal

flow rate and decrease in steam flow rate caused the location of the maximum temperature to shift toward the bottom of the reactor for the Leucite Hills case.

Utah Blind Canyon Bituminous Coal Case - The Utah Blind Canyon case depicted in Figure III. B-1D also showed the effect of increased coal and gas throughputs. Trends in measured and predicted profiles do not agree for this case. The uncertainty in the experimental measurements may explain the discrepancy. The temperature measurements were taken for two time periods. For the first time period, the measurements were repeated on two separate days, but only one set of operational data set was reported for this time period (Thimsen et al., 1984). The spread in experimental data indicates the variability in the experimental data.

User's Manual

Development of a user's manual for the one-dimensional fixed-bed model was initiated. The first draft of the manual was prepared. The manual consists of two parts. The first part includes a model formulation and a solution method while the second part includes user's and implementation guides as well as sample problems. The model formulation and the solution method have been discussed to some extent in previous reports and thus will not be presented here. The table of contents and the user's guide are included in the appendix.

Plans

During the next quarter, work will continue on developing and evaluating the fixed-bed code. Work to integrate the new version of the FG-DVC model in the fixed-bed code will be initiated. After integration, the fixed-bed code will be validated and a sensitivity analysis will be performed. The iteration method will be further modified to improve the convergence and the robustness of the code. Development of the user's manual will continue.

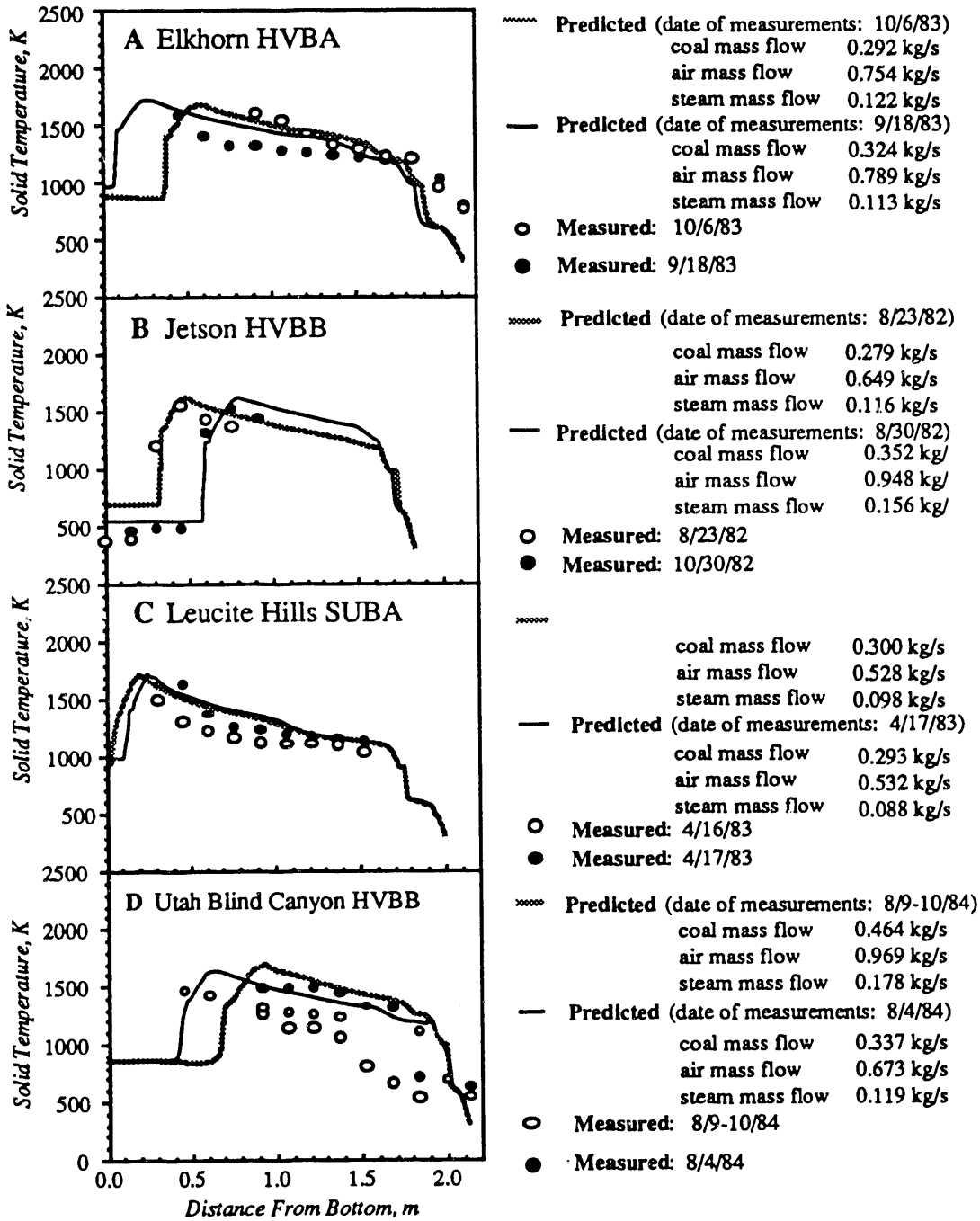

Figure III. B-1.Comparison of measured temperature and predicted solid temperature for gasification of several coals in an air-fired, low pressure Wellman-Galusha gasifier. Experimental data can be found in Thimsen et al. (1984).

III.C. SUBTASK 3.C. - GENERALIZED FUELS FEEDSTOCK SUBMODEL

Senior Investigators - B. Scott Brewster and L. Douglas Smoot
Brigham Young University
Provo, UT 84602
(801) 378-6240 and 4326

Objective

The objective of this subtask is to generalize PCGC-2 to include sorbent injection, as outlined in the Phase II Research Plan.

Accomplishments

PCGC-2 was modified to allow sorbent injection in the primary stream.

Plans

Evaluate sorbent injection submodel. Extend to additional inlets (aft sorbent injection).

SECTION IV. TASK 4. APPLICATION OF INTEGRATED CODES

Objective

The objectives of this task are to evaluate the integrated comprehensive codes for pulverized coal and fixed-bed reactors and to apply the codes to selected cases of interest to METC.

Task Outline

This task will be accomplished in two subtasks, one for the entrained-bed lasting 45 months and one for the fixed-bed lasting 36 months. Each of these subtasks will consists of three components: 1) Simulation of demonstration cases on BYU computers; 2) Implementation on a work station at AFR; and 3) Simulation of demonstration cases on the workstation.

IV.A. SUBTASK 4.A. - APPLICATION OF GENERALIZED, PULVERIZED-COAL COMPREHENSIVE CODE

Senior Investigators - B. Scott Brewster and L. Douglas Smoot
Brigham Young University
Provo, UT 84602
(801) 378-6240 and 4326

Objectives

The objectives of this subtask are 1) to simulate reactors of interest to METC and 2) to implement the comprehensive entrained-bed code at METC.

Accomplishments

A post-doctoral research associate was recruited to work on this subtask. He will begin work in January, 1991.

Potential application cases were identified at the Contract Review Meeting held at METC on October 25, 1990. They are:

1. The Texaco gasifier (a slurry feed)
2. The Shell reactor
3. A short-residence-time reactor case suggested by John Notestein of METC
4. A coal-fired gas turbine
5. An Allison gas turbine
6. The Hague International cyclone combustor

Plans

Finalize the hiring of a post-doctoral research associate and initiate simulation of an application case.

IV.B. SUBTASK 4.B. APPLICATION OF FIXED-BED CODE

Senior Investigators - Predrag T. Radulovic and L. Douglas Smoot
Brigham Young University
Provo, Utah 84602
(801) 378-3097 and (801) 378-4326

Objective

The objective of this subtask is to apply the advanced fixed-bed code developed in Subtask 3.b. to simulate fixed-bed gasifiers of interest to METC.

Accomplishments

Fixed-bed Data Collection

During the last quarter, work continued on collecting fixed-bed design and test data from organizations and individuals involved in fixed- or moving-bed gasification or combustion research or in research on non-reacting fixed- or moving-beds. No new data sets were obtained. Work also continued on collecting fixed-bed experimental data from the open literature.

Fixed-bed Code Application

No new test cases were identified or simulated.

Plans

During the next quarter, work will continue on collecting fixed-bed design and test data. Efforts will continue to identify additional test cases for simulation, and the code will be applied to these additional cases.

APPENDIX B

"COORDINATE TRANSFORMATIONS FOR GOUDEY SIMULATIONS"

The transformations consisted of two rotations and one translation from the actual x,y,z coordinates of the Goudey reactor to the ρ and ξ used by PCGC-2. The first rotation around the z axis by the 49 degrees of the burner orientation is around the resulting y axis and corresponds to the tilt of the burner. That is:

$$\begin{pmatrix} x \\ y \\ z \end{pmatrix} \xrightarrow{\Phi_z} \begin{pmatrix} x' \\ y' \\ z' = z \end{pmatrix} \xrightarrow{-\Phi'_y} \begin{pmatrix} x'' \\ y'' = y \\ x'' \end{pmatrix}$$

with $\Phi = 90 + \alpha$

$$\begin{pmatrix} x \\ y'' \\ z' \end{pmatrix} = \begin{pmatrix} -\sin\alpha & 0 & -\cos\alpha \\ 0 & 1 & 0 \\ \cos\alpha & 0 & -\sin\alpha \end{pmatrix} \begin{pmatrix} \cos\Phi & \sin\Phi & 0 \\ -\sin\Phi & \cos\Phi & 0 \\ 0 & 0 & 1 \end{pmatrix} \begin{pmatrix} x \\ p \\ -c \end{pmatrix}$$

where:

α is the tilt angle (degrees)

Φ is the burner orientation (degrees)

p is the distanced from the reactor wall to the probe (m)

c is the distance from the inlet to the probe in the z direction (m)

q is the radius of the secondary (m)

that is:

$$x'' = -\sin\alpha\,(x\cos\Phi + p\sin\Phi) + c\cos\alpha$$
$$y'' = -\sin\Phi + p\cos\Phi$$
$$z'' = \cos\alpha\,(x\cos\Phi + p\sin\Phi + c\sin\alpha$$

with the translation $\xi = z'' - q$ and using cylindrical coordinates $\rho = (x'')^2 + (y'')^2$ the following equations represent the final transformation used:

$$\xi = \cos\alpha\,(x\cos\Phi + p\sin\Phi) + c\sin\alpha - q$$

$$\rho = (\sin\alpha\,(x\cos\Phi + p\sin\Phi) + c\cos\alpha)^2 + (-\sin\Phi + p\cos\Phi)^2$$

APPENDIX C

"FIXED BED MODEL USER'S MANUAL/USER'S GUIDE

TABLE OF CONTENTS

PART TWO: CODE USER'S MANUAL

CHAPTER 5

USER'S GUIDE

5.1 General Description

MBED-1D was developed on a SUN SPARCstation 1 with the UNIX operating system. The syntax of the code should be compatible with most FORTRAN 77 compilers. Plotting or graphics routines are not distributed with the code. However, graphics are important for understanding the code's voluminous output of data, and a recommendation for graphics output is discussed in this chapter. As discussed in Chapter 4, the solution technique is based on a shooting method rather than a relaxation method. The FORTRAN code listing occupies approximately 0.5 Megabytes of disk space. The executable and object code requires an additional 1.0 Megabytes of disk space.

All input data to MBED-1D are in SI units. The input files are discussed in Section 5.3. All working variables within the program are either dimensionless or in SI units. Units associated with all variables are either given in the nomenclature or can be found in Appendix B.

CPU run time depends on the particular hardware in which the code has been implemented. Also, the degree of compiler optimization also influences CPU time. One iteration on a CONVEX C-2 requires approximately 1.8 CPU minutes. The same simulation on a SUN SPARC station IPC requires 6.6 CPU minutes.

5.2 Description of Subroutines

The computational algorithm for MBED-1D was given in Figure 4.1. A tree diagram of the structure of the program showing most of the actual computer routines is given in Figure 5.1. The routines which are not shown in Figure 5.1 are the subroutines associated with the equilibrium routines. Also, only one routine associated with the differential equation solver is shown in Figure 5.1: *lsode*. *Lsode* is shown as a black box in Figure 5.1.

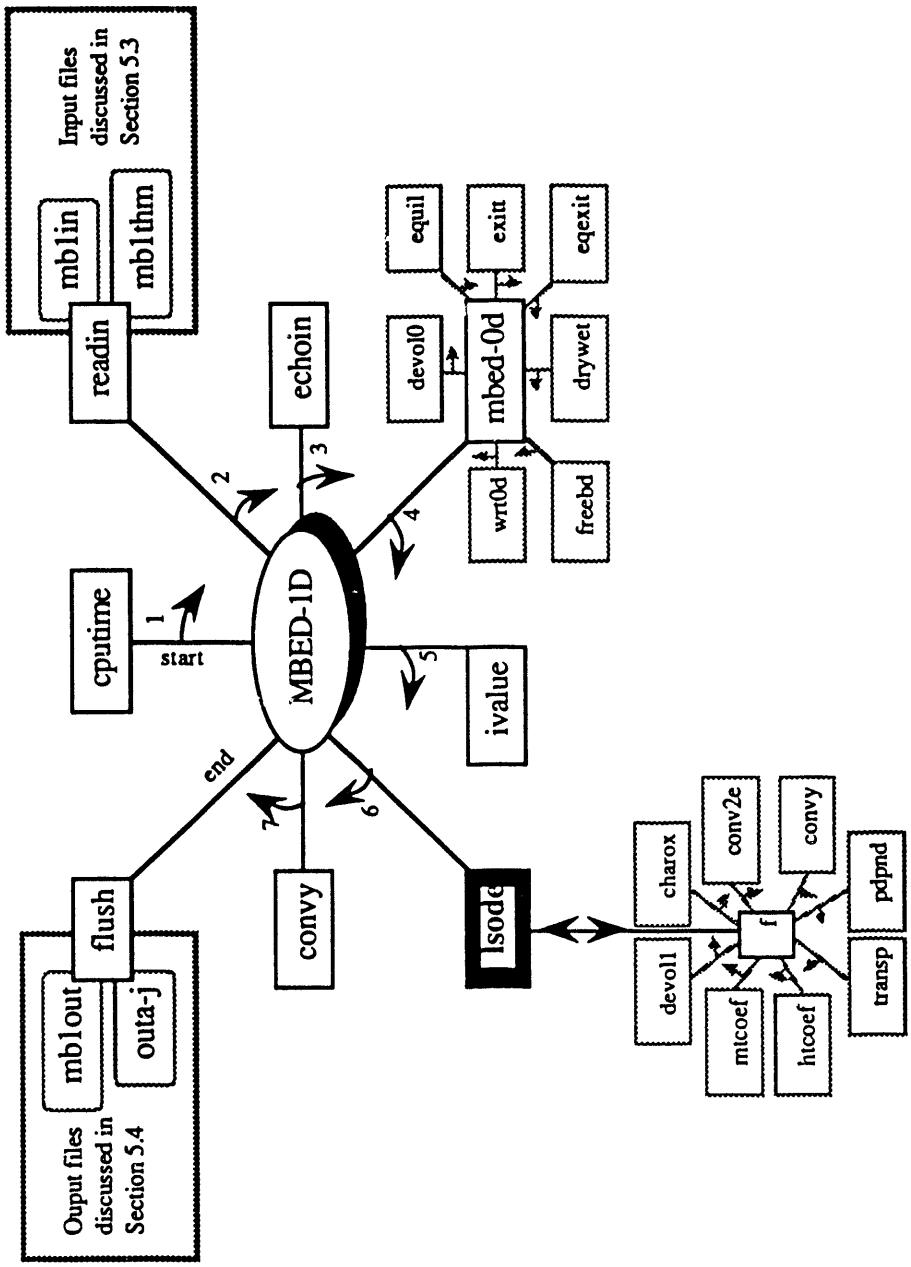

Figure 5.1 Tree diagram of the structure of MBED-1D

The main program is *mbed1d* and the routines it calls are shown in Figure 5.1. The *cputim* routine is called to track execution time and is not an integral part of the code. The *readin* routine is called to read input data from *mb1in* and *mb1thm*. The input files are discussed further in Section 5.3. The *echoin* routine is used to write the input data to the output file, *mb1out*, which is discussed in more detail in Section 5.4. The *mbed0d* routine is the two-zone fixed-bed submodel which calculates the effluent gas properties. The routines associated with *mbed0d* are also shown in Figure 5.1. The *ivalue* routine is used to determine the initial values for the set of differential equations shown in Table 3.2. The differential equations are solved by repeated calls to *lsode* which requires evaluation of the right-hand-side of the set of differential equations given in Table 3.2. The *f* routine is used to calculate the right-hand-side of the differential equation set given in Table 3.2. The *convy* routine is used to obtain calculation variables from dependent variables (i. e. temperature from enthalpy). The *flush* routine causes the contents of the logical unit to be flushed to the associated file. This routine is called for writing output to the *mb1out* and *outa* through *outj* files which are discussed in more detail in Section 5.4.

The *mbed0d* routine calculates effluent gas temperature and composition according to the two-zone model discussed in Chapter 2. The *mbed0d* routine calls *devol0, equil, exitt, eqexit, drywet, freebd,* and *wrtout* as shown in Figure 5.1. The *devol0* routine calculates the ultimate volatiles yield and composition based on Equations 2.14 through 2.19. The ultimate char yield and composition are also calculated with the *devol0* routine. The *equil* routine calculates the temperature, enthalpy and composition of the gases in the oxidation and gasification zone by assuming equilibrium. The *exitt* routine calculates the exit temperature by assuming the gases are nonreactive in the drying and devolatilization zone. The *eqexit* routine calculates the exit temperature by assuming all gases but tar in the drying and devolatilization zone are in equilibrium. The *drywet* routine determines the molar percentages on a dry and wet basis of the major gas species in the effluent gas stream. The *wrt0d* routine writes the raw gas composition on a dry basis, the drying and devolatilization zone temperature, the oxidation and gasification zone temperature, tar mass flow rate, and selected input data in both SI and English units.

The *f* routine determines the right-hand-side of the differential equation set given in Table 3.2. The *f* routine calls *convy, pdpnd, transp, htcoef, mtcoef, devol1, charox* and *conv2e* as shown in Figure 5.1. The *convy* routine is used to obtain calculation variables from dependent variables. For example, temperature is obtained from enthalpy. The *convy* routine calls the *ptemp* routine to calculate particle temperature. The *pdpnd* routine calculates the particle diameter and particle number density. The *transp* routine calculates the gas mixture transport properties (i. e. thermal conductivity, molecular diffusivity, and viscosity). The *htcoef* routine calculates heat transfer coefficients, and the *mtcoef* routine calculates mass transfer coefficients. The *devol1* and *charox* routines calculate the volumetric drying, devolatilization, oxidation, and gasification rates. The *conv2e* routine converts the drying, devolatilization, oxidation, and gasification rates to an elemental basis.

5.3 Program Input

5.3.1 Main Data File, *mb1in*

Two input files are required by MBED-1D: the main data file (*mb1in*) and the thermodynamic properties data file (*mb1thm*). The main data file is given in Table 5.1.

Table 5.1 Main data file, *mb1in*.

```
5,                                  !nsay..(say(i),i=1,nsay) follows:
**********************************************************  MBED1D
***********  ***  BRIGHAM YOUNG UNIVERSITY SIMULATION OF  ***********
***************  WELLMAN GALUSHA 10/30/82 TEST USING   ***************
***********  *********  JETSON BITUMINOUS COAL  ************************
*************************************************************** 8/30/90
-------------------------------------------------------------------------
ESSENTIAL INPUT PARAMETERS TO RUN ZERO-DIMENSIONAL MODEL:
-------------------------------------------------------------------------
    f     * l0d     (T--> do 0-d calculation only)
    t     * lgaseq  (T--> all exit gases but tar in equil., t if l0d = f)
    f     * lfreeb  (T--> do FREEBoard calculation using qfreeb)
    f     * ljkstm  (T--> calculate heat loss with flowjs latent heat)
    f     * lashcp  (T--> use ASH composition to calculate CP)
    f     * lx0     (T--> use usrx0 for x0 rather than SET model x0)
    f     * lusey0  (T--> use input y0 rather than idev specified y0)
    t     * lecho   (T--> echo input parameters to mblout)
1.9812    * diach   (DIAmeter of reactor CHamber, m)
1.8288    * chlgh   (reactor CHamber axial LenGtH, m)
101325.0  * pres    (reactor PRESsure at bed top, pa)
333.75    * twtop   (Temperature of Wall at reactor TOP, K)
287.15    * twbot   (Temperature of Wall at reactor BOTtom, K)
298.0     * tcoal   (Temperature of feed COAL, K)
-1.2e6    * qfreeb  (heat loss in FREEBoard, watts)
0.3524    * flowc   (FLOW rate of feed Coal, kg/s)
0.94813   * flowo   (FLOW rate of Oxidizer in feed, air or oxygen, kg/s)
0.15624   * flows   (FLOW rate of Steam in feed, kg/s)
0.13390   * flowjs  (FLOW rate of Jacket Steam, kg/s)
0.4000e6  * q       (wall heat loss, j/s)
0.0000    * trf     (Tar Recycle Fraction, only used if l0d = t)
387.6     * tmptrf  (TeMPerature of Tar Recycle Fraction, K)
1.0000    * brnout  (BuRNOUT or weight fraction of reacted organic matter)
elements  * elem    (flag to read ELEMent data in cree0)
thermo    * ther    (flag to read species data in cree0)
reactant  * reac    (flag to read REACtant feed stream 1, steam)
300.      * tf1     (Temperature of Feed stream 1 or steam feed, K)
 h2.0      O1.0       0.0       0.0     h2o       1.00000m
                                                          (blank Line)
reactant  * reac    (flag to read REACtant feed stream 0, oxidizer)
300.      * tf0     (Temperature of Feed stream 0 or oxidizer feed, K)
 o2.0       0.0       0.0       0.0     o2        0.20990m
ar1.0       0.0       0.0       0.0     ar        0.00980m
 n2.0       0.0       0.0       0.0     n2        0.78030m
                                                          (blank Line)
0.0426    * prxash  (PRoXimate ASH fraction, dry ash-free basis)
0.4938    * prxfc   (PRoXimate Fixed Carbon fraction, dry ash-free basis)
0.0625    * prxh2o  (PRoXimate moisture fraction, dry ash-free basis)
0.3994    * prxvm   (PRoXimate Volatile fraction, dry ash-free basis)
```

Table 5.1 Main data file, *mb1in* (continue).

```
0.8141   * wdafc  (ultimate Carbon fraction, Dry Ash-Free basis)
0.0507   * wdafh  (ultimate Hydrogen fraction, Dry Ash-Free basis)
0.1015   * wdafo  (ultimate Oxygen fraction, Dry Ash-Free basis)
0.0175   * wdafn  (ultimate Nitrogen fraction, Dry Ash-Free basis)
0.0161   * wdafs  (ultimate Sulfur fraction, Dry Ash-Free basis)
1704.0   * tmash  (Melting Temperature of ASH, K)
0.4410   * asio2  (mass fraction SIO2 in Ash, see comments below)
0.0201   * acao   (mass fraction CAO in Ash)
0.2310   * aal2o3 (mass fraction AL2CO3 in Ash)
0.0113   * amgo   (mass fraction MGO in Ash)
0.0139   * ak2o   (mass fraction K2O in Ash)
0.0013   * ana2o  (mass fraction NA2O in Ash)
0.0144   * atio2  (mass fraction TIO2 in Ash)
0.0000   * amno   (mass fraction MNO in Ash)
0.0416   * afeo   (mass fraction FEO in Ash)
0.2125   * afe2o3 (mass fraction FE2O3 in Ash)
0.0000   * afe    (mass fraction free iron, FE, in Ash)
0.0003   * ap2o5  (mass fraction P2O5 in Ash)
0.0000   * acaf2  (mass fraction CAF2 in Ash)
0.0126   * aso3   (mass fraction SO3 in Ash)
5        * idev   (DEVolatilization FLAG, SEE COMMENTS BELOW FOR MORE)
0.1567   * usrx0  (USeR supplied X0, used when 1x0 is set to t)
-------------------------------------------------------------------------
ADDITIONAL INPUT PARAMETERS TO RUN ONE-DIMENSIONAL MODEL:
-------------------------------------------------------------------------
    t    * lsp    (T--> Shell Progressive rather than ash segregation)
    f    * ltareq (T--> let TAR go to equilibrium in the gas phase)
    f    * lstiff (T--> use STIFF LSODE solver)
    t    * lstop  (T--> STOP calculation when bottom of reactor reached)
    t    * louta  (T--> print gas/solid flow rate, energy rates, etc.)
    t    * loutb  (T--> print gas/solid transport properties)
    t    * loutc  (T--> print sherwood numbers and mass transport coef.)
    t    * loutd  (T--> print film, ash and total resistances)
    t    * loute  (T--> print chemical, bulk and total resistance)
    t    * loutf  (T--> print diameters, # density, consumption rates)
    t    * loutg  (T--> print enthalpies, reynolds and prandle numbers)
    t    * louth  (T--> print heat transfer rates)
    t    * louti  (T--> print first fifteen gas mole percents)
    t    * loutj  (T--> print residence times, heating rates, & vel.)
1        * itask  (LSODE parameter used to specify output, see comments)
0.020    * deltaz (step size for output, m)
1.0e-15  * abstol (ABSolute TOLerance)
1.0e-8   * reltol (RELative TOLerance)
0.02032  * pd0    (initial Particle Diameter, m)
0.25     * gamma  (swelling parameter, fraction)
1.0      * zi     (heat of rxn partition, if zi = 1, rxn heat to solid)
0.64     * vfash  (Void Fraction in ASH zone, volume void/total volume)
0.33     * vfcoal (Void Fraction in COAL zone at reactor solid feed)
1192.0   * rhosm  (apparent coal density, kg/m^3)
0.1359   * poros  (POROSity of coal)
1092.4   * rhotar (TAR density, kg/m^3)
391.0    * tbtar  (Boiling point for TAR, K)
4.4      * ffco2  (Frequency Factor for CO2 gasification, m/K_s)
4.4      * ffh2   (Frequency Factor for H2 gasification, m/K_s)<--GUESS
1.33     * ffh2o  (Frequency Factor for H2O gasification, m/K_s)
2.3      * ffo2   (Frequency Factor for O2 oxidation, m/K_s)
1.62e8   * eco2   (activation Energy for CO2 gasification, j/kmol)
```

Table 5.1 Main data file, *mb1in* (continue).

```
1.62e8    * eh2     (activation Energy for H2 gasification, j/kmol)<--GUESS
1.47e8    * eh2o    (activation Energy for H2O gasification, j/kmol)
9.29e7    * eo2     (activation Energy for O2 oxidation, j/kmol)
1.0       * zeta    (particle area factor to account for internal burning)
0.5       * apdivt  (developing Ash Porosity DIVided by Tortuosity)
0.05      * fdgsg   (FuDGe factor for Solid to Gas heat transfer coef.)
1.0       * fdgdev  (DEVolatilization FuDGe factor)
1.0       * fdgco2  (co2 gasification FuDGe factor)
1.0       * fdgh2   (h2 gasification FuDGe factor)
1.0       * fdgh2o  (h2o gasification FuDGe factor)
1.0       * fdgo2   (o2 oxidation FuDGe factor)
1.0       * fhwg    (Fudge factor for Gas-to-Wall Heat transfer coef.)
1.0       * fhws    (Fudge factor for Solid-to-Wall Heat transfer coef.)
-------------------------------------------------------------------------
ADDITIONAL COMMENTS
-------------------------------------------------------------------------
idev  = 1  n. d. zap lignite (y0's adjusted to match ultimate)
idev  = 2  gillette subbit. (y0's adjusted to match ultimate)
idev  = 3  montana rosebud subbit. (y0's adjusted to match ultimate)
idev  = 4  illinois #6 bituminous (y0's adjusted to match ultimate)
idev  = 5  kentucky #9 bituminous (y0's adjusted to match ultimate)
idev  = 6  pittsburg #8 bituminous (y0's adjusted to match ultimate)
idev  = 7  utah blind canyon bituminous (y0's adjusted)
idev  = 8  wyodak subbituminous (y0's adjusted to match ultimate)
itask = 1  overshoot and interpolate to get t at tout
itask = 2  take one step only and return
itask = 3  stop at first internal mesh point at or beyond tout
```

When setting up a new problem for simulation, it is easiest to start by editing input files from a previous simulation, since much of the information will remain unchanged. The *mb1in* input file is divided into two major sections. The first section contains the required data to run the two-zone, zero-dimensional model. The last section contains the the additional parameters required to run the one-dimensional model.

Most of the input data in *mb1in* are single line, format free entries. After the format free data entries, an extensive comment statement is given describing the input parameter. The code variable is given in lower case followed by the description of the code variable in parenthesis. Units are also given in parenthesis if required. Upper case is used in the code variable description indicating the reason for choosing the code variable name (e. g. diach DIAmeter of reactor CHamber, m).

The *mb1in* file starts by reading the integer *nsay* which indicates the number of comment statements that are printed out at the top of the main output file *mb1out*. Any number of comment statements may be included in the header. In the example file shown in Table 5.1, five comment lines are used to describe the simulation. Following the five comment lines, three more lines are used to differentiate the zero-dimensional input parameters from the one-dimensional input parameters. These three lines are required in the input file.

Eight lines of logical input lines follow the three comment lines that describe the zero-dimensional input parameters. These parameters are l0d, lgaseq, lfreeb, ljkstm, lashcp, lx0, lusey0, and lecho. The logical parameters require an L5 format. The model options are discussed in more detail in Section 5.5. The fifteen lines following the logical inputs are format free and describe the reactor geometry (diach and chlgh), reactor pressure (pres), temperature of the wall at the top of the reactor (twtop), temperature of

the wall at the bottom of the reactor (twbot), the feed coal temperature (tcoal), the freeboard heat loss (qfreeb), the flow rate of the feed coal (flowc), the flow rate of the oxidizer in the feed (flowo), the flow rate of the steam in the feed (flows), the flow rate of jacket steam (flowjs), the 0-D overall wall heat loss (u), the tar recycle fraction (trf), the temperature of the tar recycle fraction (tmptrf), and the burnout (brnout). Not all of these fifteen parameters are used in the zero-dimensional calculation. For example, the jacket steam flow rate is used to calculate the wall heat loss based on the vaporization enthalpy of steam provided the logical ljkstm is set to "true". When the wall heat loss is calculated based on the jacket steam flow rate, the estimated wall heat loss is not used. Code operation is discussed in more detail in Section 5.5.

The keywords "elem" and "ther" are used to invoke reading of data from the thermodynamic input file *mb1thm*. The keyword "reac" invokes reading of stream temperature and composition. Only two gaseous reactant streams are allowed. The first reactant stream is for steam, and the second reactant stream is for the oxidizer which is usually oxygen or air. A blank line signifies the end of defining a reactant stream. Following the keyword "reac", the temperature of the stream is input as a format free code variable. Following the stream temperature, the stream species composition is input. A separate line is used for each species. The atomic composition of each species is described by formatted code variables, 4(a2,f7.5). The character string, formatted by a2, describes the element. For example, " h" is used for hydrogen as shown in Table 5.1. Note the blank before the "h" is required for the a2 formatted input. The real number following the element character string describes the number of atoms formatted as f4.5. For example, in Table 5.1, " h2.0 " indicates two hydrogen atoms per water molecule. The four blanks following the 2.0 are consistent with the f7.5 format specification. Following the description of the atomic composition of the species, the species name is described by the 2a4 format specification. Next, the composition of the species in the reactant stream is input with a format specification of (1x,f7.5,1a). For example, pure water is specified as " 1.00000m" in Table 5.1. There is a blank in front of the concentration fraction. The letter following the concentration fraction, "m", specifies the fraction as a mole fraction. Weight fractions can be specified by using a "w" instead of an "m" after the species concentration fraction. The complete formatted specification for the species definition is (4(a2,f7.5),2a4,1x,f7.5,a1).

The format free proximate analysis of the feed coal on a dry, ash-free basis is specified as prxash, prxfc, prxh2o, and prxvm. The dry, ash-free ultimate analysis is specified as wdafc, wdafh, wdafo, wdafn, and wdafs. Next, the melting point of the ash followed by the ash composition is specified. The last two parameters essential to run the zero-dimensional portion of the code are related to devolatilization. The variable, idev, is an integer which describes the base coal used in the functional group composition calculation. The variable, usrx0, is used to specify the potential tar-forming fraction when the flag lx0 is set to "true".

The second half of the input file *mb1in* is used to describe the additional input parameters that are necessary to run the one-dimensional fixed-bed model which is described in Chapter 3. The additional one-dimensional parameters are separated from the essential zero-dimensional input parameters by three comment lines which are followed by fifteen lines of logical input parameters: lsp, ltareq, lstiff, lstop, louta, loutb, loutc, loutd, loute, loutf, loutg, louth, louti, and loutj. Parameters essential to the differential equation solver follow the fifteen logical input parameters. The differential equation solver, *lsode*, requires itask and deltaz to specify output. Tolerances are specified with abstol and reltol. For more information on *LSODE* see Hindmarsh (1983).

The diameter of the feed coal is specified as pd0. Multiple particle sizes in the feed coal are not treated. Particle swelling is assumed to be proportional to devolatilization. The proportionality factor is input as gamma. The heat of reaction partition, zi, is not active and is ignored. The partition between the heat of reaction is not arbitrarily partitioned as discussed in Chapter 3. The void fractions at the top and bottom of the bed are represented by vfcoal and vfash, respectively. The format free apparent coal density, coal porosity, tar density, and tar boiling point are represented by rhosm, poros, rhotar, , and tbtar, respectively. The gasification and oxidation kinetics are also format free. The frequency factors are entered first followed by the activation energies: ffco2, ffh2, ffh2o, ffo2, eco2, eh2, eh2o, and eo2. The remaining parameters required to run MBED-1D are used to look at sensitivities of various parameters. Some of these values represent observed physical phenomena. The remaining format free parameters are the particle area factor which is used to account for internal particle burning (zeta), the developing ash porosity divided by tortuosity (apdivt), the solid-to-gas heat transfer correction factor (fdgsg), the devolatilization mass transfer correction factor (fdgdev), the CO_2 gasification correction factor (fdgco2), the H_2 gasification correction factor (fdgh2), the H_2O gasification correction factor (fdgh2o), the gas-to-wall heat transfer correction factor (fhwg), and the solid-to-wall heat transfer correction factor (fhws). Additional comments at the end of the *mb1in* input file are used to define different options using the integer flags idev and itask. These final comment lines are not read by MBED-1D.

5.3.2 Thermodynamic Data File, *mb1thm*

The thermodynamic properties data file, *mb1thm*, is given in Table 5.2. Typically, this file does not change unless a new species or element is needed. The thermodynamic properties data file is called from the *cree0* routine. The keywords "elem" and "ther" are used to invoke reading of data from the thermodynamic input file *mb1thm*.

The input file *mb1thm* is divided into three major sections: element data, species thermodynamic data, and species transport data. The elemental data is read in initially by specifying the species name, molecular weight, and valence. The elemental data uses the following format specification: a2,8x,2f10.6. The order in which the elements are listed is the order in which they are treated in the program calculations. A blank line is required between the elemental data and the species thermodynamic data as shown in Table 5.2.

The thermodynamic data for each species are entered on three separate lines. The first line is used to specify the species name and elemental composition. The second and third lines are used to specify heat capacity coefficients for the species. The format for specifying the species name and elemental composition is as follows: 3a4,12x, 4(a2,f3.0). The source and date of the thermodynamic data are also shown in Table 5.2 following the species name (e. g. j 9/65) The "j" indicates the source of the data as being the JANNAF thermochemical tables (Stull and Prophet, 1971). Also, the "g 300.000 5000.000" entry indicates that the species is a gas over the temperature range from 300 to 5000 K MBED-1D does not use the literature source and date, species physical state, and valid temperature range. However, this information is available in Table 5.2 for reference.

A blank line is required between the species thermodynamic data and the species transport data. The format free species transport data is read by the *readin* routine. The species transport data includes the Stockmeyer collision diameter (s), Lennard-Jones temperature parameter (ek), and the nonpolar correction factor for the Lennard-Jones parameter (delta).

Table 5.2 Thermodynamic Data File, *mb1thm*.

```
c          12.01115       4.0
h          1.00797        1.0
n          14.0067        0.0
s          32.06          4.0
o          15.9994       -2.0
ar         39.9480        0.0

ar                 l 5/66ar 1.00 0.00 0.00 0.g   300.000  5000.000
 0.25000000e 01 0.0            0.0            0.0            0.0
-0.74537500e 03 0.43660002e 01 0.25000000e 01 0.0            0.0
 0.0            0.0           -0.74537476e 03 0.43660002e 01
co                 j 9/65c  1.o  1.00 0.00 0.g   300.000  5000.000
 0.29840689e 01 0.14891387e-02-0.57899678e-06 0.10364576e-09-0.69353499e-14
-0.14245227e 05 0.63479147e 01 0.37100916e 01-0.16190964e-02 0.36923584e-05
-0.20319673e-08 0.23953344e-12-0.14356309e 05 0.29555340e 01
co2                j 9/65c  1.o  2.00 0.00 0.g   300.000  5000.000
 0.44608040e 01 0.30981717e-02-0.12392566e-05 0.22741323e-09-0.15525948e-13
-0.48961438e 05-0.98635978e 00 0.24007788e 01 0.87350905e-02-0.66070861e-05
 0.20021860e-08 0.63274039e-15-0.48377520e 05 0.96951447e 01
ch4                j 3/61c  1.h  4.00 0.00 0.g   300.000  5000.000
 0.15027056e 01 0.10416795e-01-0.39181514e-05 0.67777872e-09-0.44283706e-13
-0.99787031e 04 0.10707143e 02 0.38261929e 01-0.39794557e-02 0.24558321e-04
-0.22732920e-07 0.69626952e-11-0.10144945e 05 0.86690062e 00
c2h6               cr2178c   2h   60   00   0g   300.000  5000.000
 1.67107058e+00 1.88078150e-02-6.98943156e-06 1.16385735e-09-7.17707692e-14
-1.14683543e+04 1.26317347e+01 1.92453270e+00 1.68224303e-02-2.24906498e-06
-3.40875417e-09 1.49239675e-12-1.14789269e+04 1.16292438e+01
h2                 j 3/61h  2.0  0.0  0.0  0.g   300.000  5000.000
 0.31001883e 01 0.51119458e-03 0.52644204e-07-0.34909964e-10 0.36945341e-14
-0.87738013e 03-0.19629412e 01 0.30574446e 01 0.26765198e-02-0.58099149e-05
 0.55210343e-08-0.18122726e-11-0.98890430e 03-0.22997046e 01
hcn                000000h  1.c  1.n  1.0  0.g   300.000  5000.000
 0.37068110e 01 0.33382799e-02-0.11913307e-05 0.19992916e-09-0.12826451e-13
 0.14962633e 05 0.20794888e 01 0.24513550e 01 0.87208301e-02-0.10094202e-04
 0.67255677e-08-0.17626959e-11 0.15213000e 05 0.80830069e 01
h2o                j 3/61h  2.o  1.00 0.00 0.g   300.000  5000.000
 0.27167616e 01 0.29451370e-02-0.80224368e-06 0.10226681e-09-0.48472104e-14
-0.29905820e 05 0.66305666e 01 0.40701275e 01-0.11084499e-02 0.41521180e-05
-0.29637404e-08 0.80702101e-12-0.30279719e 05-0.32270038e 00
h2s                j12/65h  2.s  1.00 0.00 0.g   300.000  5000.000
 0.28479090e 01 0.38415990e-02-0.14099360e-05 0.24278735e-09-0.15783280e-13
-0.34469788e 04 0.74781399e 01 0.38811293e 01-0.13211856e-03 0.36517713e-05
-0.21820441e-08 0.28783779e-12-0.36350916e 04 0.25161505e 01
n2                 j 9/65n  2.0  0.0  0.0  0.g   300.000  5000.000
 0.28963194e 01 0.15154863e-02-0.57235275e-06 0.99807385e-10-0.65223536e-14
-0.90586182e 03 0.61615143e 01 0.36748257e 01-0.12081496e-02 0.23240100e-05
-0.63217520e-09-0.22577253e-12-0.10611587e 04 0.23580418e 01
nh3                j 9/65n  1.h  3.00 0.00 0.g   300.000  5000.000
 0.24165173e 01 0.61871186e-02-0.21785136e-05 0.37599057e-09-0.24448854e-13
-0.64747109e 04 0.77043467e 01 0.35912762e 01 0.49388665e-03 0.83449304e-05
-0.83833385e-08 0.27299092e-11-0.66717070e 04 0.22520962e 01
no                 j 6/63n  1.o  1.00 0.00 0.g   300.000  5000.000
 0.31889992e 01 0.13382279e-02-0.52899316e-06 0.95919314e-10-0.64847928e-14
 0.98283242e 04 0.67458115e 01 0.40459509e 01-0.34181783e-02 0.79819174e-05
```

Table 5.2 Thermodynamic Data File, *mb1thm* (continue).

```
-0.61139254e-08 0.15919072e-11 0.97453867e 04 0.29974976e 01
o2                j 9/65o  2.0  0.0  0.0  0.g    300.000  5000.000
 0.36219521e 01 0.73618256e-03-0.19652219e-06 0.36201556e-10-0.28945623e-14
-0.12019822e 04 0.36150942e 01 0.36255980e 01-0.18782183e-02 0.70554543e-05
-0.67635071e-08 0.21555977e-11-0.10475225e 04 0.43052769e 01
oh                j 3/66o  1.h  1.00 0.00 0.g    300.000  5000.000
 0.29106417e 01 0.95931627e-03-0.19441700e-06 0.13756646e-10 0.14224542e-15
 0.39353811e 04 0.54423428e 01 0.38375931e 01-0.10778855e-02 0.96830354e-06
 0.18713971e-09-0.22571089e-12 0.36412820e 04 0.49370009e 00
so2               j 6/61s  1.o  2.00 0.00 0.g    300.000  5000.000
 0.52451363e 01 0.19704204e-02-0.80375759e-06 0.15149969e-09-0.10557998e-13
-0.37558227e 05-0.10873518e 01 0.32665329e 01 0.53237863e-02 0.68437544e-06
-0.52809987e-08 0.25590450e-11-0.36908145e 05 0.96513472e 01

3.418,124.,0.,    * ar   s(i), ek(i), delta(i)
3.590,110.,0.,    * co   most data from rp&s except as noted
3.996,190.,0.,    * co2
3.758,148.6,0.0,  * ch4
4.418,230.0,0.0,  * c2h6
2.915,38.,0.,     * h2
3.0,300.0,0.0     * hcn  blind guess (after rdb above)
2.641,809.1,1.,   * h2o
3.49,343.0,0.0,   * h2s
3.681,91.5,0.,    * n2
3.15,358.0,0.7,   * nh3
3.47,119.0,0.,    ! no   bsl
3.433,113.,0.,    * o2
3.0,300.0,0.0,    ! oh   obtained from rdb
4.04,347.0,0.42,  ! so2

!*this file should always contain the following species:
! ar, co, co2, ch4, c2h6, h2, hcn, h2o, h2s, n2, nh3, and o2
! other species may be added if desired.  the subroutines wrtout and addgas
! should be modified to obtain printout of any added species.  if these
! files are not modified, the added species will be part of "others"
! in the output file.
```

5.4 Program Output

5.4.1 Main Output File, *mb1out*

Eleven output files are available from MBED-1D: the main output file (*mb1out*) and ten optional output file (*outa* through *outj*). The main output file is given in Table 5.3. The output file in Table 5.3 corresponds to the input data given in Table 5.1 and Table 5.2.

Table 5.3 Main Output File, *mb1out.*

```
************************************************************************ MBED1D
***************  BRIGHAM YOUNG UNIVERSITY SIMULATION OF  ***************
*****************  WELLMAN GALUSHA 10/30/82 TEST USING   ***************
************************  JETSON BITUMINOUS COAL  ************************
************************************************************************ 8/30/90
------------------------------------------------------------------------
Zero-dimensional input parameters:
------------------------------------------------------------------------
 F          T--> do 0-d calculation only
 T          T--> all exit gases in equil., t if l0d = f
 F          T--> do FREEBoard calculation using qfreeb
 F          T--> calculate heat loss with flowjs latent heat
 F          T--> use ASH composition to calculate CP
 F          T--> use usrx0 for x0 rather than SET model x0
 F          T--> use input y0 rather than idev
 T          T--> echo input parameters to mblout
 0.198E+01  DIAmeter of reactor CHamber, m
 0.183E+01  reactor CHamber axial LenGtH, m
 0.101E+06  reactor PRESsure at bed top, pa
 0.334E+03  Temperature of Wall at reactor TOP, K
 0.287E+03  Temperature of Wall at reactor BOTtom, K
 0.298E+03  Temperature of feed COAL, K
-0.120E+07  heat loss in FREEBoard, watts
 0.352E+00  FLOW rate of feed Coal, kg/s
 0.948E+00  FLOW rate of Oxidizer in feed, kg/s
 0.156E+00  FLOW rate of Steam in feed, kg/s
 0.134E+00  FLOW rate of Jacket Steam, kg/s
 0.400E+06  Overall wall ht coefficient, j/sm^2K
 0.000E+00  Tar Recycle Fraction, only used if l0d = t
 0.388E+03  Tar Recycle Temperature, K
 0.100E+01  BuRNOUT, wt fract of reacted organic matter
 0.426E-01  PRoXimate ASH fraction, dry ash-free basis
 0.494E+00  PRoXimate Fixed Carbon fraction, daf basis
 0.625E-01  PRoXimate moisture fraction, daf basis
 0.399E+00  PRoXimate Volatile fraction, daf basis
 0.814E+00  Dry, Ash-Free ultimate mass fraction C
 0.507E-01  Dry, Ash-Free ultimate mass fraction H
 0.102E+00  Dry, Ash-Free ultimate mass fraction O
 0.175E-01  Dry, Ash-Free ultimate mass fraction N
 0.161E-01  Dry, Ash-Free ultimate mass fraction S
 0.170E+04  melting temperature of ash, K
 0.441E+00  SIO2 weight fraction in ash
 0.201E-01  CAO weight fraction in ash
 0.231E+00  AL2O3 weight fraction in ash
 0.113E-01  MGO weight fraction in ash
 0.139E-01  K2O weight fraction in ash
 0.130E-02  NA2O weight fraction in ash
 0.144E-01  TIO2 weight fraction in ash
 0.000E+00  MNO weight fraction in ash
 0.416E-01  FEO weight fraction in ash
 0.213E+00  FE2O3 weight fraction in ash
 0.000E+00  FE (free iron) weight fraction in ash
 0.300E-03  P2O5 weight fraction in ash
 0.000E+00  CAF2 weight fraction in ash
 0.126E-01  SO3 weight fraction in ash
 5          1-zap, 2-gill, 3-rose, 4-ill6, 5-kty9, 6-pit8
  0.157E+00     USeR  supplied  X0,  used  when  lx0  is  set  to  t
```

Table 5.3 Main Output File, *mb1out* (continue).

```
------------------------------------------------------------------------
One-dimensional input parameters:
------------------------------------------------------------------------
 T           T--> Shell Progressive rather than AS model
 F           T--> T--> let TAR go to equilibrium
 F           T--> use STIFF LSODE solver
 T           T--> T--> STOP when bottom of reactor reached
 T           T--> print gas/solid flow rate, energy rates
 T           T--> print gas/solid transport properties
 T           T--> print sherwood numbers and mt coef.
 T           T--> print film, ash and total resistances
 T           T--> print chemical, bulk and total resistance
 T           T--> print diameters, # density, c rates
 T           T--> print enthalpies, re and pr numbers
 T           T--> print heat transfer rates
 T           T--> print first fifteen gas mole percents
 T           T--> print res. times, heating rates, & vel.
 1           LSODE parameter used to specify output
 0.200E-01   step size for output, m
 0.100E-14   ABSolute TOLerance used in LSODE
 0.100E-07   RELative TOLerance used in LSODE
 0.203E-01   initial Particle Diameter, m
 0.250E+00   swelling parameter, fraction
 0.100E+01   heat of rxn partition
 0.640E+00   Void Fraction in ASH zone
 0.330E+00   Void Fraction ir COAL zone
 0.119E+04   apparent coal density, kg/m^3
 0.136E+00   POROSity of coal
 0.109E+04   TAR density, kg/m^3
 0.391E+03   Boiling point for TAR, K
 0.440E+01   Frequency Factor for CO2 gasification, m/K_s
 0.440E+01   Frequency Factor for H2 gasification, m/K_s
 0.133E+01   Frequency Factor for H2O gasification, m/K_s
 0.230E+01   Frequency Factor for O2 oxidation, m/K_s
 0.162E+09   activation Energy for CO2 gasification, j/kmol
 0.162E+09   activation Energy for H2 gasification, j/kmol
 0.147E+09   activation Energy for H2O gasification, j/kmol
 0.929E+08   activation Energy for O2 oxidation, j/kmol
 0.100E+01   particle area factor for internal burning
 0.500E+00   developing Ash Porosity DIVided by Tortuosity
 0.500E-01   FuDGe factor for Solid to Gas ht coef.
 0.100E+01   DEVolatilization FuDGe factor
 0.100E+01   co2 gasification FuDGe factor
 0.100E+01   h2 gasification FuDGe factor
 0.100E+01   h2o gasification FuDGe factor
 0.100E+01   o2 oxidation FuDGe factor
 0.100E+01   Fudge factor for Gas-to-Wall HT coefficient
 0.100E+01   Fudge factor for Solid-to-Wall HT coefficient
------------------------------------------------------------------------
Calculated input parameters:
------------------------------------------------------------------------
 0.310E+03   Temperature of WALL used in 0-d calc, K
 0.373E+03   SATurated water Temp. at reactor pressure, K
 0.154E+07   VAporization enthalpy of water at TW, j/kg
 0.206E+06   heat loss through reactor walls, j/s or watts
 0.792E+01   AVeraGe Atomic Weight of coal, kg/kmol
 0.332E+08   Higher Heating Value of coal, j/kg
```

Table 5.3 Main Output File, *mb1out* (continue).

```
-0.857E+06  Heat of Formation of Coal, j/kg
-0.165E+03  SENsible enthalpy of Coal, j/kg
 0.594E+03  a in Cp(ash) = a + bT - ct^-2
 0.586E+00  b in Cp(ash) = a + bT - ct^-2
 0.000E+00  c in Cp(ash) = a + bT - ct^-2
 0.159E+04  liquid ash heat capacity, j/kg_K
 0.230E+06  heat of melting for ash, j/kg
INPUT ECHO (idev =           5)
----------
    lfreeb, ljkstm, lx0                              F    F    F
    burnout                                          1.0000
-------------------------------------------------------------------------
    u, watts/m^2K                 *****              (***** btu/hrft2F)
    Blast Steam Temp., K          300.00             ( 80.33 F)
    Blast Oxydizer Temp., K       300.00             ( 80.33 F)
-------------------------------------------------------------------------
    HHV OF DAF COAL, j/kg         0.331798E+08       (14264.7 btu/lb)
    Freeboard heat loss, watts    -.120000E+07       (-.1138E+04 btu/s)
-------------------------------------------------------------------------
    Chamber diameter, m           1.9812             ( 6.4999 ft)
    Chamber length, m             1.8288             ( 5.9999 ft)
    Wall temp., K                 310.45             ( 99.14 F)
    Chamber Pressure, KPa         .10133E+03         (  1.0 atm)
    Inlet coal temp., K           298.00             ( 76.7 F)
-------------------------------------------------------------------------
    Coal mass flow, kg/s          0.3524             ( 1.3984 t/hr)
    Oxidizer mass flow,kg/s       0.94813            ( 3.7624 t/hr)
    Steam mass flow, kg/s         0.15624            ( 0.6200 t/hr)
    Jacket steam flow, kg/s       0.13390            ( 0.5314 t/hr)
    Tar recycle wt. fraction      0.0000
-------------------------------------------------------------------------
    UA, w/K                       0.400000E+06       (0.25E+07 btu/hr.F)
    Tsat, K                       373.14             (211.99 F)
    Enthalpy of Vap., j/kg        0.1540E+07         (0.6623E+03 btu/lb)
    Wall heat loss, watts         0.4000E+06         (0.3794E+03 btu/s)
-------------------------------------------------------------------------
Proximate (ash, fc, H2O, VM)      0.0426  0.4938  0.0625  0.3994
Ultimate anal. (input-CHNSO)      0.8142  0.0507  0.0175  0.0161  0.1015
Ultimate anal. (devol-CHNSO)      0.8142  0.0508  0.0175  0.0161  0.1015
-------------------------------------------------------------------------
```

Table 5.3 Main Output File, *mb1out* (continue).

```
OUTPUT RESULTS:  V* =  0.547878048311968          x0 =  0.221957148909373
---------------
    Exit temp., K                  921.33          (1198.72 F)
    Equilibrium temp., K          1471.39          (2188.83 F)
    Product tar flow, kg/s         0.0648          ( 0.2572 t/hr)

    Recycle tar flow, kg/s         0.0000          ( 0.0000 t/hr)
    Total tar flow, kg/s           0.0648          ( 0.2572 t/hr)
                    RAW GAS COMPOSITION (DRY)-->
    COMPONENT                                      (DRY) MOLE %
    ---------                                      ------------
         CO                                            18.89
         CO2                                           10.83
         H2                                            21.32
         CH4                                            1.09
         C2H6                                           0.00
         H2S                                            0.23
         INERTS (AR =  0.59% & N2 = 47.05%)            47.64
         OTHERS                                         0.01
         (CHX =  0.00%, HCN =  0.00%, NH3 =  0.01%, etc. =  0.00%)


     ZERO-D CPU TIME:   0 hours,  0 minutes,  0.189 seconds!
```

Distance from top	ts (K)	tg (K)	mol% H2	mol% CO2	KPa	Inches H2O
0.1828800000E+01	297.6	921.3	20.13	10.23	0.000E+00	0.000E+00
0.1808800000E+01	444.7	940.9	20.38	9.34	0.278E-01	0.112E+00
0.1788800000E+01	544.5	960.5	20.40	8.56	0.547E-01	0.220E+00
0.1768800000E+01	604.0	980.3	20.35	7.98	0.800E-01	0.322E+00
0.1748800000E+01	617.5	1002.7	20.33	7.57	0.105E+00	0.424E+00
0.1728800000E+01	666.3	1032.0	20.18	7.23	0.130E+00	0.522E+00
0.1708800000E+01	972.9	1366.9	9.25	9.79	0.155E+00	0.624E+00
0.1688800000E+01	988.9	1400.2	9.01	9.63	0.181E+00	0.727E+00
0.1668800000E+01	1047.8	1432.2	8.81	9.48	0.206E+00	0.830E+00
0.1648800000E+01	1165.9	1459.0	8.66	9.38	0.231E+00	0.929E+00
0.1628800000E+01	1225.1	1480.7	8.54	9.29	0.256E+00	0.103E+01
0.1608800000E+01	1238.4	1382.5	11.12	8.14	0.280E+00	0.112E+01
0.1588800000E+01	1256.6	1394.6	11.04	8.10	0.302E+00	0.121E+01
0.1568800000E+01	1285.0	1406.1	10.95	8.06	0.323E+00	0.130E+01
0.1548800000E+01	1314.1	1416.5	10.85	8.05	0.344E+00	0.138E+01
0.1528800000E+01	1336.1	1426.1	10.75	8.05	0.364E+00	0.146E+01
0.1508800000E+01	1351.6	1435.3	10.64	8.06	0.385E+00	0.155E+01
0.1488800000E+01	1363.0	1444.4	10.52	8.09	0.406E+00	0.163E+01
0.1468800000E+01	1371.9	1453.6	10.39	8.12	0.427E+00	0.172E+01
0.1448800000E+01	1379.3	1463.0	10.26	8.15	0.442E+00	0.178E+01
0.1428800000E+01	1385.8	1472.6	10.12	8.19	0.463E+00	0.186E+01
0.1408800000E+01	1391.9	1482.6	9.97	8.24	0.476E+00	0.191E+01
0.1388800000E+01	1397.7	1492.8	9.81	8.29	0.496E+00	0.199E+01
0.1368800000E+01	1403.5	1503.5	9.65	8.34	0.509E+00	0.205E+01
0.1348800000E+01	1409.2	1514.6	9.48	8.39	0.525E+00	0.211E+01
0.1328800000E+01	1415.0	1526.1	9.30	8.45	0.544E+00	0.219E+01
0.1308800000E+01	1420.8	1538.1	9.11	8.52	0.560E+00	0.225E+01
0.1288800000E+01	1426.7	1550.6	8.91	8.58	0.577E+00	0.232E+01
0.1268800000E+01	1432.8	1563.5	8.71	8.66	0.587E+00	0.236E+01
0.1248800000E+01	1438.9	1577.0	8.49	8.74	0.603E+00	0.242E+01
0.1228800000E+01	1445.2	1591.1	8.27	8.82	0.617E+00	0.248E+01
0.1208800000E+01	1451.5	1605.7	8.03	8.91	0.631E+00	0.254E+01

Table 5.3 Main Output File, *mb1out* (continue).

0.1188800000E+01	1458.0	1620.9	7.79	9.00	0.647E+00	0.260E+01
0.1168800000E+01	1464.7	1636.8	7.53	9.11	0.657E+00	0.264E+01
0.1148800000E+01	1471.4	1653.3	7.27	9.21	0.672E+00	0.270E+01
0.1128800000E+01	1478.3	1670.4	6.99	9.33	0.686E+00	0.276E+01
0.1108800000E+01	1485.3	1688.2	6.70	9.45	0.696E+00	0.280E+01
0.1088800000E+01	1492.5	1706.8	6.40	9.58	0.708E+00	0.285E+01
0.1068800000E+01	1499.9	1726.2	6.08	9.72	0.721E+00	0.290E+01
0.1048800000E+01	1507.4	1746.6	5.75	9.87	0.732E+00	0.294E+01
0.1028800000E+01	1515.2	1768.2	5.40	10.04	0.747E+00	0.300E+01
0.1008800000E+01	1523.4	1791.2	5.02	10.23	0.757E+00	0.304E+01
0.9888000000E+00	1531.9	1815.9	4.61	10.45	0.767E+00	0.309E+01
0.9688000000E+00	1540.8	1842.4	4.17	10.70	0.780E+00	0.314E+01
0.9488000000E+00	1550.3	1870.9	3.70	10.99	0.791E+00	0.318E+01
0.9288000000E+00	1560.3	1901.5	3.20	11.33	0.801E+00	0.322E+01
0.9088000000E+00	1570.9	1934.3	2.67	11.71	0.814E+00	0.327E+01
0.8888000000E+00	1582.2	1969.4	2.10	12.15	0.824E+00	0.331E+01
0.8688000000E+00	1594.2	2006.7	1.51	12.65	0.836E+00	0.336E+01
0.8488000000E+00	1606.6	2044.8	0.89	13.22	0.846E+00	0.340E+01
0.8288000000E+00	1617.6	2067.3	0.32	13.68	0.858E+00	0.345E+01
0.8088000000E+00	1615.7	2005.4	0.08	13.12	0.868E+00	0.349E+01
0.7888000000E+00	1597.6	1889.8	0.02	11.89	0.878E+00	0.353E+01
0.7688000000E+00	1571.6	1754.6	0.00	10.46	0.888E+00	0.357E+01
0.7488000000E+00	1540.2	1606.6	0.00	8.95	0.896E+00	0.360E+01
0.7288000000E+00	1504.0	1447.2	0.00	7.40	0.904E+00	0.364E+01
0.7088000000E+00	1462.7	1276.7	0.00	5.80	0.911E+00	0.366E+01
0.6888000000E+00	1416.4	1100.9	0.00	4.22	0.917E+00	0.369E+01
0.6688000000E+00	1363.5	917.6	0.00	2.67	0.922E+00	0.371E+01
0.6488000000E+00	1302.8	731.8	0.00	1.17	0.926E+00	0.372E+01
0.6288000000E+00	1233.8	573.8	0.00	0.00	0.929E+00	0.374E+01
0.6088000000E+00	1220.6	548.9	0.00	0.00	0.932E+00	0.375E+01
0.5888000000E+00	542.2	528.1	0.00	0.00	0.935E+00	0.376E+01
0.5688000000E+00	528.2	528.3	0.00	0.00	0.938E+00	0.377E+01
0.5488000000E+00	528.5	528.6	0.00	0.00	0.941E+00	0.378E+01
0.5288000000E+00	528.8	528.9	0.00	0.00	0.944E+00	0.379E+01
0.5088000000E+00	529.2	529.2	0.00	0.00	0.947E+00	0.381E+01
0.4888000000E+00	529.5	529.5	0.00	0.00	0.949E+00	0.382E+01
0.4688000000E+00	529.8	529.9	0.00	0.00	0.951E+00	0.383E+01
0.4488000000E+00	530.1	530.2	0.00	0.00	0.954E+00	0.384E+01
0.4288000000E+00	530.4	530.5	0.00	0.00	0.956E+00	0.385E+01
0.4088000000E+00	530.7	530.8	0.00	0.00	0.959E+00	0.386E+01
0.3888000000E+00	531.1	531.1	0.00	0.00	0.961E+00	0.386E+01
0.3688000000E+00	531.4	531.5	0.00	0.00	0.963E+00	0.387E+01
0.3488000000E+00	531.7	531.8	0.00	0.00	0.966E+00	0.388E+01
0.3288000000E+00	532.0	532.1	0.00	0.00	0.968E+00	0.389E+01
0.3088000000E+00	532.3	532.4	0.00	0.00	0.970E+00	0.390E+01
0.2888000000E+00	532.7	532.8	0.00	0.00	0.972E+00	0.391E+01
0.2688000000E+00	533.0	533.1	0.00	0.00	0.974E+00	0.392E+01
0.2488000000E+00	533.3	533.4	0.00	0.00	0.976E+00	0.392E+01
0.2288000000E+00	533.7	533.7	0.00	0.00	0.978E+00	0.393E+01
0.2088000000E+00	534.0	534.1	0.00	0.00	0.979E+00	0.394E+01
0.1888000000E+00	534.3	534.4	0.00	0.00	0.981E+00	0.394E+01
0.1688000000E+00	534.6	534.7	0.00	0.00	0.983E+00	0.395E+01
0.1488000000E+00	535.0	535.1	0.00	0.00	0.984E+00	0.396E+01
0.1288000000E+00	535.3	535.4	0.00	0.00	0.986E+00	0.397E+01
0.1088000000E+00	535.7	535.8	0.00	0.00	0.988E+00	0.397E+01
0.8880000000E-01	536.0	536.1	0.00	0.00	0.989E+00	0.398E+01

Table 5.3 Main Output File, *mblout* (continue).

```
0.6880000000E-01     536.3     536.4     0.00      0.00     0.991E+00     0.398E+01
0.4880000000E-01     536.7     536.8     0.00      0.00     0.992E+00     0.399E+01
0.2880000000E-01     537.0     537.1     0.00      0.00     0.994E+00     0.400E+01
0.8800000000E-02     537.4     537.5     0.00      0.00     0.995E+00     0.400E+01
-.1120000000E-01     537.7     537.8     0.00      0.00     0.996E+00     0.401E+01
-------------------------------------------------------------------------------
Overall Heat Loss =   0.2602E+06 j/s
TOTAL CPU TIME:   0 hours,  1 minutes, 49.144 seconds!
```

The main output file, ***mblin***, consists of input parameters, variables calculated from input data, effluent output from the two-zone model, and axial output from the one-dimensional model. Overall heat loss and cpu time are also reported at the end of the *mblout* file. The axial output consists of the axial distance from the top of the coal bed (m), the solid and gas temperatures (K), the mole percent H_2 and CO_2 (%), and the pressure drop from the top of the reactor (KPa and inches of water).

5.4.2 Optional Output Files, *outa* Through *outj*

Ten optional output files are shown in Table 5.4. These files are created when the logical flags outa through outj are set to "true". Each file begins with the distance from the top of the reactor in meters (z).

Table 5.4 Optional Output Files and Parameters.

outa	outb	outc	outd	oute	outf	outg	outh	outi	outj
z	z	z	z	z	z	z	z	z	z
Wg	tg	ncall	frco2	crco2	pd	hrxn1	hw	ar	stime
Ws	ts	cfrac	frh2	crh2	pdu	hrxn2	hwg	co	gtime
Wghg	cpg	areap	frh2o	crh2o	brnout	hrxn3	hws	co2	gashr
Wshs	gk	sco2	fro2	cro2	rco2	hrxn4	hsg	ch4	solhr
ydot(1)	gmw	sh2	arco2	zirihi	rh2	smrihi	hrs	c2h6	s2gk
ydot(2)	gvisc	sh2o	arh2	rw	rh2o	re	hrv	h2	fdgsg
ydot(3)	sk	so2	arh2o	trco2	ro2	pr	sk	hcn	gvel
ydot(4)	difco2	rc	aro2	trh2	risum	rskgk	gk	h2o	svel
gasflo	difh2	rh	trco2	trh2o		phi	ergk	h2s	
flochr	difh2o	rn	trh2	tro2			ersk	n2	
	difo2	ro					qwg	nh3	
		rs					qws	no	
							qpg	o2	
								oh	
								so2	

The *outa* output file contains the gas and solid mass flow rates (Wg and Ws), gas and solid energy rates (Wghg and Wshs), and the right hand side of the gas and solid continuity and energy equations (ydot), gas mass flow rate (gasflo), and the char mass flow rate (flochr).

The *outb* output file contains the gas and solid temperature (tg and ts), the gas heat capacity (cpg), the gas mixture conductivity (gk), the gas mixture molecular weight (gmw), the gas mixture viscosity (gvisc), the solid conductivity (sk), the diffusivity of CO_2 (difco2), the diffusivity of H_2 (difh2), the diffusivity of H_2O (difh2o), and the diffusivity of O_2 (difo2).

The *outc* output file contains the number of calls to the f routine (ncalls), the fraction of carbon remaining in the char particle (cfrac), the surface area of the particle (areap), the Schmidt number for CO_2, H_2, H_2O, and O_2 (sco2, sh2, sh2o, and so2), the Reynolds number (re), and the volumetric heterogeneous elemental reaction rate for carbon, hydrogen, nitrogen, oxygen, and sulfur (rc, rh, rn, ro, and rs).

The *outd* output file contains the film resistances for gasification and oxidation (frco2, frh2, frh2o, and fro2), the ash resistances for gasification and oxidation (arco2, arh2, arh2o, and aro2), and the total resistances for the CO_2 and H_2 gasification reactions (trco2 and trh2).

The *oute* output file contains the chemical resistances to gasification and oxidation (crco2, crh2, crh2o, and cro2), the energy term associated with mass exchange between solid and gas phases (zirihi), the volumetric drying rate (rw), and the total resistance to gasification and oxidation (trco2, trh2, trh2o, and tro2).

The *outf* output file contains the overall particle diameter (pd), the unreacted core diameter (pdu), the dry ash-free particle burnout (brnout), the volumetric H_2 and H_2O gasification rates (rh2 and rh2o), the volumetric oxidation rate (ro2), and the total volumetric gasification and oxidation rate (risum).

The *outg* output file contains the total enthalpy production rate for the gasification and oxidation reactions (CO_2 is hrxn1, H_2 is hrxn2, H_2O is hrxn3, and O_2 is hrxn4), the overall volumetric energy production from gasification and oxidation (smrihi), Reynolds number (re), Prandtl number (pr), ratio of the solid conductivity to the gas conductivity (rskgk), and the bed packing parameter (phi).

The *outh* output file contains the bed-to-wall heat transfer coefficient (hw), the gas-to-wall heat transfer coefficient (hwg), the solid-to-wall heat transfer coefficient (hws), the solid-to-gas heat transfer coefficient (hsg), the solid radiation coefficient (hrs), the void-to-void radiation coefficient (hrv), the solid thermal conductivity (sk), the gas mixture thermal conductivity (gk), the effective radial gas conductivity (ergk), the effective radial solid conductivity (ersk), the volumetric heat transfer from the gas to the wall (qwg), the volumetric heat transfer from the solid to the wall (qws), and the volumetric heat transfer from the solid to the gas (qpg).

The *outi* output file gives the concentration in mole percent of the gas phase. Only the mole percentages for the first 15 gas species in the *mb1thm* file are printed. For the example in Table 5.4, the mole percentages are for AR, CO, CO_2, CH_4, C_2H_6, H_2, HCN, H_2O, H_2S, N_2, NH_3, NO, O_2, OH, and SO_2.

The *outj* output file gives the solid residence time (stime), the gas residence time (gtime), the gas heating rate (gashr), the solid heating rate (solhr), the k factor (s2gk) used in calculating the correction factor for solid-to-gas heat transfer in a reacting bed following Dzhapbyev et al. (1986), the calculated correction factor for solid-to-gas heat transfer in a reacting bed (fdgsg) following Dzhapbyev et al. (1986), the gas velocity (gvel), and the solid velocity (svel).

5.4.3 Plotting Output Files

As discussed at the beginning of this chapter, plotting or graphics routines are not distributed with the code. However, graphics are important for understanding the code's voluminous output of data, and a recommendation for graphics output is discussed in this section.

Simple graphics can be viewed using inexpensive software available on personal computers. During development of MBED-1D, data was transferred between the SUN™ workstation and an Apple Macintosh™ by logging into the workstation with an Apple Macintosh™ using the terminal emulator VersaTerm Pro™. Output files were transferred to the Macintosh™ by using the UNIX command "cat". The output file to be plotted was concatenated to the screen and placed into the Macintosh™ clipboard by using the " • copy table" command which is located in the "Edit" menu of VersaTerm Pro™. This command is also available with other terminal emulators. The copy table command copies the columns of output with a "tab character" as the delimiter between data columns. With tabs placed between data columns, the data in the clipboard is formatted correctly to be pasted into either a spreadsheet (e. g. Excel™) or a graphics program (e. g. Cricket Graph™). The data can then be viewed with the graphics software. Data can also be plotted using packages available for the workstation. However, the choice of graphics software is left to the discretion of the user.

5.5 Code Operation

MBED-1D is a "user-specialist" code that requires familiarity with the theory and structure of the code in order to be used correctly and efficiently. This section gives several hints for new users. A thorough understanding of the problem physics and numerical assumptions is essential. Several iterations are required to obtain a converged solution. Presently, these iterations are done by hand to gain insight into the solution method. The iteration procedure is also discussed in this section.

5.5.1 Selecting Logicals

Several logical parameters can be set to run different code options. The "l0d" flag is available to let the user run either the complete one-dimensional model (see Chapter 3) or just the two-zone model (see Chapter 2). Only effluent properties are calculated when the "l0d" flag is set to "true."

The "lgaseq" flag is used to control the gas phase submodel. Two model assumptions can be made: 1) all gases in the drying and devolatilization zone are nonreactive ("lgaseq" is set to "false"), and 2) all gases in the drying and devolatilization zone, except tar, are in chemical equilibrium ("lgaseq" is set to "true"). Both these options are specifically for the two-zone model calculation. When the one-dimensional model is executed (i. e. "l0d" is set to "false"), "lgaseq" is automatically set to "true" since there is no allowance to keep all gases nonreactive in the one-dimensional portion of MBED-1D. One additional flag related to the gas phase chemistry is available when running MBED-1D, "ltareq." Setting "ltareq" to "true" causes the tar in the gas phase to react to equilibrium. If "ltareq" is set to "false," tar is assumed to be nonreactive in the gas phase.

The "lfreeb" flag is used to calculate the freeboard temperature using the freeboard heat loss which is input as "qfreeb". Heat loss is input as a negative quantity. If "lfreeb" is set to "false," the freeboard temperature is not calculated. Typical temperature drop

from the top of the coal bed to the top of the freeboard in a Wellman-Galusha reactor may be 10-20 K (Hobbs, 1990).

The "ljkstm" flag is used to calculate the reactor heat loss based on the jacket steam flow rate which can be specified using the variable "flowjs." The heat of vaporization is calculated using the Pitzer-Chen equation (Reid and Sherwood, 1966). This equation gives acceptable results at high pressures but should be used with caution at atmospheric conditions.

The "lashcp" flag is used to specify the method of calculating the heat capacity of the ash. The complete ash composition is used if "lashcp" is set to "true." Otherwise, the correlation given by Merrick (1983) is used for the ash heat capacity.

The "lx0" flag is used to specify the potential tar-forming fraction. The potential tar-forming fraction is calculated with a semi-empirical model (Ko, et al., 1988) if "lx0" is set to "false". Otherwise, the potential tar-forming fraction is specified with the variable "usrx0."

The "lusey0" flag is used to specify the dry, ash-free functional group fractions. Actual functional group data can be used for calculations if "lusey0" is set to "true." The dry, ash-free functional group data should be entered after the "usrx0" variable. Otherwise, the functional group compositions are calculated based on a base set of eight coals. The base coal is specified with the integer flag "idev" as shown in Table 5.1.

The "lecho" flag is used to print input data to the "mb1out" file. Input data are printed to the "mb1out" file for verification if "lecho" is set to "true".

The "lsp" flag is used to specify the shell progressive or ash segregation char oxidation and gasification model. The shell progressive model is used if "lsp" is set to "true". Otherwise, the ash segregation model is used.

The "lstiff" flag is used to control the type of algorithm used to solved the set of first order differential equations. A stiff solver is used if "lstiff" is set to "true." Otherwise, a non-stiff solver is used to solve the differential equations. Both methods give the same results. However, the non-stiff solver is faster.

The "lstop" flag is used to terminate the integration of the differential equations when the bottom of the reactor has been reached. For example, the integrator stops at the bottom of the reactor if "lstop" is set to "true." Otherwise, the integrator continues to march past the bottom of the reactor. Either a ^C or the UNIX command KILL must be used to terminate the program when "lstop" is set to "true".

The "lout" flags control printing of output variables. Printing is enabled when the flags are set to "true". The various output files were discussed in Section 5.4.

5.5.2 Iteration Procedure

The two-zone, well-mixed model discussed in Chapter 2 is used to convert the split boundary value problem into an initial value problem by providing an initial estimate of the effluent gas composition and temperature. However, the gas exit temperature predicted by the two-zone model is always high due to the assumption that the devolatilization zone is at a single temperature. Likewise, the exit solid temperature is high due to the well-mixed assumption. Thus after integrating from the top to the bottom of the reactor, the calculated feed gas temperature will be higher than the input feed gas temperature. Therefore, a new exit gas temperature must be estimated which is smaller than the temperature predicted by the two-zone model discussed in Chapter 3. This procedure can be repeated in an iterative manner until the calculated feed gas temperature is equal to the input feed gas temperature. Detail on this iteration technique is given in this section.

To start a calculation, the heat loss from the reactor must be estimated. The heat loss can be estimated using the jacket steam flow rate. Using this estimate of heat loss, the effluent gas temperature and composition can be determined using the two-zone model discussed in Chapter 2. The differential equations listed in Table 3.2 are integrated from the top of the reactor to the bottom of the reactor. At the bottom of the reactor, the calculated gas temperature can be compared to the known gas temperature. If the calculated feed gas temperature is equal to the known feed gas temperature, convergence is obtained. However, the initial calculated effluent temperature using the two-zone model is expected to be high since the exit temperature is calculated by assuming the drying and devolatilization zone to be one temperature.

After the initial guess, the zero-dimensional wall heat loss can be adjusted to reguess the effluent gas temperature. For these subsequent iterations, "ljkstm" is set to "true" and the overall 0-D heat loss is used as an iteration variable. Increasing the overall 0-D heat loss causes the exit temperature to decrease. An example iteration scheme is shown in Table 5.5. After the initial temperature is guessed using the two-zone model, the exit temperature is lowered by estimating the 0-D heat loss. Four iterations were required to match the calculated feed gas temperature with the "known" feed gas temperature using this method as shown in Table 5.5. The 0-D heat loss represents the heat loss necessary to lower the exit gas temperature and is significantly different than the calculated 1-D heat loss as shown in Table 5.5. The 0-D heat loss is only used as a method to iterate exit gas temperature. Measured heat loss values should be compared to the calculated 1-D heat loss values.

Table 5.5 Iteration of MBED-1D using feed gas temperature as an iteration variable

Iteration #	0-D Heat Loss, MW§	Tg_{exit}, K	Tg_{feed}, K‡
1	Jacket steam flow+	1030	791
2	0.80	892	403
3	0.70	906	453
4	0.69§	907	459

§ The 1-D heat loss for iteration #4 was 0.23 MW. The one-dimensional heat loss should be compared to measurements since the 0-D heat loss is used for iteration purposes only.

‡ The known feed gas temperature is 460 K for this case.

+ The jacket steam flow rate was used to estimate the overall heat loss which was 0.21 MW.

END

DATE
FILMED
1/15/92

I